Characteristics and Air Pollution Effects of Particulate Matters from Rubber Wood Combustion in Rubber–Smoking Process

Jiraporn Chomanee

A Thesis Submitted in Partial Fulfillment of the Requirements
for the Degree of Master of Science in Physical Chemistry
Prince of Songkla University
2008

Thesis Title	Characteristics and Air Pollution Effects of Particulate Matters from Rubber Wood Combustion in Rubber–Smoking Process
Author	Mrs. Jiraporn Chomanee
Major Program	Physical Chemistry

Major Advisor

..……..……...

(Asst. Prof. Dr. Surajit Tekasakul)

Co-advisor

…….....……..…...……...

(Assoc. Prof. Dr. Perapong Tekasakul)

Examining Committee:

……...……..Chairperson

(Asst. Prof. Dr. Orawan Sirichote)

..…...…….……Committee

(Asst. Prof. Dr. Surajit Tekasakul)

..…....…….……..Committee

(Assoc. Prof. Dr. Perapong Tekasakul)

….....……...……...……..Committee

(Assoc. Prof. Wongpun Limpaseni)

The Graduate School, Prince of Songkla University, has approved this thesis as partial fulfillment of the requirements for the Master of Science Degree in Physical Chemistry

…….……

(Assoc. Prof. Dr. Krerkchai Thongnoo)

Dean of Graduate School

ชื่อวิทยานิพนธ์ คุณลักษณะและผลกระทบของมวลอนุภาคจากการเผาไหม้ไม้ยางพาราในกระบวนการรมควันยางแผ่นต่อมลภาวะทางอากาศ
ผู้เขียน นางจิราพร ช่อมณี
สาขาวิชา เคมีเชิงฟิสิกส์
ปีการศึกษา 2551

บทคัดย่อ

งานวิจัยนี้เป็นการศึกษาคุณลักษณะทางกายภาพและทางเคมีของอนุภาคควันที่เกิดจากการเผาไหม้ของไม้ยางพาราในกระบวนการรมควันยางแผ่นของสหกรณ์สวนยาง (สกย.) และศึกษาผลกระทบของมวลอนุภาคต่อการเกิดมลภาวะทางอากาศโดยรอบของสหกรณ์สวนยางและเมืองหาดใหญ่ โดยศึกษาค่าความเข้มข้นของอนุภาคฝุ่นโดยรวมด้วยเครื่องเก็บตัวอย่างปริมาณสูง (High Volume Air Sampler) ซึ่งทำการเก็บตัวอย่างอากาศระหว่างเดือนมกราคม 2549 ถึงเดือนมกราคม 2550 และศึกษาการกระจายขนาดของอนุภาคฝุ่น/ควันโดยใช้เครื่องเก็บตัวอย่างแบบแยกขนาดอนุภาคแอนเดอร์เซน (Andersen Sampler) ที่สามารถแยกขนาดของอนุภาคได้ 8 ช่วง ต่อมาศึกษาวิเคราะห์ชนิดและปริมาณสารโพลีไซคลิกอะโรมาติกไฮโดรคาร์บอน (PAHs) 16 ชนิด ในอนุภาคด้วยเทคนิคลิควิดโครมาโตกราฟีสมรรถนะสูง (HPLC) ร่วมกับตัวตรวจวัดชนิดยูวี (UV) จากการศึกษาพบว่าอนุภาคควันจากการเผาไหม้ไม้ยางพาราแสดงการกระจายขนาดอนุภาคที่ 1 โหมด ซึ่งขนาดอนุภาคส่วนใหญ่เท่ากับ 0.68 ไมโครเมตร ตัวอย่างทั้งจากบริเวณพื้นที่ทำงานในสกย.และจากเมืองหาดใหญ่มีการกระจายของขนาดอนุภาคเป็น 2 โหมด ประกอบด้วยอนุภาคขนาดปานกลาง (accumulation mode) มีอนุภาคขนาด 0.54 ไมโครเมตร และอนุภาคหยาบ (coarse-mode) มีอนุภาคขนาด 4.00 ไมโครเมตร จากการศึกษาค่าความเข้มข้นของอนุภาคพบว่าความเข้มข้นของอนุภาคโดยรวมในบริเวณทำงานของสกย. และเมืองหาดใหญ่มีค่าไม่เกินเกณฑ์มาตรฐานของกรมควบคุมมลพิษ (330 ไมโครกรัมต่อลูกบาศก์เมตร) ค่าความเข้มของอนุภาคฝุ่นโดยรวมเฉลี่ยของตัวอย่างจากห้องรมควัน พื้นที่การทำงาน และเมืองหาดใหญ่มีค่าตามลำดับอยู่ที่ 15,806.11, 164.42 และ 31.86 ไมโครกรัมต่อลูกบาศก์เมตร ผลการวิเคราะห์องค์ประกอบทางเคมีพบการเปลี่ยนแปลงของค่าความเข้มข้นของสารโพลีไซคลิกอะโรมาติกไฮโดรคาร์บอนของตัวอย่างอากาศทั้งที่บริเวณทำงานและตัวเมืองหาดใหญ่ มีความสัมพันธ์กับปริมาณยางแผ่นรมควัน ปริมาณน้ำฝนและทิศทางลม นอกจากนี้พบว่าสารโพลีไซคลิกอะโรมาติกไฮโดรคาร์บอนชนิดหลายวงแหวนมีปริมาณมากเป็นพิเศษที่อนุภาคขนาดเล็กของตัวอย่างจากบริเวณพื้นที่ทำงานของสกย. แสดงถึงค่าความเสี่ยงต่อการเกิดปัญหาสุขภาพของคนงานในสกย. และจากการศึกษาวิเคราะห์โดย

จำแนกตามจำนวนวงแหวนของสารโพลีไซคลิกอะโรมาติกไฮโดรคาร์บอน พบว่ารูปแบบการกระจายของสารโพลีไซคลิกอะโรมาติกไฮโดรคาร์บอน มีการเปลี่ยนแปลงขึ้นอยู่กับพื้นที่ในการเก็บตัวอย่าง โดยสารโพลีไซคลิกอะโรมาติกไฮโดรคาร์บอนชนิด 4-6 วงแหวน เป็นกลุ่มหลักที่พบในตัวอย่างจากห้องรมควันและพื้นที่ทำงานของสกย. ส่วนตัวอย่างจากเมืองหาดใหญ่พบสารโพลีไซคลิกอะโรมาติกไฮโดรคาร์บอนชนิด 2-3 วงแหวนเป็นกลุ่มหลัก แสดงให้เห็นถึงอิทธิพลของอนุภาคจากการเผาไหม้ของไม้ยางพาราต่อมลภาวะทางอากาศของเมืองหาดใหญ่อยู่ในระดับต่ำ ทั้งนี้เป็นผลของปริมาณน้ำฝน ทิศทางลม และการเกิดปฏิกิริยาของอนุภาคในอากาศระหว่างการเคลื่อนที่ทำให้เกิดการเจือจางของสารมลภาวะในอากาศ

Thesis Title	Characteristics and Air Pollution Effects of Particulate Matters from Rubber Wood Combustion in Rubber–Smoking Process
Author	Mrs. Jiraporn Chomanee
Major Program	Physical Chemistry
Academic Year	2008

ABSTRACT

Physical and chemical characteristics of particles from rubber-wood combustion in a rubber sheet smoking cooperative were studied, and their influences to workplace environments and surrounding atmosphere were evaluated. Particle samples were collected at three different sites: smoking room, workplace area, and Hat Yai City. The samples were collected during January 2006 to January 2007. Total suspended particulate matter (TSP) and total smoke particulate concentration were measured using a commercial portable high-volume sampler and a modified high-volume air sampler, respectively. The size distribution of particulate matter was collected by an 8-stage Andersen sampler. Sixteen polycyclic aromatic hydrocarbons (PAHs) in the extracts from the particulates were analysed using a high performance liquid chromatography (HPLC) with diode-array ultraviolet-visible (UV) detection. Smoke particle size distribution shows single-mode behavior. It has been demonstrated that the partitioning of the mass median aerodynamic diameter (MMAD) is 0.68 μm. The particle size distribution of workplace and ambient air clearly shows bi-modal behavior with the accumulation-mode peak taking place at a particle size of 0.54 μm and the coarse-mode peak taking place at 4.0 μm. The variable of total smoke concentration depends on wood moisture content and wood burning period. The TSP in workplace and ambient air at Hat Yai City are within the limits regulated by the Thailand Pollution Control Department (330 μg m^{-3}). The average TSP is about 15,806.11, 164.42, and 31.86 μg m^{-3} for particles sampled from source, workplace, and Hat Yai City, respectively. Behaviors of PAH concentration for both workplace and Hat Yai are influenced by the precipitation, the ribbed smoked sheet production and the wind direction. The PAH concentration inside the

workplace was higher, particularly of the ones with larger numbers of aromatic rings in the fraction of fine particles, which may lead to serious health problems of the workers. The PAH distribution pattern varied with the sampling sites. Particle-bound PAHs from source and workplace were dominated by 4-6 ring PAH compounds, while PAHs from Hat Yai City were dominated by 2-3 ring PAH compounds. Here, the effect of smoke particles to the city of Hat Yai seems to be less. The concentrations and fractions of the PAHs are different at different sites, indicating dilution, mixing, and degradation of the pollutants.

ACKNOWLEDGEMENTS

The author would like to express a gratitude to her advisors, Assistant Professor Dr. Surajit Tekasakul and Associate Professor Dr. Perapong Tekasakul, for their valuable instruction, expert guidance and excellent suggestion.

Thanks also go to Associate Professor Wongpun Limpaseni and Assistant Professor Dr. Orawan Sirichote, for their expert comments and suggestion.

The author would also like to express her gratitude to the staff of the Department of Chemistry, Faculty of Science, Prince of Songkla University for their support throughout the course of study. This study could not have taken place without the samples from Saikao rubber smoking cooperative, Songkhla Province. An acknowledgement also goes to Professor Dr. Masami Furuuchi and Dr. Yunhe Bai from Kanazawa University, Japan for their technical support, and Dr. Helmut Duerrast of Physics Department, Prince of Songkla University for correcting the use of English.

Financial supports from the Center of Excellence for Innovation in Chemistry (PERCH-CIC), NRCT-JSPS Joint Research Project and the Graduate School, Prince of Songkla University are gratefully acknowledged. Finally, none of this would have been possible without love and encouragement of her parents and friends. The author thanks them for their kindness and valuable advice. Everything will be kept always in her mind.

Jiraporn Chomanee

CONTENTS

CONTENTS (Continued)

CONTENTS (Continued)

List of Tables

List of Figures

List of Figures (Continued)

List of Figures (Continued)

List of Figures (Continued)

List of Figures (Continued)

List of Figures (Continued)

LIST OF ABBREVIATION AND SYMBOLS

Abbreviation

Ace	Acenaphthene
Act	Acenaphthylene
Ant	Anthracene
BaA	Benz(a)anthracene
BaP	Benzo(a)pyrene
BbF	Benzo(b)fluoranthene
BghiPe	Benzo(g,h,i)perylene
BkF	Benzo(k)fluoranthene
BP	boiling point
Chr	Chrysene
DBA	Dibenzo(a,h)antracene
DMSO	Dimethyl sulphoxide
DOM	dissolved organic matter
EPA	Environmental protection agency
EPAQS	Expert panel of air quality standard
Fle	Fluorene
Flu	Fluoranthene
GSD	Geometric standard deviation
HPLC	High performance liquid chromatography
IARC	International agency for research on cancer
IDP	Indeno(1,2,3-cd)pyrene
MMAD	Mass median aerodynamic diameter
MOUDI	Micro orifice uniform deposit impactor
MP	melting point
MW	molecular weight
NAAQS	National ambient air quality standard
Nap	Naphthalene
NR	Natural Rubber

NO_2	Nitrogen dioxide
PAHs	Polycyclic Aromatic Hydrocarbons
Phe	Phenanthrene
PM	Particulate Matters
PSU	Prince of Songkla University
Pyr	Pyrene
RSS	Ribbed Smoked Sheet
S	water solubility
TEFs	Toxicity equivalency factors
TSP	Total suspended particulates
USE	Ultrasonic extraction
UV	Ultraviolet-Visible
VP	Vapor pressure
WP	Workplace

Symbols

d.b.	dry basis
d_{ave}	average aerodynamic diameter
μg	microgram
μL	microliter
μm	micrometer
mL	milliliter
mg	milligram
ng	nanogram
ppm	part per million
ppb	part per billion
C	particle concentration (g m^{-3})
f	mass fraction
M_{dry}	mass of the wood samples after drying
M_f	mass of filter sample after sampling (g)
M_i	mass of blank filter (g)

M_j mass collected in each stage (g)

M_{total} total mass collected (g)

M_{wet} mass of the wood samples before drying (g)

Q flow rate (L m^{-1})

R recovery (%)

V volume (m^{-3})

V_{total} total sampling volume (m^3)

CHAPTER 1
INTRODUCTION

1.1 General Background

Thailand is currently the largest natural rubber (NR) producing and exporting country in the world. Natural rubber is commercially produced in four forms: ribbed smoked sheet (RSS), block rubber, rubber concentrated latex, and miscellaneous forms. Most natural rubber products are used in vehicle tire production. The main consuming NR countries in the world are United States of America, Japan, China and India. At present, a part of RSS is produced in community-level rubber cooperatives, which are small-scale factories. There are totally about 700 such cooperatives throughout the country, mostly in the south of Thailand, such as, Nakhonsi Thamarat, Surat Thani and Songkhla. Especially in Songkhla Province, there are about 101 rubber cooperatives.

The smoke drying or smoking procedure of RSS production is shown in the diagram in Fig. 1.1. In the production of RSS, fuel wood (usually rubber-wood) is burned to supply heat (and smoke) to rubber sheets in the rubber smoke room. Burning of fresh rubber-wood causes a high concentration of smoke particles. Each rubber cooperative does not have a pollution control device, therefore the smoke will be released into the factory workplace area through the ventilating lids on the roof of the drying room, which is directly opened to the inside of the factory building. Workers also need to operate inside the smoke room periodically. Kalasee et al. (2003) found that the mass median aerodynamic diameter (MMAD) of particulates from rubber-wood combustion was 0.95 μm. Moreover, the smoke particles contained extremely high concentrations of hazardous pollutants, for example polycyclic aromatic hydrocarbons (PAHs) (Furuuchi et al., 2006). Most PAHs associated with fine airborne particles, typically 0.5 μm or less (De martinis et al., 2002). Fine particles in this size range efficiently evade the mucocolitis defense system and are deposited in the peripheral airways, where they may exert toxic

effects. Choosong et al. (2007) studied the working environment in a rubber sheet smoking factory and found that concentrations of particle-bond PAHs in smoke particles were extremely large, particularly in fine particles. Worker's main discomforts were smoke and odor. The upper respiratory symptoms were very likely related to pollutants in the workplace.

In addition, PAHs are associated with fine airborne particles that can be transported over a long distance. This implies that particles can distribute PAHs to the atmosphere. This is one of the major sources of air pollution to nearby surroundings.

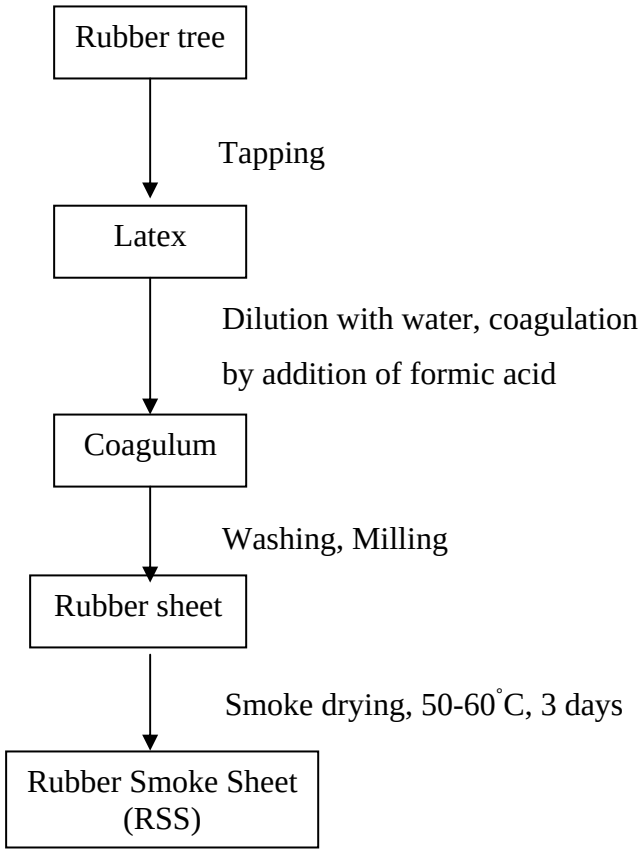

Figure 1.1 Procedure of RSS production (Prom tong and Tekasakul, 2007).

1.2 Review of Literature

1.2.1 Smoke from wood combustion

For better understanding of the physical characteristics of smoke particles from rubber-wood combustion, the size distribution and concentration of particles are studied first. The size distribution and concentration of smoke particles have been investigated in many references.

Hedberg et al. (2002) attempted to characterize many chemical compounds, including PAHs emitted from combustion of birch-wood, which was commonly used in Swedish household appliances. Results showed that fluorene, phenanthrene, anthracene, fluoranthene, and pyrene contributed to more than 70% of the total mass PAHs. The relative carcinogenic potency contribution of fluoranthene (Flu) in the wood smoke would be about 40% of benzo(a)pyrene (BaP).

Venkataraman et al. (2002) investigated the size distribution of PAHs from biofuel combustion i.e. wood (Acacia nilotica, local names keeker or babul in India), briquette, and dung cake in cooking stoves. Their results indicated that the PAH size distribution from all stove-fuel systems was unimodal with mass median aerodynamic diameters (MMADs) in submicron range 0.40-1.01 μm.

Kalasee et al. (2003) studied the soot particles produced from rubber-wood combustion in the rubber smoking process. Particle size distribution was measured with the use of an eight-stage cascade (Andersen) impactor. It was found that the size distribution of soot particles in the smoking room ranged from less than 0.43 μm to 4.7 μm. The mass median aerodynamics diameter (MMADs) was found to be 0.95 μm. Particle concentrations depended strongly on moisture content of the rubber-wood.

Saez et al. (2003) investigated the characteristics of smoke particles from biomass combustion processes (i.e. poplar wood) using a multistage cascade

impactor method (Andersen Mark ÏÏÏ). The concentration of 16 PAH components in particulates was measured. Most of heavy the PAHs were associated with small particles with an aerodynamic diameter less than 2 μm, and the size distribution characteristics of the particles were dominantly unimodal.

Francisco et al. (2005) studied PAHs emitted from combustion of Pine wood, Pine needle, Prickly Pear, and Almond skin in agricultural and sylvicultural debris using two different kinds of combustion devices. Low molecular weight PAHs, including naphthalene 1- and 2-methylnaphthalene, acenaphthylene and phenanthrene were the most common PAHs found in all types of smoke samples, ranging 61%-72% of the total PAH concentration from the biomass combustion samples. In addition, the results showed that the naphthalene concentration can be used as an indicator of the total hydrocarbon content in the smoke.

Furuuchi et al. (2006) studied the characteristics of smoke particles from the rubber-wood combustion and evaluated their influences on workspace environment in a rubber cooperative as well as on the surrounding atmosphere in the city of Hat Yai, Thailand. The particle size distributions showed a single-mode behavior in the accumulation mode while the particle size distribution in the workspace and in the ambient at Prince of Songkla University showed a bi-modal behavior. The PAH concentration for particles smaller than 3.3 micron is higher than 10^5 ng m^{-3}, while the concentration for larger particles is about 10^3 ng m^{-3}.

The effects of the condition in the combustion process, including wood type, burning rate, temperature, and wood moisture content on the particles and PAH concentration were studied by many researchers.

Oanh et al. (2005) investigated the influence of the type of fuel and type of cooking stove used in the combustion process on the physicochemical properties of the smoke particles. The PM and PAH content varied with type of cooking stove. PM emission factors for wood fuel, rice husk briquettes, and anthracite coal, were around 2-5 g kg^{-1}, 5 g kg^{-1} and 7 g kg^{-1}, respectively while the emission factors of total PAHs were 24-114 mg kg^{-1} and 140 mg kg^{-1} for wood fuel

and rice husk briquettes, respectively. The variation of PAHs was 0.08-1.64 mg g^{-1} of PM for total PAHs, 0.06-0.98 mg g^{-1} for genotoxic PAHs, and 0.001-0.147 mg g^{-1} for BaP alone.

Chao et al. (2008) investigated the influence of wood moisture content, biomass blending ratio, excess air ratio, and biomass grinding size on the physicochemical properties of the fly-ash. The concentrations of PAHs in PM10, PM2.1 and ultra fine particles were evaluated. It was reported that the reduced combustion time could improve the particle and PAH emission during the co-combustion of biomass with coal. The heating value decreased with the increase of biomass in the fuel resulting in a reduction of the combustion temperature. The moisture content in the biomass was a predominant factor for the increase of PM10 and PM2.1 emissions. However, the enlarged biomass grinding size did not significantly affect the combustion performance. Coagulation of the particles increased the PM10 and PM2.1 ratio and shifted the peak of the PM number distribution towards larger diameters as the amount of biomass increased.

1.2.2 Particulate matter bond PAHs

One of the major problems with wood combustion is the emission of gaseous pollutants such as CO, NO_x, SO_x, and solid particulate matters from incomplete combustion (Zimmerman et al., 2000). More over, toxic PAHs were released. They are detected in the gaseous phase (smoke, particulate emission), the solid phase (soot, fly ash, tars, creosote), and in the condensable liquids.

PAHs are a large group of organic compounds with two or more fused aromatic rings. They have a relatively low solubility in water while they are highly lipophilic. Most of the PAHs with low vapour pressure in the air are adsorbed on particles. Ultraviolet light from solar radiation can decompose PAHs adsorbed on particulate matters. Moreover, PAHs associated with particles in the atmosphere can be related with several air pollutants, like O_3, NO_x, and SO_2 (WHO, 1987).

PAHs are ubiquitous compounds in the environment. Emission from combustion may be through two independent ways: gas or vapor phase (smoke)

consisting of semi-volatile and volatile compounds directly from a combustion facility, and solid or particulate phase (fly ash, soot) emitted and then evaporated or dissipated into the environment (Khalili et al., 1995 and Liu et al., 2002). A number of studies have been focused on the anthropogenic sources of PAHs. As product of incomplete combustion, PAHs are commonly found in coal tars and petroleum residues (Wise et al., 1988, Wornat et al., 1999, and Harvey et al., 2002), wood emission and biomass combustion (Kamen et al., 1985, Lee et al., 2000, Fine et al., 2001, Hay et al., 2003, and Hedberg et al., 2002).

The effects of emission source, distance from source, temperature, wind direction, season, and precipitation on the physicochemical properties of aerosol particles were studied by many researchers.

Odabasi et al. (1999) measured the concentration of PAHs in Chicago air between June and October 1995 using a modified high-volume sampler (PS-1 sampler) to collect airborne PAHs in both particulate and gas phases. From their report, the particle/gas phase distribution varied widely. PAHs in gas phase ranged from 1.1 to 99.4% and generally decreased with increasing molecular weight. Moreover, the amount of PAHs associated with the particulate phase increased with decreasing temperature.

Venkataraman et al. (1999) studied PAH size distribution of urban aerosol in Mumbai, India, by using an eight-stage Anderson impactor. Bimodal size distribution was obtained with a predominance of non-volatile PAH species in the fine mode and semi-volatile PAH species in the coarse mode.

Martinis et al. (2002) measured PAH concentration in airborne particles (PM10). A high-volume air sampler with a size-selective inlet was used to collect samples from urban site of Sao Paulo City, Brazil, during February-May 1994. Samples were Soxhlet extracted sequentially with dichloromethane and acetone, followed by solid phase fractionation. PAHs were analyzed by gas chromatography/mass spectrometry and *Salmonella* microsuspension bioassay. Results showed that the concentration of the individual PAHs ranged from 0.8 ng m^{-3}

for perylene to 12.8 ng m^{-3} for benzofluoranthene. The total PAH concentration was found to be 95.5 ng m^{-3}. Contribution from wood combustion to atmospheric aerosol was concluded.

Park et al. (2002) measured the concentration of PAHs in ambient particles from urban site in Seoul, Korea, during October 1998 and December 1999. The chemical characteristics, seasonal variation, and emission source of PAHs were examined. PAHs on particles were extracted using dichloromethane with ultrasonication and supercritical fluid extraction method. PAHs were analyzed by GC/MSD/SIM. A one-way analysis of variance (ANOVA) was conducted to determine temporal variations in daily average PM2, particulate-phase PAHs, and total PAH concentration. The results of the analysis showed that the PM2.5 level was not statistically different for each season, while clear seasonal trends were seen for particulate-phase PAHs and total PAH concentration. Moreover, temperature and PAHs showed a moderate level of negative correlation, the higher temperatures were associated with lower PAH concentrations. In addition, the influence of gas pollutants on the concentration of PAHs was studied. The relationship between particulate PAHs and O_3 concentration showed a negative correlation. While the relationship between particulate PAHs and NO_2 was a positive correlation. The reason might be that both PAHs and NO_2 were emitted from combustion.

Duan et al. (2005) studied the difference of the size distribution of PAHs between urban and rural sites in Guangzhou, China. The MOUDI sampler was used to study the size distribution of aerosol samples. The concentration of PAHs was analyzed by gas chromatography with mass selective detection (GC-MS). Different PAH size distribution models were found for urban locations and a suburban location. This can be explained by three mechanism controlling the size distribution of PAHs, such as the adsorption on available aerosol surface area for 5-7 ring PAHs, absorption in available aerosol organic mass for all PAHs, and multilayer adsorptive accumulation on the coarse mode aerosols for 3-4 ring PAHs. Otherwise the change in the ratio of total PAHs/TSP depended on the sampling period (season).

Poppi and Silva (2005) measured the concentration of PAHs in ambient air of Campo Grande City, Brazil. Particle-bond PAHs were collected on PTFE filter and gas-phase PAHs were collected in a sorbent tube with XAD-2 resin. PAHs were extracted with a dichloromethane/methanol ratio 4:1 v/v and analyzed by using gas chromatography-mass spectrometry (GC-MS). Total PAH concentrations were in the range of 8.94-62.5 ng m^{-3} with an average of about 21.05 ng m^{-3}. In addition, the source of the emission of PAHs in atmosphere was investigated by using molecular diagnostic criteria and found that biomass burning (e.g. wood fuel) from the rural zone was the main source of PAHs in the atmosphere.

Rehwagen et al. (2005) studied a profile of PAHs bound to air dust from industrial and controlled areas in La Plata, Argentina and Leiplzig, Germany. PAH distribution in inhalable and respirable particulate matters was investigated. A high volume cascade impactor was used to separate six size fractions of particles. PAH concentration was analyzed with HPLC/UV/fluorescence detection. The results showed that the size distribution of particles demonstrated the greater relevance of smaller particles. Moreover, the BgP/InP ratio was lower in winter than in summer in both places. This ratio indicates the main sources of PAHs from wood burning in domestic.

Tsapakis et al. (2005) studied the influence of source and ambient temperature on the gas/particle concentration and distribution of PAHs in an urban region of Heraklion, Greece. An artifact-free sampling device was used to collect particles. Total concentration (gas and particulate) of PAHs ranged from 44.3 to 129.2 ng m^{-3} with a mean concentration of 79.3 ng m^{-3}. Total PAH concentrations in gas phase showed no observable seasonal variation. In contrast, the PAHs in particulate phase depended on seasonal variation. Moreover, higher PAH concentrations in the particulate phase were observed in winter than in summer.

Vasilakos et al. (2006) studied the influence of meteorology on gas/particle PAH phase in the atmosphere from suburban areas in Athens, Greece during June and November 2003. The results of the analysis showed that PAHs were

positive correlated with NO, NO_2, O_3, wind speed, wind direction and temperature. One of the main sources of PAHs during studied period was wood burning in a nearby agricultural area.

1.2.3 Health effect of wood smoke and particle-bond PAHs

A lot of interest has been drawn in the study of PAHs because of its mutagenic and carcinogenic effects (Agency for Toxic Substances and Disease Registry (ATSDR), 1990 and 1995). In general, PAHs are a group of over 100 different chemicals. Some of the PAHs are lighter (low molecular weight) and can evaporate into air (PAHs in gas phase). These PAHs decompose by reacting with sunlight and other chemicals in the air. This generally takes days to weeks. The more sunlight, the quicker these PAHs will decompose. Low molecular weight PAHs (2-3 rings) are less toxic to humans and not carcinogenic. While heavier PAHs (higher molecular weight, more than 4 ring PAHs) do not dissolve in water, but stick to solid particles (PAHs in particulate phase) and settle to the sediment in bottom of lakes, rivers, or streams. These PAHs stick to soil and sediment and will generally take weeks to months to break down in the environment. Microorganisms in soil and sediment are the main cause of break down. These heavy PAHs are carcinogenic to lab animals and may be carcinogenic to humans (ATSDR, 1990 and 1995).

Since smoke from wood burning contains a large number of chemicals and fine particles, which can affect both the lungs and the heart. Wood smoke may be a significant source of fine particle pollution.

Many researchers have studied the health effects of residential wood combustion (RWC) on humans, both in indoor and outdoor environments, and found that smoke from wood-burning stoves and fireplaces comprise a complex mixture of gases and particles. The size of particles is directly linked to their potential for causing health problems. Sizes of wood smoke less than 10 μm in diameter pose the greatest problems, because the particles in this size range can get deep into the lungs. In addition, fine particles with 2.5 μm in diameter and smaller than 2.5 μm can affect both lung and heart.

Heuman et al. (1991) studied the lung function of 410 schoolchildren in Klamath Falls, OR. During winter in high- and low-exposure areas. PM10 level in the high exposure area ranged 50 to 250 μg m^{-3}. In contrast, low exposure level area ranged from 20 to 75 μg m^{-3} and found that the lung function decreased during the wood-burning season for the children in the high-exposure area only.

Tesfaigzi et al. (2002) investigated the potential respiratory health responses to subchronic wood smoke exposures in a Native American community in New Maxico. The experiment used Brown Norway rats for exposure to air as control, 1 or 10 mg m^{-3} of smoke particles from *pinus edulis*. The wood smoke consisted of fine particles (<1 μm); the particle-bound materials primary composed of carbon and a majority of identified organic compounds. The result showed that the severity of alveolar macrophage hyperplasia and pigmentation increased with smoke concentration.

1.3 Scopes and Research Objectives

The characteristics of smoke particles from the rubber-wood combustion and their influences on workplace environments and surrounding atmosphere are studied. Concentration, size distribution, and chemical components are evaluated for particles sampled at different sites in Hat Yai, Thailand, including emission source, workplace area at Saikaw rubber cooperative, and ambient air at Prince of Songkla University. The objectives for this work are:

1. To study the physical and chemical characteristics of smoke particles from rubber-wood combustion in rubber smoking process.
2. To evaluate the effect of wood moisture content and burning period on PM and emission of particulate-phase PAHs from rubber-wood combustion.
3. To evaluate the effect of wood combustion and meteorological parameter on the PM and PAH concentration of particles sampled at workplaces and surrounding atmosphere (Hat Yai).

CHAPTER 2
THEORY

2.1 Ambient aerosol

Aerosol is a system of airborne particles suspended in gas medium, one generally considers the gas properties and flow dynamics first and then evaluates how individual particle follows or deviates from the gas motion. The difference in trajectories between particles and gas molecules is the basis for many aerosol particle size measurement techniques. It is also the basis for many devices controlling aerosol contaminants and for techniques manipulating aerosol particles for manufacturing purposes. Changes in gas properties generally affect the particle trajectories.

As an example, one may appreciate the need for dealing with air flow characteristic first by asking how much aerosol deposition will occur 50 km from an aerosol-emitting power plant. The wind velocity determines the speed with which the aerosol is transported away from the power plant. Large particles gravitationally settling in a shorter time than available for transport to the 50 km distant site will not be found at the receptor site. The mechanism of settling and dispersion is determined by the degree and mode of turbulence. Returning to aerosol measurement principle, a commonly used instrument, the horizontal elutriator, size-selectively removes particles in a horizontal flow channel. Here, the gas flow is generally "well behaved" by the careful avoidance of air turbulence.

Most of the world's data on suspended particle mass concentration are obtained by drawing a measurable volume of air through a particle-efficient filter over a 24 h period. The filter is weighed in a temperature-and humidity-controlled laboratory before and after sampling to determine the particle deposit. The deposit weight is then divided by the sample volume to determine the particle mass concentration. The U.S. Environmental Protection Agency (EPA) has designated federal reference methods (FRMs) for total suspended particulate (TSP), PM-10, and PM-2.5 (mass of particles with aerodynamic diameters less than approximately 40 μm,

<10 μm, and <2.5 μm, respectively), applying this method to determine compliance with national ambient air quality standard (NAAQS).

2.2 Ambient air sampling

Goals for ambient sampling for suspended particulate matter include (1) determining compliance with air quality standard; (2) evaluating the extent and causes of high mass concentration, deposition, and visibility impairment; (3) enhancing understanding of the chemical and physical properties of atmospheric pollution; (4) apportioning the chemical constituents of suspended particulate matters to their emitting source: and (5) evaluating adverse health effects. A sampling system that serves one objective does not necessarily meet the needs of other objectives. Most notably, filter samplers designed to determine compliance with mass based air quality standards have limited applicability to sampling for chemical characterization, hourly and daily sequential sampling, quantification of volatile aerosol, and particle sizing.

2.3 Workplace air sampling

Aerosol sampling in the workplace is ultimately concerned with measuring aspect of the aerosol that leads to specific health effects. Thus, the method and metric used aims to provide biologically relevant information. Aerosol particles can cause health problems when deposited on the skin and eyes, but generally the most sensitive route of entry into the body is through the respiratory system. The biological effects resulting from deposition of aerosol in the respiratory tract will depend on the dose received and the body's response to the deposited particles. Physiological response to aerosol depends on the chemical and physical nature of the particles and the location of the interaction (i.e., deposition region). The ultimate goal of industrial hygiene aerosol measurement is therefore to ascertain the dose of aerosol delivered to the body and to evaluate whether the dose or potential dose is sufficient to cause adverse health effects.

Many instrument types have been used in the workplace (Mark et al., 1984). A cascade impactor is often the instrument of choice, giving an indication of the mass-weighted size distribution of aerosol. Impactors are generally capable of giving the size distribution of aerosol between a 0.1 and 15 μm aerodynamic diameters and above. Static cascade impactors, such as the Andersen eight-stage impactor and the Micro Orifice uniform deposit Impactor (MOUDI) have found relatively widespread use in the workplace. The Andersen consists of eight multi-orifice stages with cut points between 10 and 0.4 when operated at 4.72 x 10^{-4} m^3 s^{-1} or 28.3 L min^{-1} as show in Fig. 2.1. Collection is usually onto aluminum foil, although other substrates are available. The use of multi-orifices in the Andersen impactor allows deposits to be distributed with relative evenness onto substrates. This is taken further within the MOUDI, where many orifices per stage, together with rotating substrates, lead to highly uniform deposits. The MOUDI is available in an 8- or 10-stage version and is capable of making aerosol size distribution measurements down to 0.056 μm at 5x 10^{-4} m^3 s^{-1} [30 L min^{-1}].

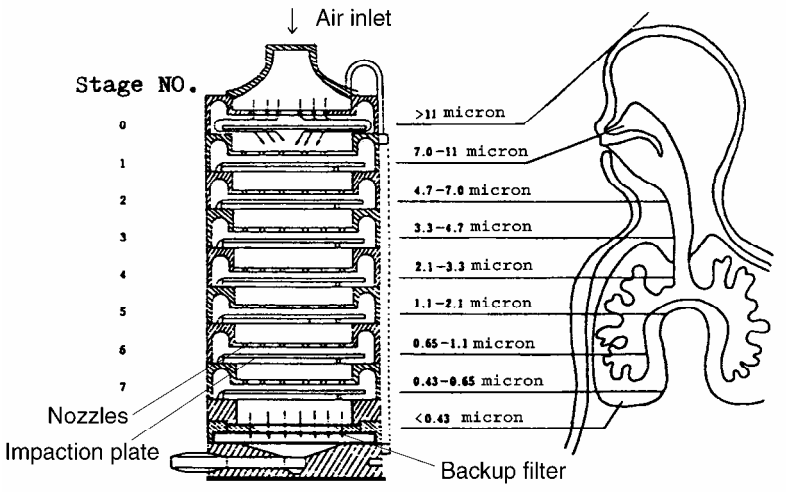

Figure 2.1 An eight- stage Andersen impactor.

Sampling strategy

While “static” or “area” sampling with fixed point samplers is still used in many situations, it is now widely accepted that representative aerosol sampling in the workplace should be carried out in the breathing zone - frequently defined as a region of the body not more than 0.3 m from the mouth and nose (Vincent et al., 1995). Breathing zone measurements generally give a better representation of the workers exposure. However, Vincent noted that the placement of sampling devices in this region does not guarantee representative sampling, and that large variations of sampled aerosol concentration can be seen across the front of the body, depending on the workers orientation, placement of the aerosol source, and local air movements (Raynor et al., 1975).

2.4 Conventional impactors

The most common type of impactor consists of a single jet of particle-laden gas (aerosol) impinging on a flat plate, as shown in Fig. 2.2. Particles larger than the cut size of the impactor will slip across the streamlines and impact on the plate, while smaller particles will follow the streamlines and will not be collected. The most important impactor characteristic is the collection efficiency curve. The collection efficiency (as a function of particle size) is defined as the fraction of particles passing through the nozzle that are collected on the impaction plate. The ideal impactor has a perfectly sharp efficiency curve, which means that, all particles larger than the cut size of the impactor are collected on the plate, while all smaller particles follow the gas flow out of the impaction region.

A nozzle and an impaction plate constitute a single-stage impactor that is useful when classifying particles into two size fractions. For example, this is the case when analyzing particles that are less than 10 μm (PM10) or less than 2.5 μm (PM2.5). In these types of impactors, the particles larger than the cut size are removed from the air stream, while the smaller particles penetrate the impactor stage to be either colleted on a filter, where they can be analyzed (e.g., for mass

concentration or elemental composition), or passed into some other instrument for real-time mass or number concentration measurement.

Often, it is desirable to determine the entire size distribution of the aerosol and not just the quantity less than a certain size. In this case, a series of impactor stages are used in a cascaded fashion such that the gas passes from one stage to the next, as shown in Fig. 2.3 to remove particles in discrete size ranges (Londge and Chan, 1986). This is known as a cascade impactor and is widely used for determining size distribution of aerosols.

A cascade impactor makes use of the fact that particle collection is governed by the Stokes number. The velocity of the particle-laden gas stream is increased in successive stages, resulting in the collection of successively smaller particles in the subsequent stage. For example, if a four-stage cascade impactor has a cut-size of 10, 5, 2.5, and 1.25 μm, the first stage will collect particles larger than 10 μm, the second stage will collect particles between 5 and 10 um, the third stage between 2.5 and 5 μm, and the fourth stage between 1.25 and 2.5 μm. Particles less than 1.25 μm penetrate the final stage of the impactor and can be collected on an after-filter.

The particles deposited on the impaction place can be evaluated by a variety of methods. A few of the more common methods are: (1) the particles are collected on glass plates, membrane filters, or foils and are inspected or counted under a microscope; (2) the particles are collected on foils and weighed to determine the mass of particles at each stage; (3) the particles are collected on quartz crystals, and the mass of particles is determined by the change in the natural frequency of the crystals (Fairchid and Wheat, 1984); (4) the particles are charged before passing though the impactor, and the current is measured at each impaction place to determine the number of particles being collected (Keskinen et al., 1992). The first two methods provide size distribution data integrated over time, while the latter two methods provide size distribution data in near real time.

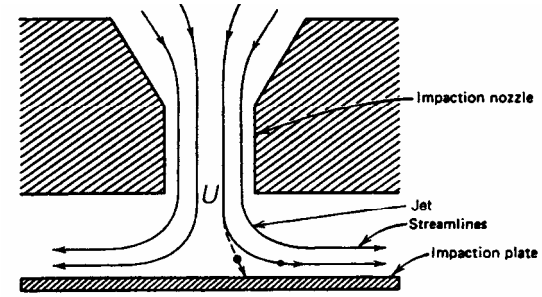

Figure 2.2 Schematic diagram of a conventional impactor (Willeke, 2001).

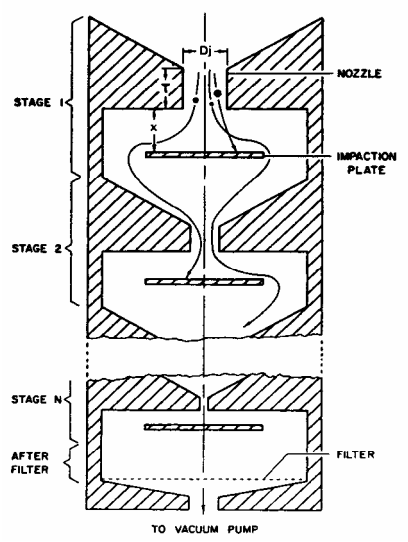

Figure 2.3 Schematic diagram of a cascade impactor (Willeke, 2001)**.**

2.5 Polycyclic aromatic hydrocarbons

Polycyclic aromatic hydrocarbons (PAHs) are a group of hydrocarbon compounds containing fused aromatic rings with synonyms polynuclear aromatic hydrocarbons, arenes, or polyarenes. There are 1896 possible structures for PAHs containing two to eight rings. Chemical transformation of PAHs in the environment results in the formation of homocyclic and heterocyclic derivatives of PAHs containing nitrogen, oxygen, or sulfur atoms. When combined with PAHs, this larger group of aromatic compounds are referred to polyaromatic compounds (PACs). Fig. 2.5 shows the molecular structures of the sixteen PAHs or EPA16, which have been

designated by the United States Environmental Protection Agency (USEPA) as priority pollutants. Compounds marked with an asterisk (*) have been selected by the European Union (EU) for monitoring.

Anthropogenic input of PACs to the environment stems from incomplete combustion of fossil fuels, waste incineration, and industrial operations, such as coke oven and aluminum smelter operations. In addition, motor vehicle emissions may contribute up to 35% of PAHs input to the environment in industrialized countries. PAHs are also produced when foods, especially meats, are cooked at high temperatures by smoking, roasting, or grilling. Leachate from oil and coal products, including asphalt and creosote, used as a wood preservative, can contain high level of PAHs. Except for spills and leaching, anthropogenic PAHs enter the environment as air pollutants and are transported over time in to water, soil, sediments, and biota. Forest fires, volcanic eruptions, and soil diagenesis (primarily perylene) are the greatest natural source of PACs.

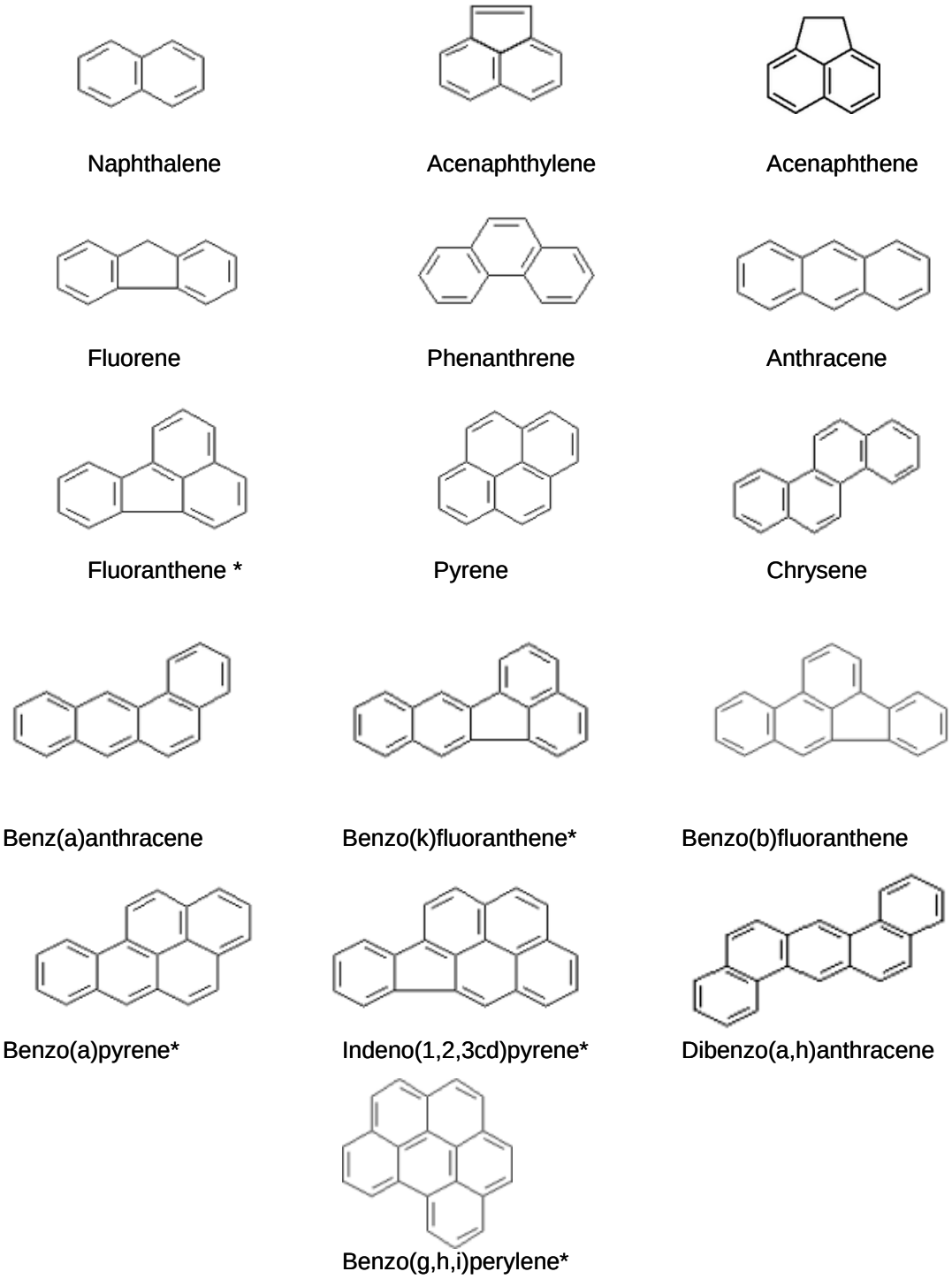

Figure 2.4 Structures of sixteen PAH compounds (EPA_{16}), *European Union priority pollutants (EU_6). (http:// www.ecochem.biz/PAH/pah_primer.htm).

2.5.1 Physical properties

The physical properties of selected PAHs is shown in Table 2.1. The vapor pressure of PAHs decreases over 11 orders of magnitude as the number of fused rings increases from two to seven order. Because of naphthalene's high vapor pressure, it tends to partition to a greater degree into the vapor phase in the environment. Larger PAHs (3- and 4-rings) will partition between the gaseous and solid phases in the environment. PAHs with five or more aromatic rings are found almost exclusively associated with particulate or solid phases. Water solubility of PAHs with two to six-rings decreases over five orders of magnitude with increasing molecular weight. Therefore, 2- and 3-ring PAHs are more likely to be found in aquatic environments, in dissolved organic matter (DOM), and in solid phases such as soot. The tendency of PAHs to accumulate in soil, sediments, and biota also increases with the size of the molecule. Since chromatographic separations are primarily based on differences in physical properties, the considerable variability described above for PAHs makes sampling, sample preparation, and especially analysis challenging. When several PAHs are measured as a group, a single sample collection, extraction or analysis method may not be adequate. This is further complicated when the more polar derivatives of PAHs are added to the list of compound to be analyzed.

PAH concentrations in various envious environmental compartments depend on the proximity of emission source, meteorological conditions, seasons, and the physical properties of the compounds themselves.

Table 2.1 Physical Properties of selected PAHs.

Compound	Abbreviation	MW ($g\ mol^{-1}$)	MP (°C)	BP (°C)	VP (Pa)	S ($g\ m^{-3}$)
Naphthalene	Nap	128	81	218	10.4	31
Acenaphthene	Ace	152	96	278	$3x10^{-1}$	38
Acenaphthylene	Act	154	92	265	$9x10^{-2}$	16
Fluorene	Fle	166	116	295	$9x10^{-2}$	1.9
Anthracene	Ant	178	216	340	$1x10^{-3}$	0.045
Phenanthrene	Phe	178	101	339	$2x10^{-2}$	1.1
Fluoranthene	Flu	202	111	375	$1.2x10^{-3}$	0.26
Pyrene	Pyr	202	156	360	$6x10^{-4}$	0.13
Benz[a]anthracene	BaA	228	160	435	$2.8x10^{-5}$	0.011
Chrysene	Chr	228	255	448	$5.7x10^{-7}$	-
Benzo[b]fluoranthene	BbF	252	168	481		0.0015
Benzo[k]fluoranthene	BkF	252	217	481	$5.2x10^{-8}$	0.0008
Benzo[a]pyrence	BaP	252	175	495	$7x10^{-7}$	0.0038
Indeno[1,2,3-cd]pyrene	IDP	276	164	536	-	0.00019
Benzo[ghi]Perylene	BghiPe	276	277	-	-	0.00026
Dibenz[a,h]anthracene	DBA	278	267	524	$3.7x10^{-10}$	0.0006

Note: MW = molecular weight, MP = melting point, BP = boling point, VP = vapor pressure of the solid, S = water solubility (Leo, 2006).

2.5.2 Environmental transformations and toxicity

PAHs are generally unreactive and have low acute toxicities, but degraded and biotransformed products of PAHs can be very potent mutagens and carcinogens. PAHs may induce cancer of the lungs, bladder, and skin. Several PAHs have been classified by the International Agency for Research on Cancer (IARC) as probable human carcinogens. Exposure to high levels of PAHs has been shown to produce immunosuppressive effects.

PAHs require metabolic activation to produce their mutagenic or carcinogenic effects. The primary mechanism of PAH biotransformation in higher organisms is by cytochrome P450-based monooxygenases leading to detoxification and excretion. However, an attack by cytochrome P4501A1 can activate certain PAHs, such as BaP to form a mutagenic diol epoxide capable of forming DNA

adducts. The carcinogenesis of nitro-PAHs involves ring oxidation and nitro-reduction to form N-hydroxyamino-PAH intermediates that can bind with DNA. The formation of hydroxyl-PAH metabolites allows PAHs to be excreted by higher organisms. PAHs can be bioconcentrated or bioaccumulated in aquatic invertebrates such as mollusks that do not posses the ability for their biotransformation, while fish can effectively biotransform PAHs, preventing biomagnification up the food chain.

2.5.3 Regulations

There are no specific regulations limiting PAH levels or emissions in the atmosphere, although USEPA and the EU have set limits on the amount of particulate matter (PM) in ambient air. This provides indirect regulations for PAHs, since most are so strongly associated with atmospheric particles. The EU Working Group on Polycyclic Aromatic Hydrocarbon is currently assessing the need for a PAH atmospheric monitoring program. The U.K. Expert Panel on Air Quality Standards (EPAQS) has recommended an annual of 0.25 ng m^{-3} using BaP as a marker.

Risk assessment for PAHs is complicated by a lack of understanding of the cancer potency of PAH mixtures. Toxicity equivalency factors (TEFs) have been determined for many PAHs relative to BaP. The concentration of PAH x TEF for each individual PAH gives a concentration known as the BaP equivalent. Since the background level of PAH is generally below 1 mg kg^{-1} for most rural sites, USEPA remediation goals are usually set at that level for BaP equivalents, and 10 mg kg^{-1} for industrial sites or well-vegetated areas, where human contact with soil is less likely. The EU has set limits for Flu, BbF, and BaP of 5, 2.5, and 2 mg kg^{-1}, respectively, in sewage sludge to be spread on agricultural land (Leo, 2006).

2.5.4 Ultrasonic extraction

Ultrasound-assisted extraction (USE) is a solid-liquid leaching technique done in the batch mode. Solvent is added to samples before they are placed in a sonication bath. The procedure is usually repeated two or three times for quantitative extraction. Ultrasonication produces very localized, extremely high effective temperatures that increase the extraction efficiencies of the solvents, and it is

inexpensive and fast. Combined extracts are centrifuged or filtered, cleaned up, and concentrated by an evaporator before the analysis.

CHAPTER 3
EXPERIMENT

The objectives of this work were to study the characteristics of smoke particles from the rubber-wood combustion and to estimate their air pollution effect in the workplace environments and the surrounding atmosphere. The experimental method was designed to investigate evolution of concentration, size distribution, and chemical components of particulate samples.

3.1 Chemicals

3.1.1 Standard chemicals

EPA 610 Polycyclic Aromatic Hydrocarbons Mix (certified solution with purity 98.5%-99.9%, Supelco, USA)

Acenaphthane	: 1000 μg mL^{-1}
Acenaphthylene	: 2000 μg mL^{-1}
Anthracene	: 100.0 μg mL^{-1}
Benz (a) anthracene	: 100.2 μg mL^{-1}
Benzo (a) pyrene	: 100.2 μg mL^{-1}
Benzo (b) fluoranthene	: 200.0 μg mL^{-1}
Benzo (g, h, i) perylene	: 200.2 μg mL^{-1}
Benzo (k) fluoranthene	: 100.0 μg mL^{-1}
Chrysene	: 100.0 μg mL^{-1}
Dibenz (a,h) anthracene	: 200.2 μg mL^{-1}
Fluoranthene	: 200.0 μg mL^{-1}
Fluorene	: 200.0 μg mL^{-1}
Indeno (1, 2, 3-cd) pyrene	: 100.1 μg mL^{-1}
Naphthalene	: 1000 μg mL^{-1}
Phenanthrene	: 100.2 μg mL^{-1}

Pyrene : 100.2 μg mL^{-1}

3.1.2 Chemicals for PAH extraction

Acetonitrile (HPLC grade, Lab-scan, Thailand)
Ethanol (AR grade, Merck, USA)
Benzene (AR grade, Merck, USA)
DMSO (HPLC grade, Merck, USA)

3.1.3 Chemicals for NO_2 extraction

Phosphoric acid (AR grade, Merck, USA)
Sulfanilic acid (AR grade, Merck, USA)
N-(1-Naphthy) ethylene diamine dihydrochloride (AR grade, Merck, USA)

3.1.4 Chemicals for HPLC assay

Ultra pure water (H_2O, water was de-ionized with reverse osmosis system and purified with a Maxima ultrapure water instrument to obtain the resistivity of 18.2 MΩ, ELGA, England)
Acetonitrile (HPLC grade, Lab-scan, Thailand)

3.2 Instrumentation

3.2.1 Samplers

High volume sampler model HV500F (Sibata, Japan)
Andersen sampler model AN200 (Tokyo Dylec, Japan)
Source high volume sampler (modified in the laboratory)
Personal passive sampler NO_2 (Advantec, Japan)

3.2.2 Apparatus used for filter extraction

Ultrasonic bath model 2800 HT (Tru-sweep, London)

Vacuum Pump (Buchi, Swizerland)

Rotary evaporator (Buchi, Swizerland)

PTFE Syringe filter, pore size 0.45 μm, diameter 25 mm and 13 mm (Vertical, Thailand)

Filter paper, No 42, diameter 125 mm (Whatman, USA)

PTFE membrane disc filter, pore size 0.45 μm, 47 mm diameter (Vertical, Thailand)

Nylon membrane disc filter, pore size 0.45 μm, 47 mm diameter (Vertical, Thailand)

Disposable syringe 1 mL (Vertical, Thailand)

Five-digit readability analytical balance model CP225D (Sartorius, Germany)

Amber vial 2 mL with polypropylene screw cap blue and white silicone/red PTFE septa (Vertical, Thailand)

Amber vial 20 mL with polypropylene cap (Wheaton, USA)

Microlitre pipette : model NPX-200, 50-200 μL (Nichiryo, Japan)

General glassware, such as round bottom flask 100 mL: volumetric flask 100 mL ; 50 mL.

3.2.3 Apparatus used for HPLC assay

High-performance liquid chromatography with UV detector (HPLC-UV) model 1100 (Agilent, USA) consists of a pump model 1311A (Agilent, USA), autosampler model G1313A (Agilent, USA), degasser model G1322A (Agilent, USA), photodiode array detector model G1315A (Agilent, USA), Chemstation software (Agilent, USA), and computer system (Hewlette Packard, USA). Reverse phase HPLC was performed using Vertisep C18 (250 x 4.6 mm I.D., particle size 5 μm) column with a Vertisep C18 (7.5 x 4.6 mm I.D., particle size 5 μm) guard column.

3.2.4 Apparatus used for NO_2 analysis

UV-vis spectrophotometer model S100 (Analytikjena, Germany)

3.3 Methods

3.3.1. Sampling sites

Hat Yai is one of the major cities in Thailand, located in Songkhla Province. The city accommodates government offices, shopping complexes, medical, agricultural and educational institutions, industrial units and residential areas. Growing urbanization, traffic volume, commercial and industrial activities have resulted in an increasing concentration of airborne particulate matters and other gaseous pollutants. Mass measurements are generally documented, but there are few data investigating size distribution of particulate that are now becoming of interest, and even less data exist regarding the chemical composition of ambient particle aerosols.

Songkhla Province is located in the south of Thailand as shows in Fig. 3.1. The climate of Songkhla is humid sub-tropical. The weather is under the Asian monsoon system, which is characterized by a marked change of wind direction, temperature, humidity and rainfall of each month. During January to April, the wind direction is from east-northeast, while the wind direction during May to October is from west-southwest. During November-December when the precipitation is highest, the wind direction shifts back to from the northeast direction. The wind direction pattern for the whole year is shown in Fig 3.2 (a). The wind pattern affects the transport of aerosol particles in the atmosphere. The stability of the weather conditions and the ability to disperse particles are factors that profoundly influence the air quality of urban areas in Hat Yai. Beside the wind, the mass concentration is also affected by rainfall and relative humidity.

Particulate matter (PM) and gas samples were collected every month for one year from three different sites, workplace (WP) and source (S) in Saikaw rubber cooperative, and a background at Prince of Songkla University, PSU. Fig. 3.2 (b) shows the locations of the sampling sites in Songhkla Province.

The Saikaw rubber cooperative, around 20 km east-northeast of Hat Yai city, was chosen as a sampling location for studying the characteristics of smoke particles emitted from rubber-wood combustion. There are three sampling sites in the rubber cooperative, including a smoking room for source sampling and two workplace areas, workplace sampling site 1 and workplace sampling site 2, as shown in Fig. 3.3 (a). Fig. 3.3 (b) shows the rubber-wood burning furnace and Fig. 3.4 shows the experimental set up for source sampling. For the workplace sampling site 1 is about 2-m above the ground floor near a wall at the front of the workplace, and workplace sampling site 2 is about 2-m above the ground floor over the workspace area in the middle of the cooperative as shown in Fig. 3.5 and Fig. 3.6.

The Prince of Songkla University (PSU), located in the northeast of Hat Yai city, was chosen for investigating the influences of smoke particles from rubber wood combustion to Hat Yai. This site is representative for a complex mix of pollutants. The site is in the downwind direction of most of the Rubber cooperatives. During May to October the wind direction is from southwest and the pollutants from there can be transport to PSU. Therefore, PSU was chosen as a receptor for smoke particles from rubber wood burning from rubber cooperative in Songkhla Province.

Figure 3.1 Location of Hat Yai City in Songkhla Province in the south of Thailand.

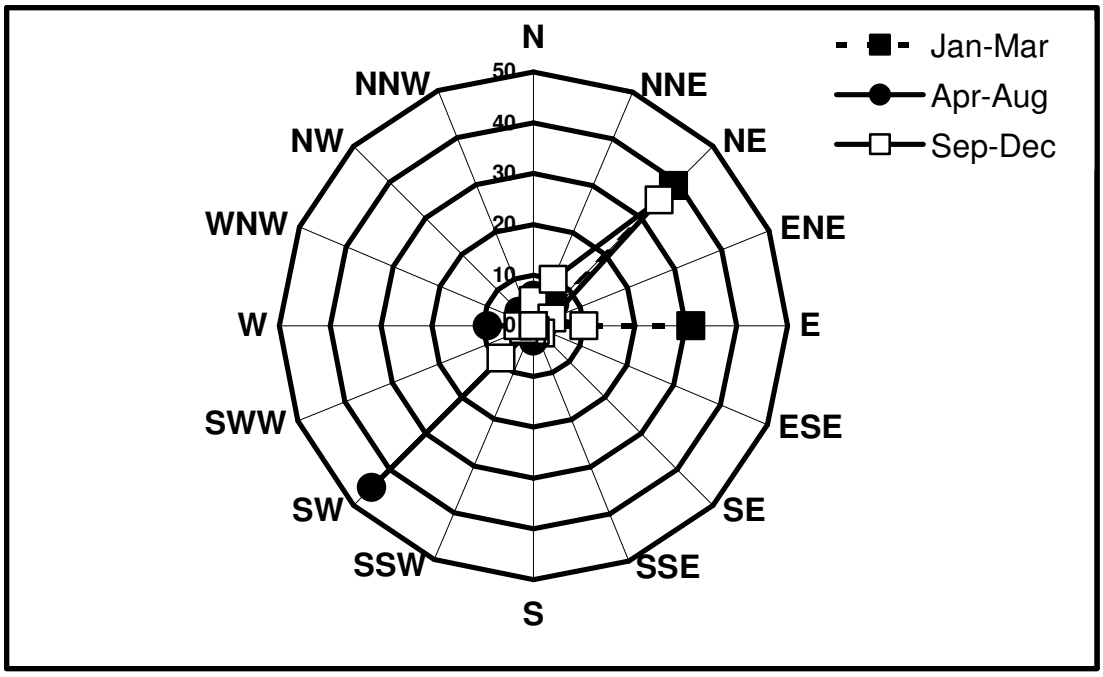

(a)

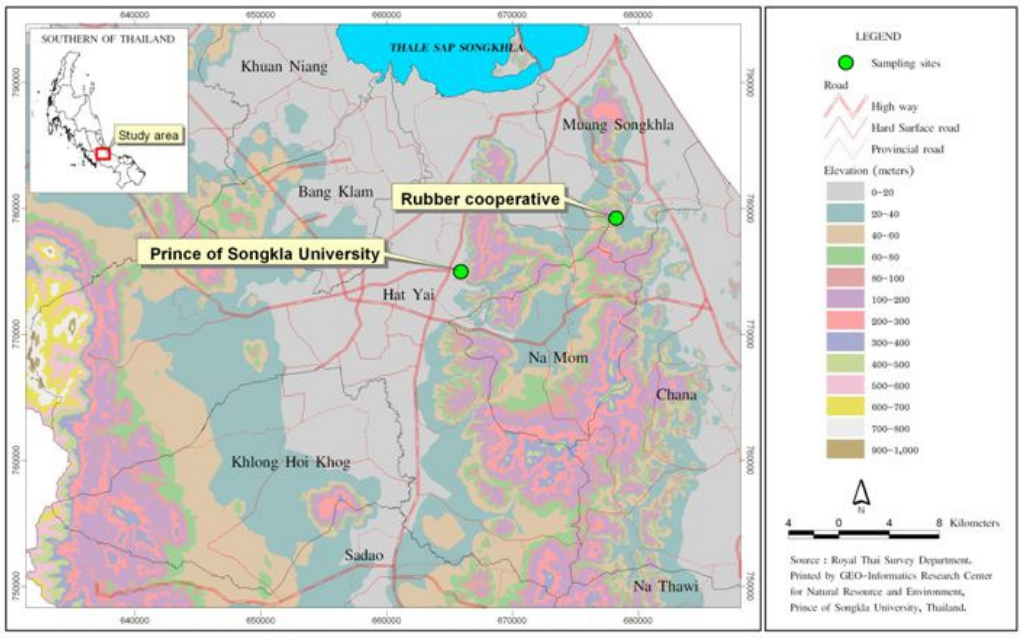

Figure 3.2 (a) Wind direction patterns of Hat Yai. **(b)** Location of sampling sites in Songkhla Province.

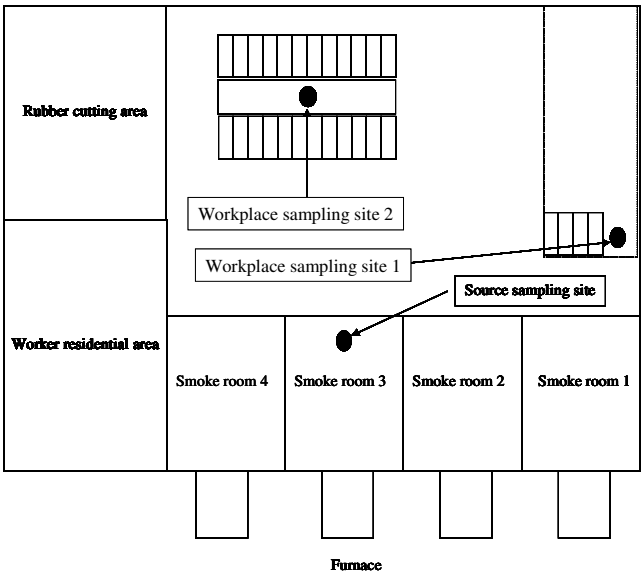

(a)

(b)

Figure 3.3 (a) Plan view of a rubber cooperative and sampling positions. (b) Photograph of rubber wood burning furnaces**.**

Figure 3.4 Photograph of source sampling and smoking rooms in Saikaw rubber cooperative.

Figure 3.5 Photograph of workplace sampling site 1 (WP1)**.**

Figure 3.6 Photograph of workplace sampling site 2 (WP2).

3.3.2 Sampling methods

Particulate matter (PM) has been sampled by three equipment sets: total suspended particulate (TSP) concentration was determined by a commercial high volume sampler and source high volume sampler, while PM size distribution of samples was obtained using a cascade impactor. Gas NO_2 was sampled using a passive gas samplers.

Treatment of filters

First the test filters were treated in the desiccator at room temperature (25°C) and 50-60 % relative humidity for at least 72 hours. They were then weighed using the five-digit readability analytical balance (Sartorius, CP225D). Quartz fiber filter (ADVANTEC, QR-100) with 110 mm-diameter was used for collected TSP, while Quartz fiber filter (ADVANTEC, QR-100) with 80 mm-diameter was used for collected particle size distribution. After sampling, the filters were folded in half and separately put in a Polyethylene bag and then the filters were treated in the desiccator at room temperature (25°C) and 50-60 % relative humidity for at least 72 hours. Then the weight of the collected particles on the filter sample was measured using the identical analytical balance. The set of filter samples was kept together, wrapped with

an aluminum foil, and then kept in a polyethylene bag again. All samples were stored in a refrigerator at -20°C in order to avoid the degradation of PAHs by UV and evaporation until extraction.

Total suspended particulate matter

Total suspended particulate matter (TSP) concentration of workplace (WP) and ambient aerosol (PSU) was measured by the commercial portable high-volume sampler (Sibata, HV500F). The sampler operates at a constant flow rate of 500 $Lmin^{-1}$ for a period of 12 hours at WP and 24 hours at PSU. For both sites, the sampling was carried out one time/week for one year, during January 2006-January 2007. Particles were collected on identical-type quartz fiber filter (ADVANTEC, QR-100) with 110-mm-diameter. Photographs of the quartz fiber filter (diameter 110 mm) and the high volume sampler are shown in Figs. 3.7 and 3.8, respectively. The sampling time and sampling period for the measurements of TSP at each sampling site were summarized in Table 3.1.

Total smoke concentration

Total smoke particulate concentration from the source sampling site was measured by the modified high-volume air sampler. The identical-type quartz fiber filter (ADVANTEC, QR-100) with 110-mm-diameter was equipped with an aluminium filter holder. The smoke particles were introduced to the filter using a vacuum cleaner. The flow rate was controlled at 100 L min^{-1} by adjusting the valve and monitoring an orifice meter with corresponding U-tube manometer. The sampling period was 10 minutes in the smoking room and sampling was carried out at different burning periods, 15, 30, 60, 75, 120, and 135 minutes after the rubber-wood was fed in to the furnace.

To study the effect of wood moisture content, the experiments were carried out using different wood moisture contents. Moisture content of rubber-wood was determined using dry basis. Each piece of wood sample 6 to 10 cm in diameter

was cut as shown in Fig. 3.9 and dried in an electric oven at 110 ℃. The moisture content (MC) was determined on a dry basis, as given:

$$Moisture\ Content = \frac{M_{wet} - M_{dry}}{M_{dry}} * 100$$

Where M_{wet} is the mass of the wood samples before drying.

M_{dry} is the mass of the wood samples after drying.

The schematic diagram and photograph of the experimental setup for source sampling are shown in Fig. 3.10 and Fig. 3.11.

The TSP or total smoke concentration of each sample is determined by knowing the particulate mass collected and the total volume of air sampled, then the concentration is calculated from

$$C = \frac{M}{V}$$

Where M is the total collected mass and V is the sampling volume determined from

$$V = Q\ t$$

Where Q is the flow rate (Lm^{-1}) and t is the sample time (min).

The sampled filters from the rubber cooperative and the ambient air were also analyzed for PAHs concentration from source, workplace, and ambient air.

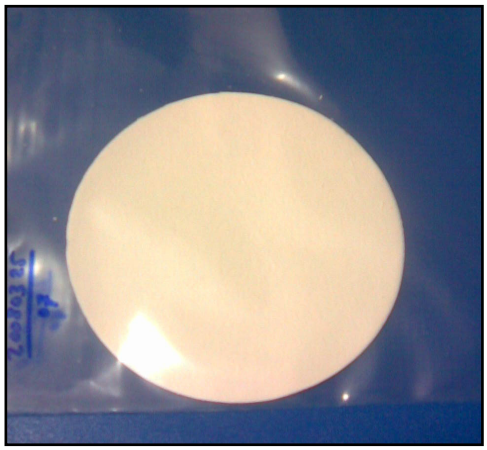

Figure 3.7 Photograph of a quartz fiber filter (ADVANTEC, QR-100) with 110-mm-diameter.

Figure 3.8 Photograph of the high volume sampler (Sibata, HV500F) used for measuring the total suspension particulate matters.

Table 3.1 Sampling time and period for TSP measurements at each sampling site.

Sampling site	Sampling time	Sampling period
WP	1/week	12 h
PSU	1/week	24 h

Figure 3.9 Photograph of the wood samples used to determine the moisture content.

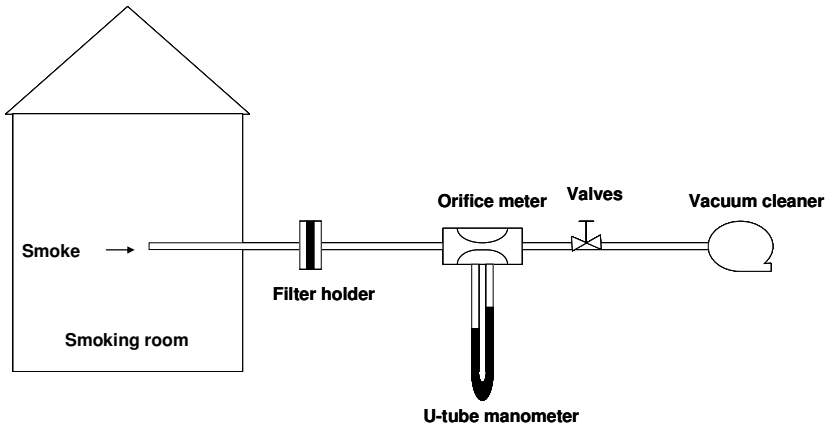

Figure 3.10 Schematic representation of the experimental set-up for measuring the concentration of total smoke particles.

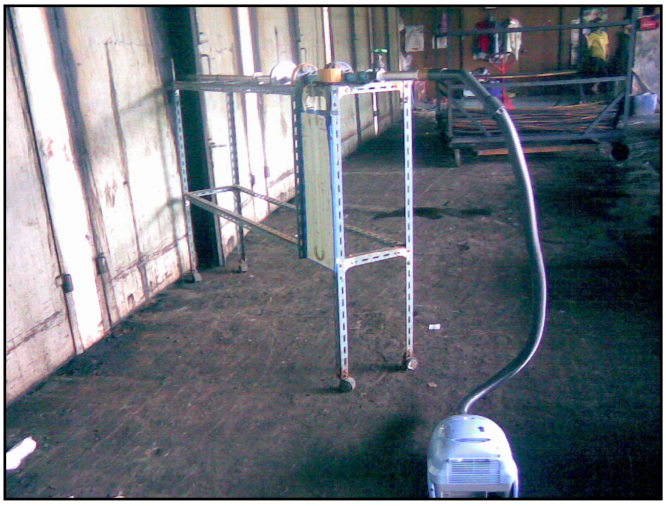

Figure 3.11 Photograph of the experimental set-up for measuring the concentration of total smoke from wood burning in smoking room.

Size distribution of particulate matter

The size distribution of particulate matter was collected by an 8-stage Andersen sampler (Dylec, AN200). The impactor has a 50% cut-off aerodynamic diameter of 11.0, 7.0, 4.7, 3.3, 2.1, 1.1, 0.65 μm for stage 1-8, respectively, and collects all particles smaller than 0.43 micron on an after-filter. The impactor was connected to a continuous duty, vacuum pump and a constant air flow rate at 28.3 L min^{-1} was controlled with an in-line rotameter. The sampling period was 3 weeks for each sample to ensure a sufficient amount of particles collected for PAH analysis (size distribution of PAHs). Particles were collected on identical-type quartz fiber filters (ADVANTEC, QR-100) with 80-mm-diameter, put on the plate of each stage in the sampler. Fig. 3.12 shows the schematic representation of the experimental set-up for measuring the size distribution of particulate matter. Figs. 3.13 and 3.14 show the Andersen sampler and the filters of each stage after sampling with Andersen sampler). The sampling time and period for measuring the concentration and size distribution of particles from each sampling site were summarized in Table 3.2.

To determine the size distribution of particulate matter samples, the normalized mass fraction $\left(f/\Delta d\right)$ was plotted as a function of the average

aerodynamic diameter, d_{ave} [µm]. Here, f is the mass fraction and Δd is the particle size interval of each stage of the Andersen sampler. Mass fraction (f) can then be calculated from

$$f = \frac{M_j}{M_{total}}$$

M_{total} is the total mass collected, calculated from

$$M_{total} = \sum_{n=1}^{n} M_j$$

Where M_j is the mass collected in each stage, calculated from

$$M_j = \left(m_f - m_i\right)$$

Where m_f is the mass of the filter after sampling and m_i is the mass of the blank filter.

The total mass concentration can then be calculated from :

$$Total \quad mass \quad concentration = \frac{M_{total}}{V_{total}}$$

Where V_{total} is the total sampling volume determined from :

$$V_{total} = Qt$$

Here Q is the flow rate and t is the sampling time.

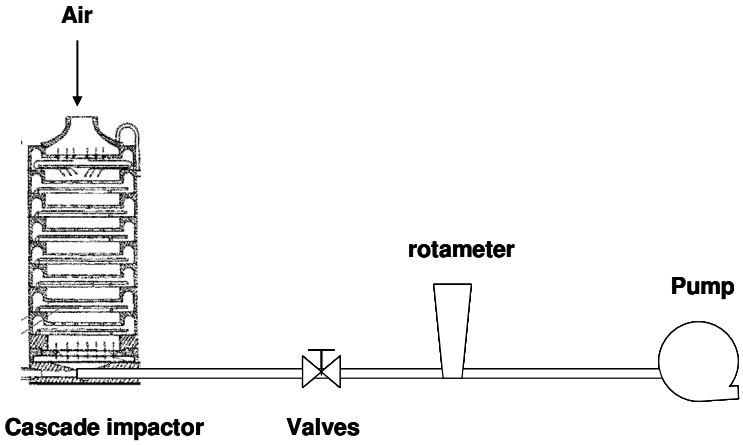

Figure 3.12. Schematic representation of the experimental set-up for measuring the size distribution of particulate matter.

Figure 3.13 Photograph of the Andersen sampler (Dylec, AN-200) used for measuring the particle size distribution.

Figure 3.14. Photograph of filters of each stage after sampling with Andersen sampler.

Table 3.2. Summary of sampling methods for each sampling site.

Sampling site	Sampling method			
	Modified high volume sampler (Total smoke concentration)	High volume sampler model 500F (TSP)	Andersen sampler (Particle size distribution)	Personal passive sampler (NO_2 concentration)
S (Source)	18	-	3	-
WP1 (workplace area)	-	1/week	1/month	2/month
WP2 (workplace area)	-	-	-	2/month
PSU (Prince of Songkla University)	-	1/week	1/month	2/month

Gas sampling method

A NO_2 personal passive sampler as shown in Fig. 3.15 (a) was used to collect NO_2 gas at both workplace (site 1, site 2) and the background (PSU) sampling sites. The filter badge was removed from the aluminum bag and immediately placed

at sampling site as shown in Fig. 3.15 (b). Sampling began as soon as the package was opened and the badge was exposed to ambient air. The badge was avoided from strong wind and high temperature. After exposure for 24 hours the badge was immediately put in the zip lock bag to terminate NO_2 sampling and kept in the aluminum bag. The analysis was performed as soon as possible to obtain the best result.

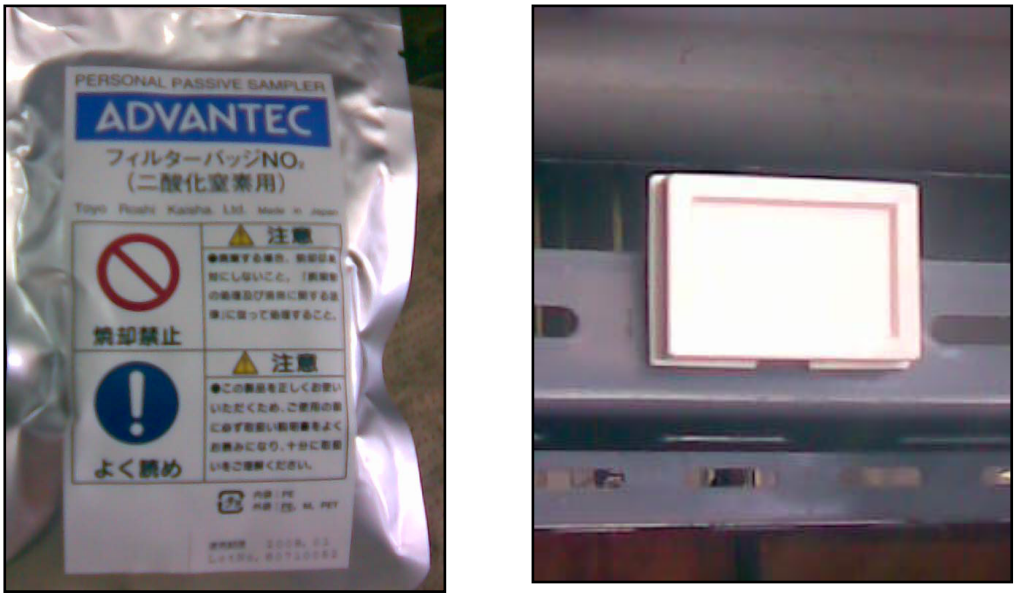

(a) (b)

Figure 3.15 Photograph of NO_2 personal passive sampler : (a) aluminum bag and (b) filter badge at sampling site.

3.3.3 Analysis of NO_2 samples

The filter inside the sampled badge was extracted and analyzed using ultraviolet spectrophotometer technique.

Extraction method

The badge case was opened by inserting a sturdy metallic blade (such as a flat-blade screwdriver) into the slot/opening in the back of the badge case. The absorption layer (filter paper) was removed from the inner frame of the badge case

and put in the vial. Then 10 mL of coloring solution was added and the vial was closed and gently shaken occasionally for 40 min.

NO_2 analytical method

The concentration of NO_2 was determined using spectrophotometer with 10 mm glass cell. The absorbance of sample solution was measured at a wavelength of 545 nm. The coloring solution was used as blank.

The concentration of NO_2 can then be calculated from

$$NO_2 = 55(I - I_o) \quad \text{ppb}$$

Where NO_2 is the concentration of NO_2 in the sample, I is the absorbance of the absorption layer after exposed and I_0 is the absorbance of the unexposed absorption layer.

Coloring solution preparation method

Coloring solution was prepared by dissolving 5 g of sulfanilic acid in 700 mL of distilled water. After 50 mL of phosphoric acid was added, the solution was mixed well. Then 50 mL of 0.1 wt% N-(1-naphthyl) ethylenediamine dihydrochloride was added and distilled water was added to total 1 L and the liquid temperature was kept at 25 to 30 $^{\circ}$C.

3.3.4 Analysis of polycyclic aromatic hydrocarbons

The 16 PAHs in the particulate matter samples, including Naphthalene(NaP), Acenaphthylene(Act), Acenaphtene(Ace), Fluorene(Fle), Phenanthrene(Phe), Anthracene(Ant), Fluoranthene(Flu), Pyrene(Pyr), Benz(a)anthracene(BaA), Chrysene(Chr), Benzo(b)fluoranthene(BbF), Benzo(k)fluoranthene(BkF), Benzo(a)pyrene(BaP), Dibenzo(a,h) anthracene(DBA),

Benzo(ghi)perylene(BghiPe), Indeno(1,2,3-cd)pyrene(IDP), were analyzed using HPLC with UV detector.

PAHs extraction method

PAHs on sampled filters were extracted using Ultrasonic extraction (USE) technique. This method was modified from the method of Tang et al. (2005). The filters were weighed for approximately 4-5 mg of particulates. They were thoroughly cut into small pieces (about 5x5 mm) and put in a 125 mL flask. The filters were extracted ultrasonically twice with 40 mL of ethanol:benzene (1:3 v/v), for 15 min each. The extracts were combined and later filtered with filter paper and 0.45 µm PTFE syringe filter as shown in Fig. 3.16 (a) and then 50 µL of DMSO was added. The solution was concentrated using a Buchi Rotary evaporator to remove ethanol and benzene, then redissolved with 450 µL of acetonitrile. Interfering compounds once again were removed by 0.45 µm syringe filter as shown in Fig. 3.16 (b). The filtrate was kept in a 1.5 mL amber glass vial, and stored in the refrigerator (-20 °C) until analyzed. Fig. 3.17 shows the diagram of the extraction procedure.

(a) (b)

Figure 3.16 Photograph of (a) PTFE syringe filter 25 mm in diameter and (b) sample filtration set-up.

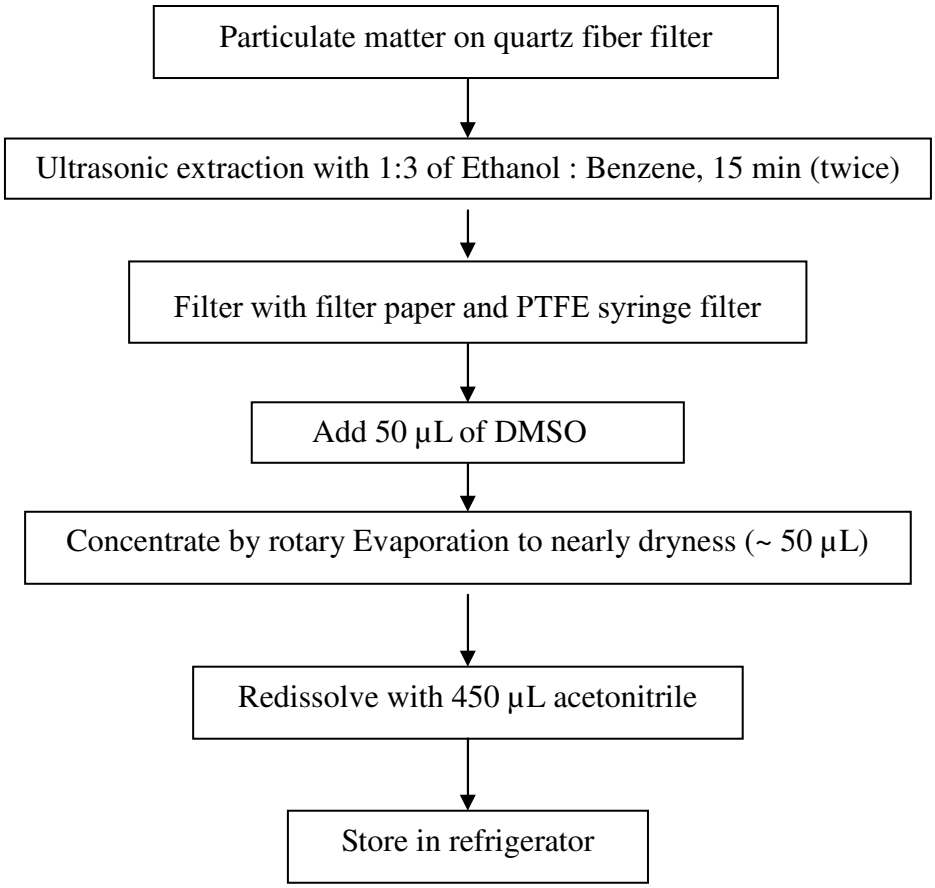

Figure 3.17 Diagram of extraction procedure.

HPLC system

The PAH extracts were analyzed using high-performance liquid chromatography: HPLC (Agillent 1100, USA) with ultraviolet absorption detection as shown in Fig 3.18. The conditions used for HPLC/UV detection were modified from the application note for the determination of PAH in extracted environmental samples (Dionex, 2003), and from Venkataraman et al. (1998), Oanh et al. (2002), and Luigi et al. (2005). A portion of the extract (25 µL) was injected into UPS C-18 reversed phase column with guard column (Vertisep, Thailand). The gradient elution of water/acetonitrile mobile phase was applied for compound separation at flow rate of 1.0-1.2 mL min^{-1}. The gradient condition is described in Table 3.3. The PAHs were detected using UV detective at 254 nm wavelength. The conditions used for HPLC analysis were described in Table 3.4. The standard solutions were prepared from the

16 PAHs mix standard (Supelco catalog number 4-8743). The resulting chromatograms present the different PAHs, which were then identified by matching the retention times and UV absorbance spectra with reference standards using the Chemstation program. The concentration of each compound was quantified from peak area. Some sample extracts were spiked with the standard solution to verify the location of each compound peak in the sample chromatograms. Fig 3.19 presents the HPLC chromatogram of the mixture of 16 PAH standard. The elution order of the identified PAHs is : Naphthalene, Acenaphthylene, Fluorene, Acenaphthene, Phenanthrene, Anthracene, Fluoranthene, Pyrene, Benz(a)anthracene, Chrysene, Benzo(b)fluoranthene, Benzo(k)fluoranthene, Benzo(a)pyrene, Dibenzo(a,h)antracene, Benzo(g,h,i)perylene, Indeno(1,2,3-cd)pyrene.

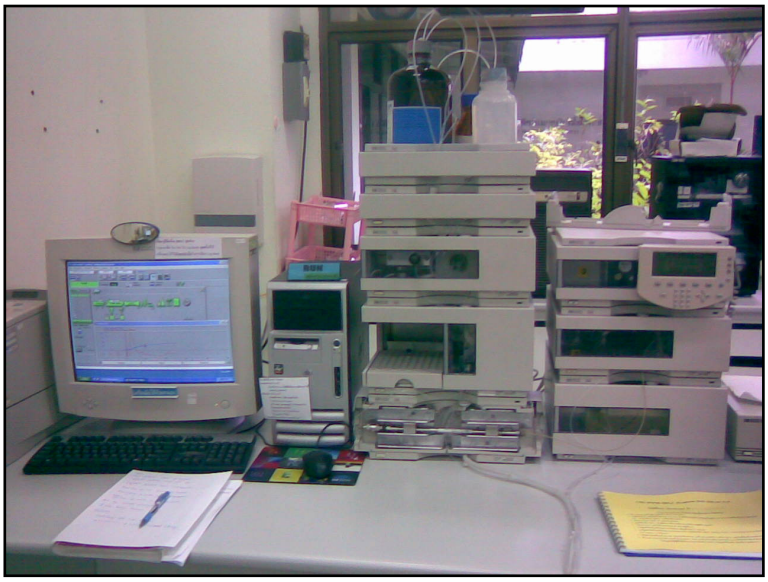

Figure 3.18 Photograph of the HPLC/UV system (Agillent, model 1100) used for measuring the concentration of PAHs in the samples.

Table 3.3 Gradient condition.

Time (min)	Acetonitrile (%)	Ultra pure water (%)	Flow rate (mL/min)
0	35	65	1
5	35	65	1
20	80	20	1
35	100	0	1.2
37	100	0	1.2
40	100	0	1

Table 3.4 HPLC conditions.

Column	VERTISEP UPS C18 column 4.6x250 mm, 5 µm
Guard	Vertisep 5 µm
Temperature	25 °C
Mobile Phase	A : Acetonitrile B : Ultra pure water
Inject Volume	25 µL
λ for detection	254 nm

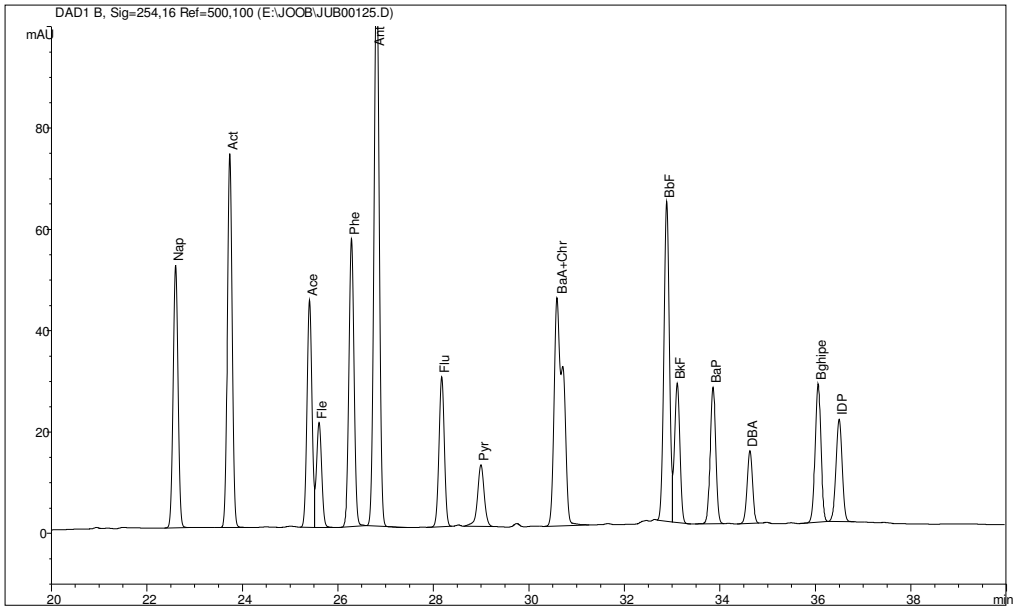

Figure 3.19 The HPLC/UV Chromatogram of 16 PAH standard.

Standard solution preparation

The HPLC system was calibrated using external standards. The standard solutions were prepared from the stock solution, which was the ten-times dilution of the 16 PAHs mix standard (Supelco catalog number 4-8743). The solvent used for dilution was acetonitrile. The concentrations of each PAH in the stock solution are given in table 3.5.

Calibration curves using PAHs standard solution in the range of 0.52-10.52 μg mL^{-1} Nap were prepared by diluting the standard PAH from stock solution with acetonitrile. Each concentration was injected into the HPLC system operated at conditions as shown in Tables 3.4 and 3.5.

Table 3.5 Concentrations of each PAH compound in stock solution.

No.	Polycyclic aromatic hydrocarbon	Abbreviation	Concentration ($\mu g\ mL^{-1}$)
1	Naphthalene	Nap	105.2
2	Acenaphthylene	Act	210.3
3	Fluorene	Fle	20.91
4	Acenaphthene	Ace	105.6
5	Phenanthrene	Phe	10.34
6	Anthracene	Ant	10.37
7	Fluoranthene	Flu	21.42
8	Pyrene	Pyr	96.9
9	Benz(a)anthracene	BaA	10.44
10	Chrysene	Chr	10.41
11	Benzo(b)fluoranthene	BbF	21.00
12	Benzo(k)fluoranthene	BkF	10.41
13	Benzo(a)pyrene	BaP	10.70
14	Dibenzo(a,h)anthracene	DBA	20.70
15	Benzo(g,h,i)perylene	BghiPe	20.64
16	Indeno(1,2,3-cd)pyrene	IDP	10.18

Limit of detection

Limit of detection was considered as the lowest concentration that the detector could provide a signal to noise ratio (S/N) more than 3. To determine the limit of detection, the PAH standard solutions were prepared for concentrations in the rang of 0.0105-10.5200 $\mu g\ mL^{-1}$ of NaP. Each concentration was injected into the HPLC system operated at conditions as show in Tables 3.4 and 3.5. The limit of detection for all PAHs or the concentrations of PAHs, which gives a S/N of more than 3.0 are summarized in Table 3.6.

Table 3.6 The limit of detection for individual PAHs by HPLC analysis in this study.

No.	PAHs	Limit of detection ($ng\ mL^{-1}$)
1	NaP	<52.60
2	Act	<105.15
3	Ace+Fle	<63.25
4	Phe	<5.17
5	Ant	<5.18
6	Flu	<10.71
7	Pyr	<4.84
8	BaA+Chr	<10.42
9	BbF	<10.50
10	BkF	<5.20
11	BaP	<5.35
12	DBA	<10.35
13	BghiPe	<10.32
14	IDP	<5.09

Recovery

The term recovery (R) is used to indicate the yield of an analyte in a pre -concentration or extraction stage in an analytical method. Actually, the recovery value is presented as a percent recovery (%R) and it can be calculated from equation given by Rubinson (1987):

$$\%R = \frac{Measured\ value}{Real\ value} \times 100$$

When $\%R$ is the percent recovery.

To determine PAH recovery, the PAH standard solution for three concentrations was prepared. Then they were spiked on blank filters using micropipette. then the filters were allowed to dry in the dark desiccator for 72 hours. The spiked filters were extracted and analyzed by HPLC/UV at the same conditions used for the samples. The percent recovery of 16 PAHs are shown in Table 3.7.

Table 3.7 The percent recovery for individual PAHs.

No.	PAHs	Recovery (%)
1	Nap	47.50
2	Act	61.84
3	Ace+Fle	86.30
4	Phe	62.67
5	Ant	104.20
6	Flu	63.88
7	Pyr	126.24
8	BaA+Chr	71.44
9	BbF	73.78
10	BkF	74.75
11	BaP	100.62
12	DBA	74.55
13	BghiPe	72.55
14	IDP	81.50

CHAPTER 4
RESULTS AND DISCUSSION

In this work, the characteristics of smoke particles from rubber-wood combustion in rubber smoking process from a rubber cooperative were investigated. The influence of smoke particles on workers inside the cooperative and on the atmospheric air of Hat Yai City were assessed. Size distribution, concentration, and chemical components (PAHs) were evaluated from sampled particles. A high performance liquid chromatography with UV detector (HPLC-UV) was used for quantification of PAHs from sampled particles.

4.1 Characteristics of smoke particles from rubber-wood burning

4.1.1 Size distribution of smoke particles

The size distribution of smoke particles from rubber-wood combustion in smoking rooms was investigated by using an 8-stage Andersen sampler (Dylec, AN200). The samples were taken at the gas inlets to the smoking room and the results are shown in Fig. 4.1. Apparently, the size distribution of the smoke particles shows a single-mode behavior. Mass median aerodynamic diameter (MMAD) was found to be 0.68 μm and the geometric standard deviation (GSD) was 3.04 μm.

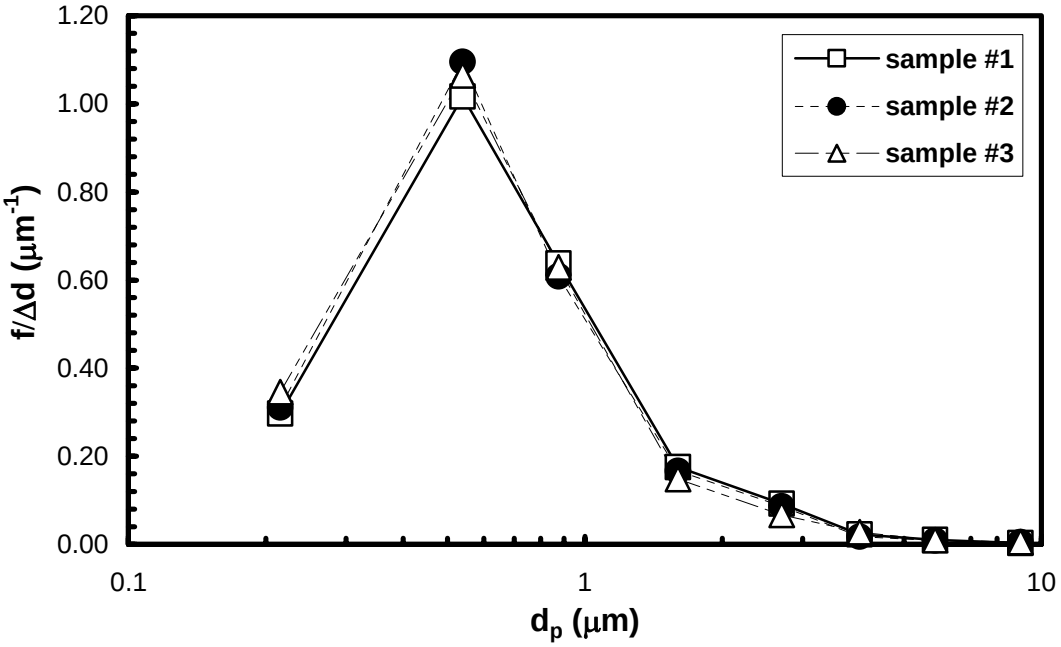

Figure 4.1 Size distribution of smoke particles from rubber-wood burning**.**

4.1.2 Concentration of smoke particles

The variation of concentrations of smoke particles for different burning time and fuel moisture contents is shown in Fig. 4.2, for rubber-wood moisture contents from 37.4% to 73.6% (dry basis). The average smoke concentration is 15806.11 μg m^{-3} or mass emission to workplace is 4.33 kg $month^{-1}room^{-1}$. Initially, the concentration was highest and it was reduced during the course of combustion. The increase of wood moisture content exponentially enhances the concentration of smoke particles as shown in Fig. 4.3. The reason for the increase is that the combustion temperature decreases during the combustion as the moisture content of the rubber-wood diminished. This results in an increase of the unburned carbon fraction (Chao et al., 2007). In addition, a relatively high amount of the evaporated water cannot be transferred through the porous structure inside the fuel. Pressure is built up and cracking of the particles occurrs and thus, more fly-ash can crack from the ash with higher mass of moisture (Kurose et al., 2001).

The effect of moisture contents of rubber-wood on particle concentration were also investigated and the results are shown in Fig. 4.2 as well. The presence of water in the rubber-wood results in incomplete combustion and hence,

a cloud of smoke particles. Therefore, when the moisture content is high, the resulted concentration is also high.

The initial total smoke concentration is 47.54 mg m^{-3} for 73.6% moisture content and 23.35 mg m^{-3} for 37.4% moisture content, while the concentrations after 135 minute are 4.57 and 3.65 mg m^{-3} for 73.6 and 37.4% moisture content, respectively.

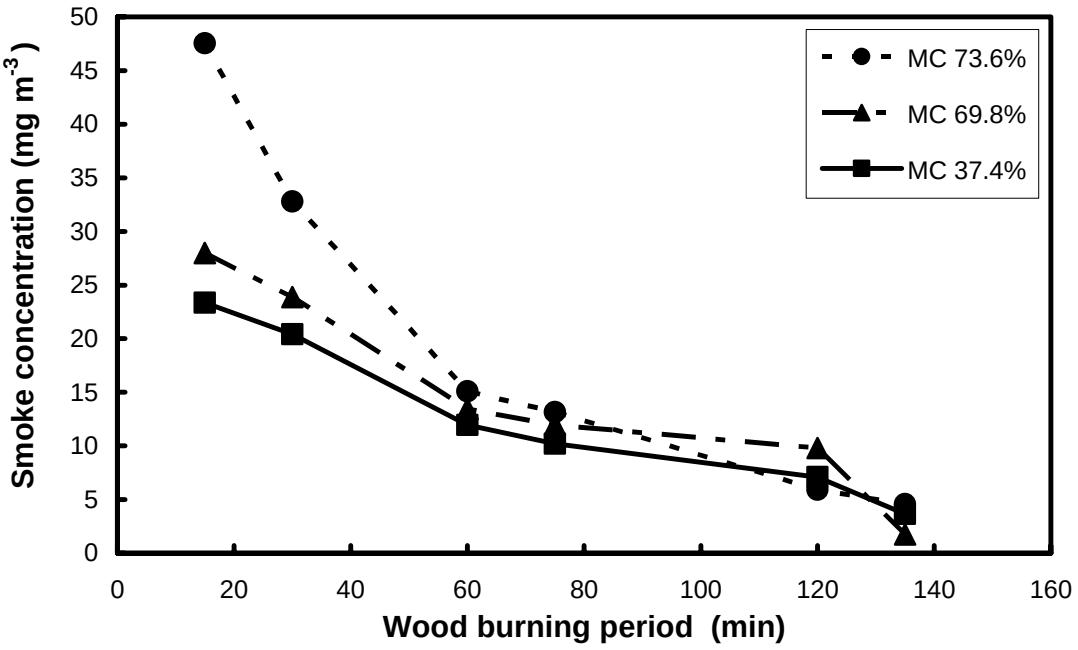

Figure 4.2 Effect of wood burning period on the concentration of smoke particles for different fuel moisture contents (MC).

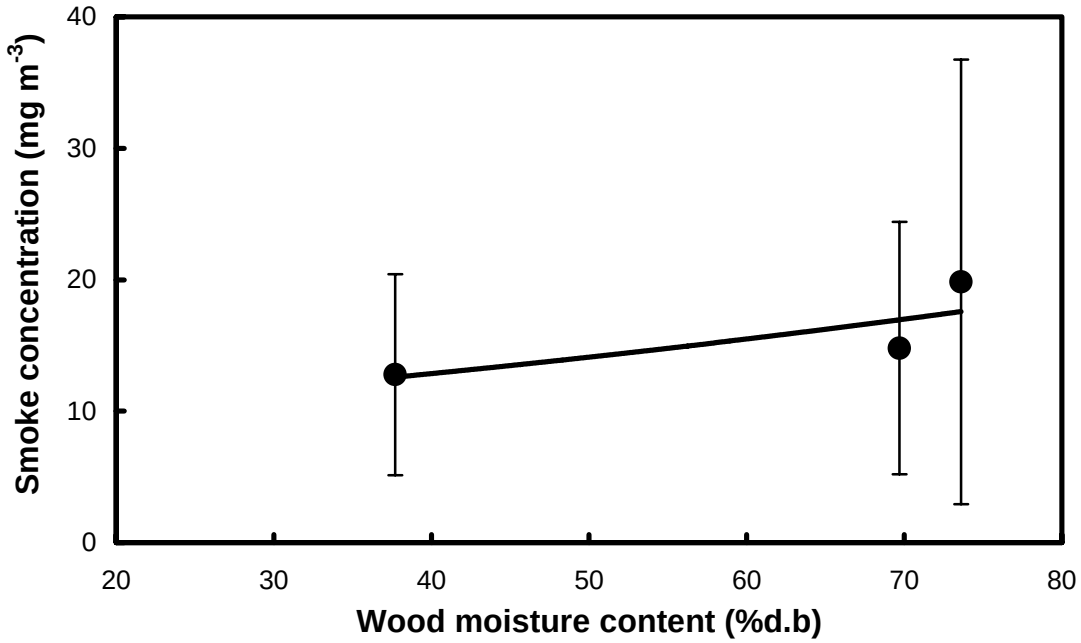

Figure 4.3 Relationship between the concentration of smoke particles and wood moisture content.

4.1.3 Concentration of PAHs

The PAHs monitored in this study comprised: Naphthalene (Nap), Acenaphthylene (Act), Acenaphthene (Ace), Phenanthrene (Phe), Anthracene (Ant), Fluorene (Fle), Fluoranthene (Flu), pyrene (Pyr), Benz[a]anthracene (BaA), Chrysene (Chr), Benzo[a]pyrene (BaP), Benzo[b]fluranthene (BkF), Benzo[k]fluoranthene (BkF), Dibenz[a,h]anthracene (DBA), Indeno[1,2,3-cd]pyrene (IDP), and Benzo[ghi]perylene (BghiPe).

Variations of total concentration of sixteen PAH compound in smoke particles and the concentration of smoke particles at different burning period and different fuel moisture content were plotted in Fig. 4.4.

The reduction rate of total PAH concentration during the course of combustion is in agreement with the reduction of particle concentration. This indicates the rather uniform presence of PAHs or the particles. Initially, the moisture content has a large impact on the PAH concentration as well as for the case of particle concentration.

The total PAH concentration is 118.06 μg m^{-3} for 73.6% moisture content and 60.58 μg m^{-3} for 37.4% moisture content, while the concentrations after 135 minute are 1.69 and 2.39 μg m^{-3} for 73.6 and 37.4% moisture content, respectively as shows in Fig. 4.4. The behaviors of the PAH concentration influenced by the burning period and fuel moisture content are in similar fashion to those of the particle concentration.

From a previous study by Promtong and Tekasakul (2007) it was found that the rate of rubber-wood supply in a rubber smoked sheet is 10 kg h^{-1} (20 kg of wood was added every 2 hours). The combustion temperature reached the highest value 1 h after fed rubber-wood, and then the temperature decreased. A proportion of PAH/smoke at 30 minutes was lower than that at 15 minutes of burning period, as shown in Fig. 4.4, since more evaporation of PAHs at higher temperature occured.

The influence of particle concentration on total PAH concentration is shown in Fig. 4.5. It was found that the correlation demonstrates a power function of PAH concentration with respect to smoke particle concentration. Low concentrations after a long period of combustion may be in part resulted from the decomposition of PAHs.

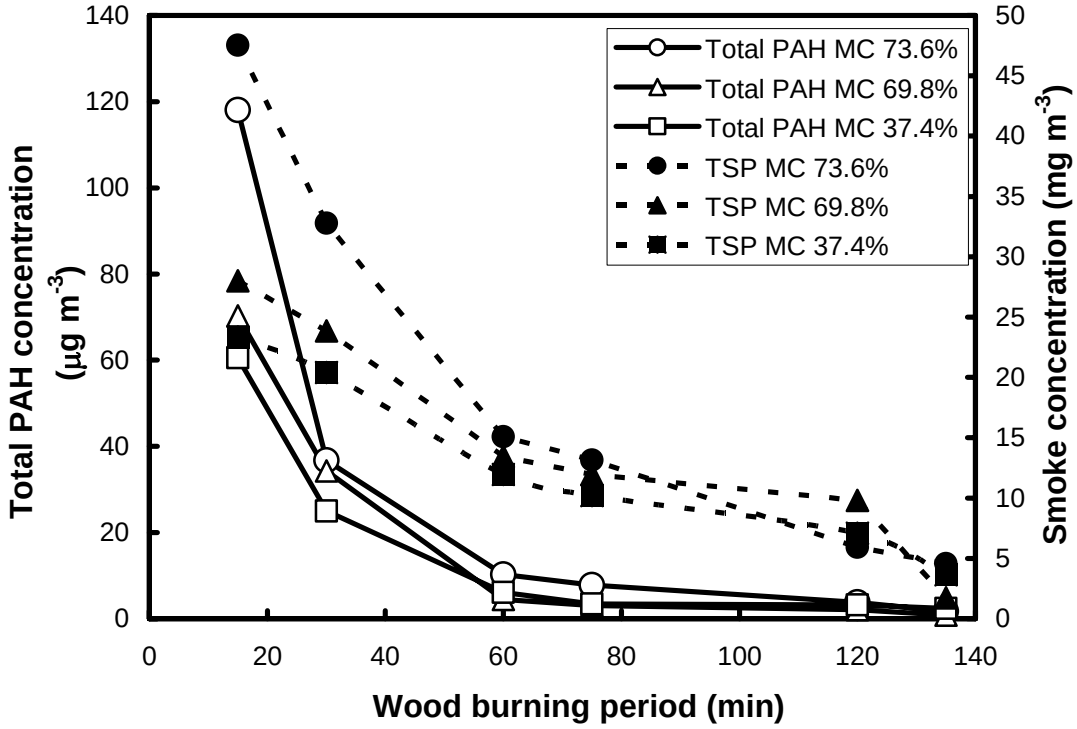

Figure 4.4 Effect of wood burning period on the concentrations of total PAHs and smoke particles for different wood moisture contents.

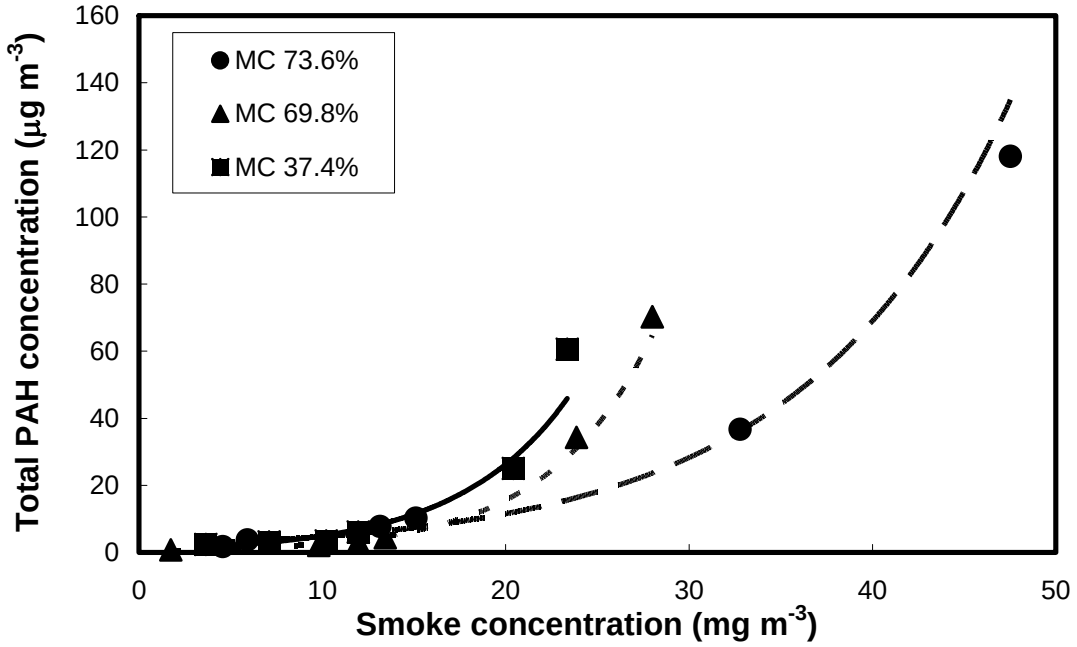

Figure 4.5 Relationship between total PAH concentration of smoke particles and smoke particle concentration for different wood moisture contents.

The relationship between 4-6 ring PAHs, which are particle-bound, and wood burning period is shown in Fig. 4.6. It was found that the PAH concentration is reduced powerfully during the course of combustion.

The initial 4-6 rings PAH concentration is 83.93 μg m^{-3} for 73.6% moisture content and 44.93 μg m^{-3} for 37.4% moisture content while the concentrations after 135 minute are 0.85 and 1.62 μg m^{-3} for 73.6 and 37.4% moisture content, respectively. The behaviors of 4-6 rings PAHs concentration influenced by burning period and fuel moisture content are in similar fashion to those of total PAHs concentration and particle concentration. The influence of particle concentration on 4-6 rings PAHs concentration is shown in Fig. 4.7. It was found that the correlation demonstrates a power function of 4-6 rings PAHs concentration with respect to smoke particle concentration.

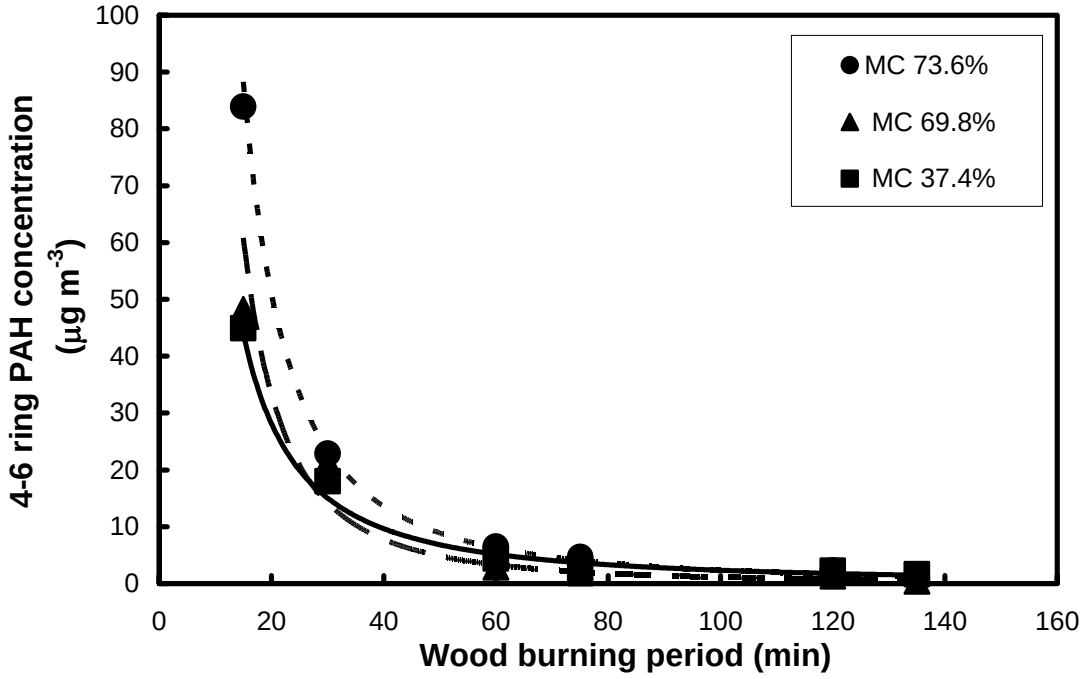

Figure 4.6 Relationship between the concentration of 4-6 ring PAHs in smoke particles and wood-burning period for difference wood moisture contents.

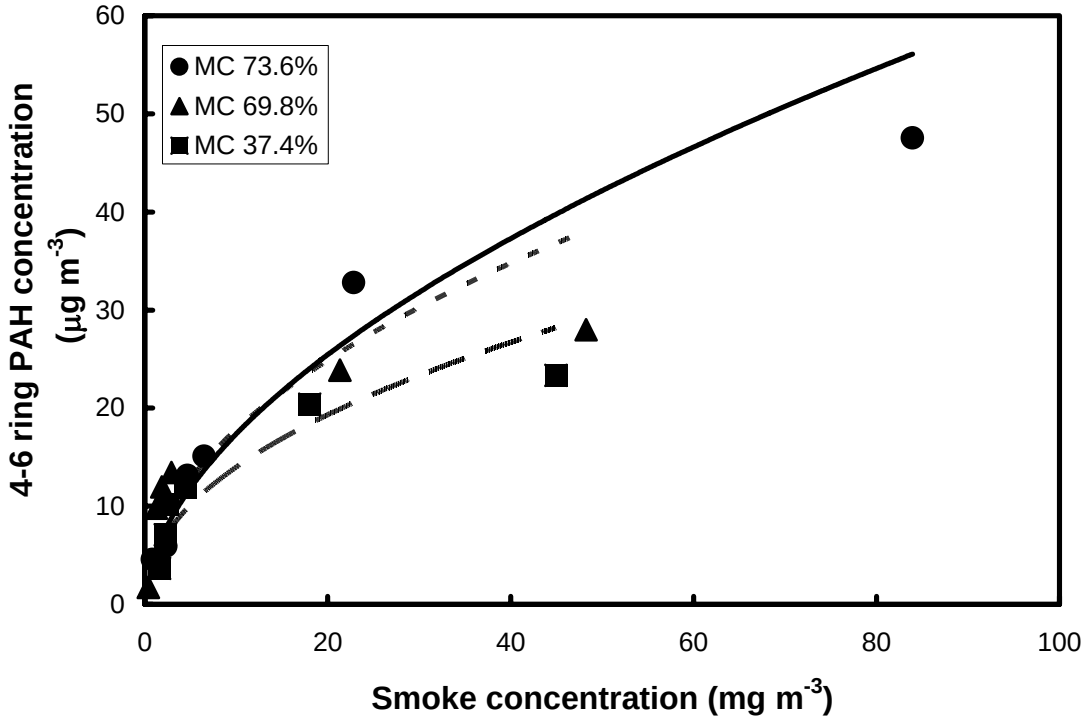

Figure 4.7 Relationship between the concentration of 4-6 ring PAHs and smoke concentration for difference wood moisture contents.

4.1.4 Profile of PAHs

The composition profile of PAHs in smoke particles generated from rubber-wood combustion in smoking room is presented in Fig. 4.8. The mass fractions presented were the average values from 18 samplings. It shows that the PAHs relative contribution is dominated by the BghiPe compound, which in average accounted for about 16.8% of the total PAHs. However, Hay et al. (2003) found a predominate of BaP from white-wood combustion, which is not the case here. It might be the result from the difference in fuel wood. The Ace+Fle fraction is the highest, because it is a combination of two compounds (Ace and Fle).

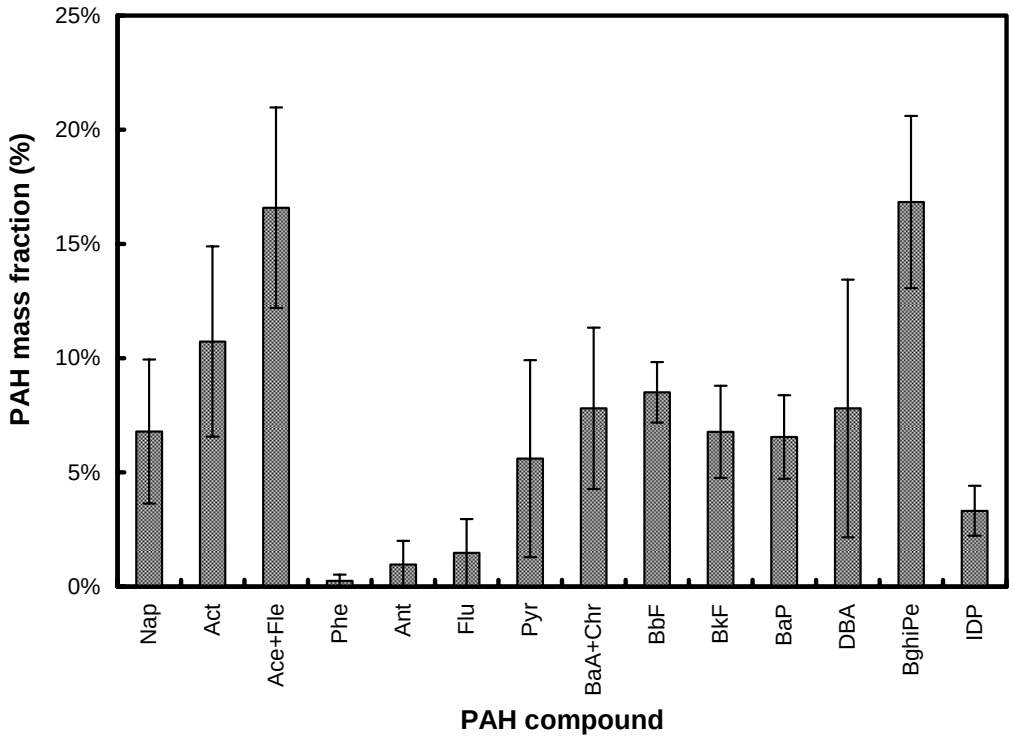

Figure 4.8 Mass fraction of each PAH compound in smoke particle samples from rubber-wood burning (n = 18).

Effect of wood burning period and fuel moisture content on PAHs contribution

The effects of wood burning period and wood moisture content on PAHs concentration were investigated. The profile of PAHs for different wood-burning period is shown in Fig. 4.9. It was found that the fraction characteristics of each PAH compound is not clear for different burning periods. However, the PAH mass fraction is dominated by BghiPe, Ace+Fle, Act, and NaP, which contribute to more than 45% of the total PAHs for all wood-burning periods. While, using birch-wood, the major emissions of PAHs are Fle, Phe, Ace, Flu and Pyr, which contribute to more than 70% of the total PAHs (Hedberg et al., 2002). Fig. 4.10 to 4.12 show the mass ratio of PAH compositions and burning period for 37.4% to 73.6% wood moisture content. A fraction of high molecular weight PAHs (4-6 rings) contributes more than 60% of the total PAHs for all values of wood moisture contents. PAH

mass fractions of 2-3 ring PAHs consisting of NaP, Act, Ace+Fle, Phe, and Ant, and 4-6 ring PAHs consisting of Flu, Pyr, BaA+Chr, BbF, BkF, BaP, DBA, BghiPe, and IDP are shown in Fig. 4.13. The relationship between 4-6 ring PAH mass fraction and wood-burning period is shown in Fig. 4.14. The mass fraction of 4-6 ring PAHs is decreased as the wood-burning period increases. This may be due to for longer period of combustion, the decomposition of 4-6 ring PAHs is more.

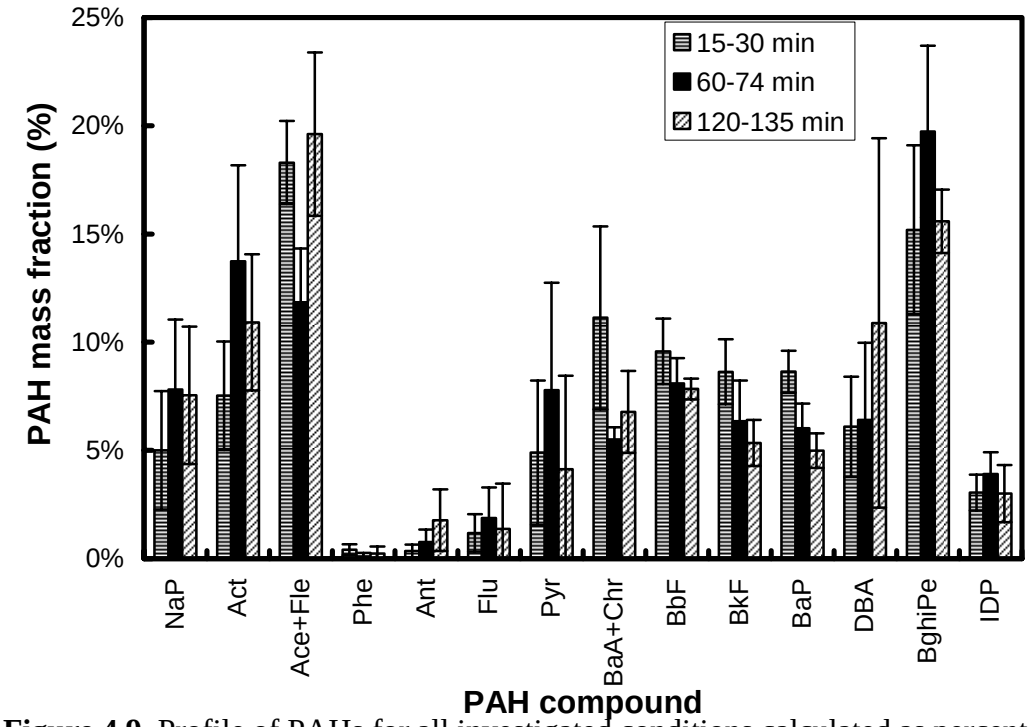

Figure 4.9 Profile of PAHs for all investigated conditions calculated as percentage for each compound in relation to the total amount of PAHs for different burning periods.

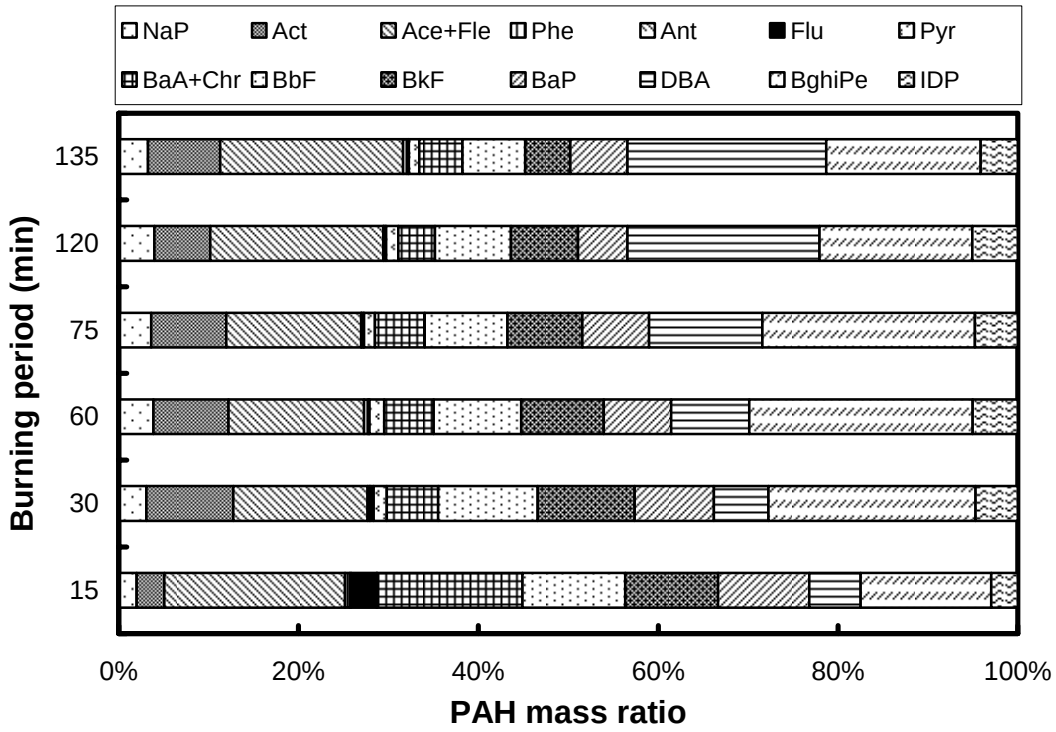

Figure 4.10 PAH mass ratio to total PAHs for each burning period for wood moisture content of 37.4%.

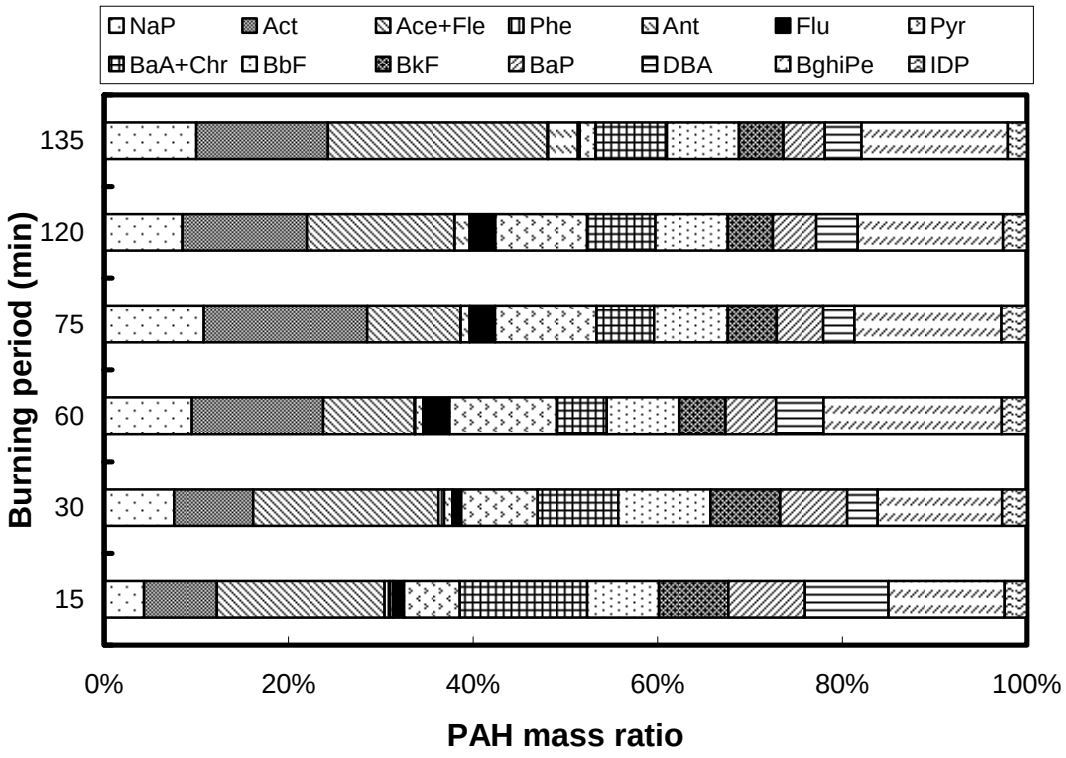

Figure 4.11 PAH mass ratio to total PAHs for each burning period for wood moisture content of 69.8%.

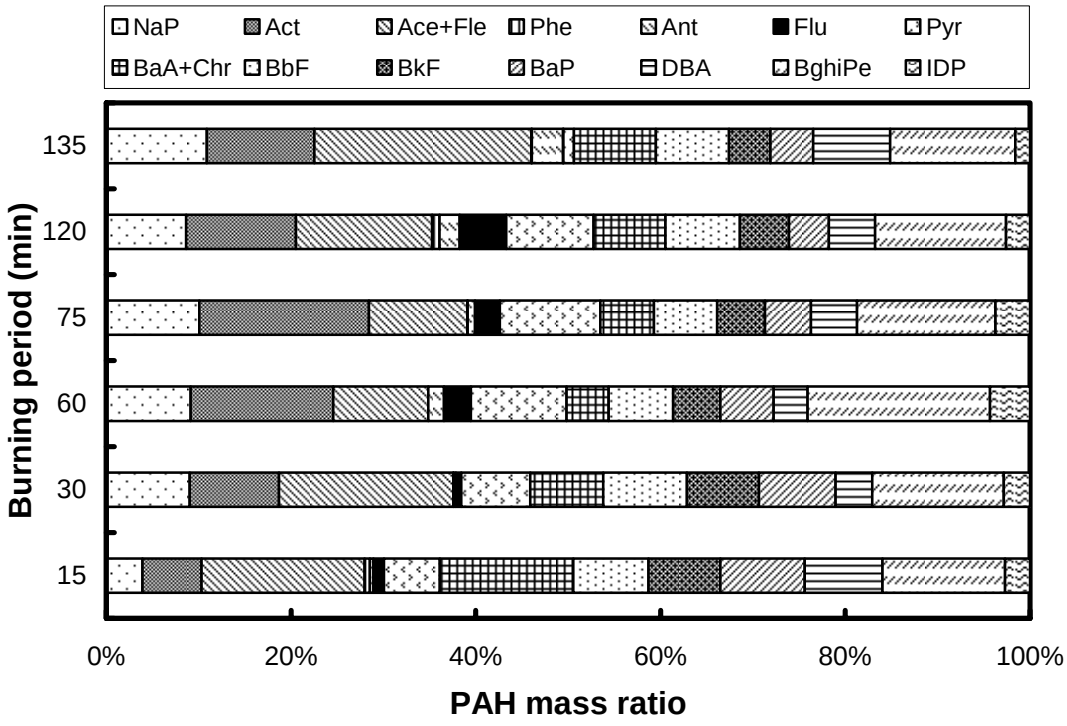

Figure 4.12 PAH mass ratio to total PAHs for each burning period for wood moisture content of 73.6%.

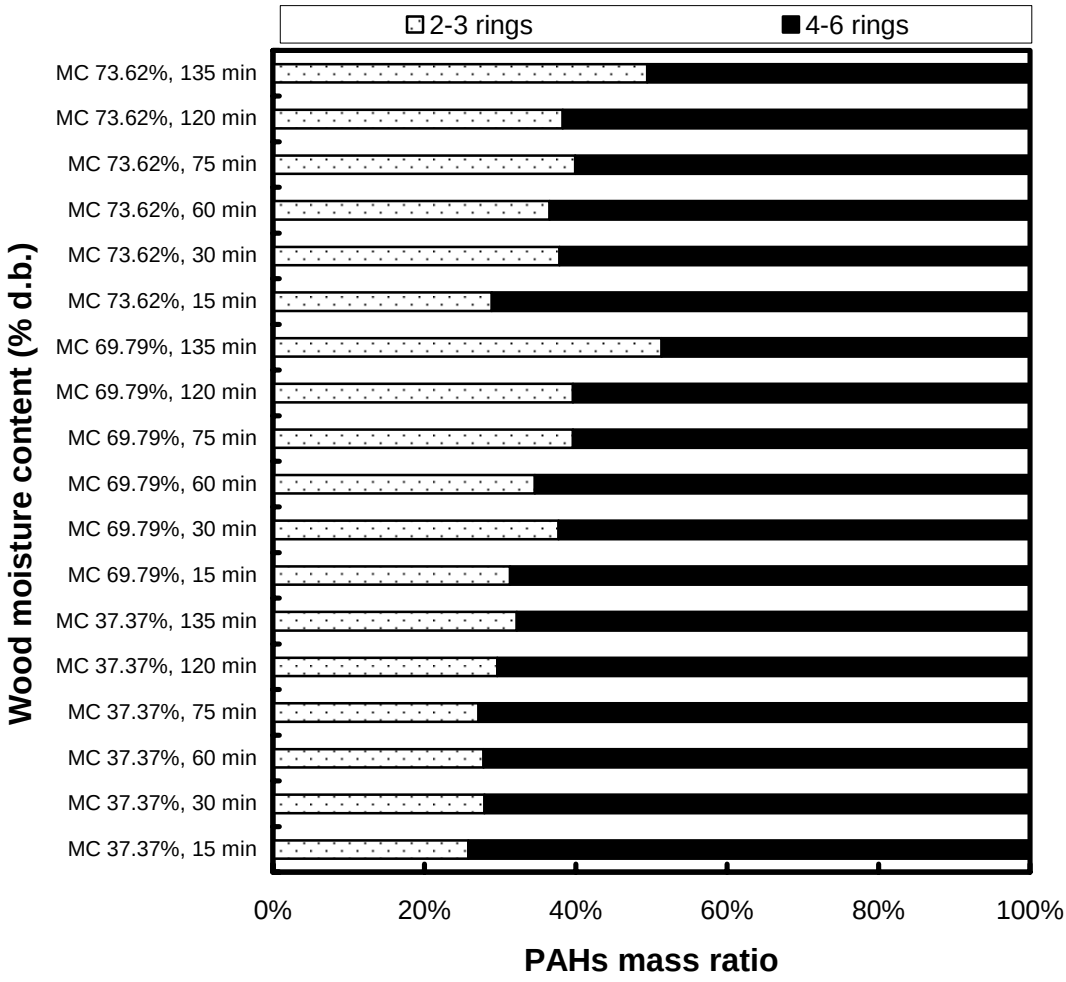

Figure 4.13 PAH mass ratio of total PAHs for each wood burning period for different wood moisture contents, showing the fractions of 2-3 ring and 4-6 ring PAHs.

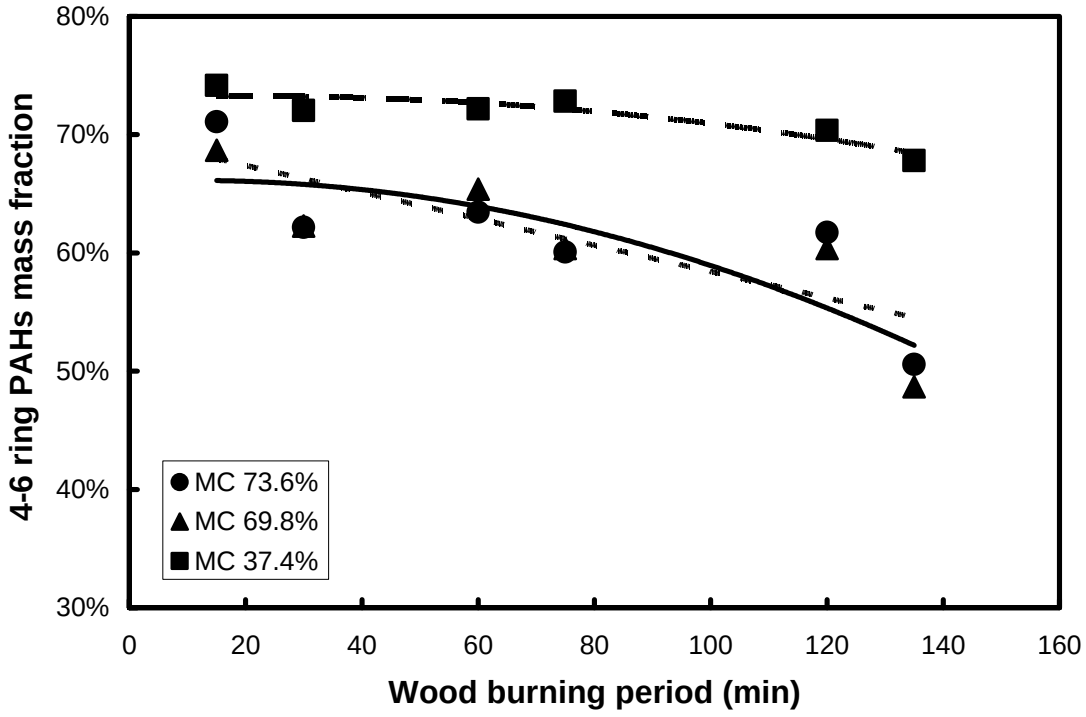

Figure 4.14 Relationship between mass fraction of 4-6 ring PAH compounds and wood burning period for different fuel moisture contents.

4.2 Characteristics of aerosol particles in workplace

4.2.1 Size distribution of particles

Aerosol sampling in the workplace is ultimately concerned with the study of the aspect of the aerosol that leads to specific health effects. Thus, the method and metric used are aimed to provide biologically relevant information. Aerosol particles can cause health problems when deposited on the skin and eyes, but generally the most sensitive route of entry into the body is through the respiratory system. The biological effects resulting from deposition of an aerosol in the respiratory tract will depend on the dose received and the body's response to the deposited particles. Physiological response to an aerosol depends on the chemical and physical natures of the particles and the location of the interaction (i.e., deposition region). The ultimate goal of industrial hygiene aerosol measurement is therefore to ascertain the dose of aerosol delivered to the body and to evaluate whether the dose or potential dose is sufficient to cause adverse health effects. To study the effect of

rubber-wood combustion to worker in a rubber sheet smoking cooperative, physical and chemical and characteristics of particulate matters were investigated.

Many types of instrument have been used for aerosol sampling in the workplace (Mark et al., 1984). Cascade impactor is often the instrument of choice, giving an indication of the mass-weighted size distribution of an aerosol. The size distribution of smoke particles at workplace area (WP) in a cooperative was measured using an identical 8-stage Andersen cascade sampler (Dylec, AN 200). The result of PM size distribution is shown in Fig. 4.15. It shows a bi-modal behavior of aerosol particles dominated by fine particles with a peak at 0.54 μm, an accumulation mode, similar to that from smoke particles, and the coarse-mode (peak at 4.00 μm) probably from the soil dust near the rubber cooperative. The source of these particles is then attributed to the smoke particles from wood burning in the cooperative.

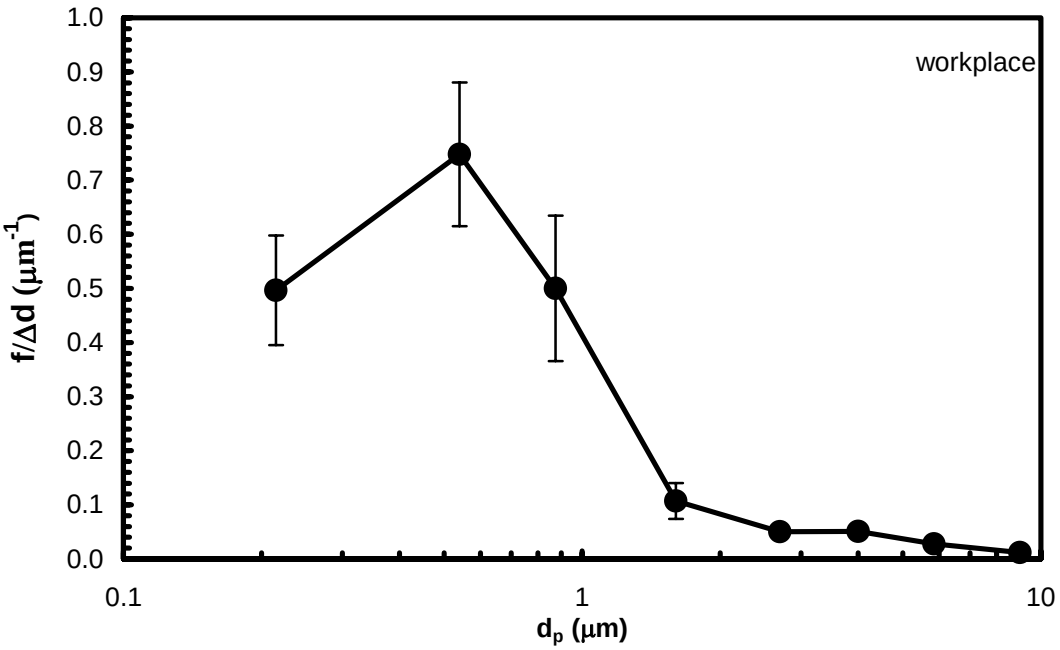

Figure 4.15 Size distribution of particulate matters from workplace (WP) sampling site.

4.2.2 Concentration of particles

The total suspended particulates (TSP) were measured by using high-volume air sampler (SIBATA, HV500F). The yearly TSP collected during January

2006 to January 2007 at workplace ranges from 43.69 to 366.83 μg m^{-3}, with an average of 164.42 ± 80.59 μg m^{-3}. In contrast, the minimum value of TSP at the workplace area was observed during the lowest RSS production period of the cooperative, while the maximum TSP value at the workplace area was observed during the highest RSS production period.

Effect of RSS production

The effect of the amount of rubber-wood used in the combustion on the particle concentrations was investigated. The amount of rubber-wood used is directly proportional to the RSS production. The average TSP of particle sampled at the workplace in each month from January 2006 to January 2007 and the RSS production of the rubber cooperative is shown in Fig. 4.16. TSP at workplace is found to depend on the RSS production. Increasing of the RSS production linearly enhances the TSP at the workplace as shown in Fig. 4.17.

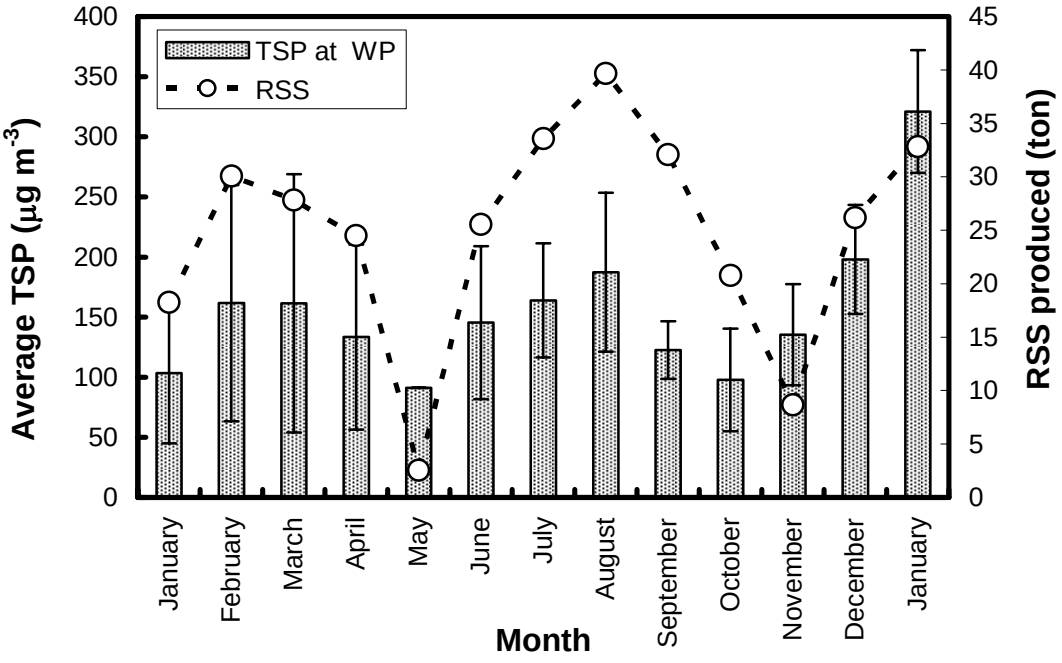

Figure 4.16 Effects of RSS production on the average monthly TSP at workplace area during January 2006 to January 2007.

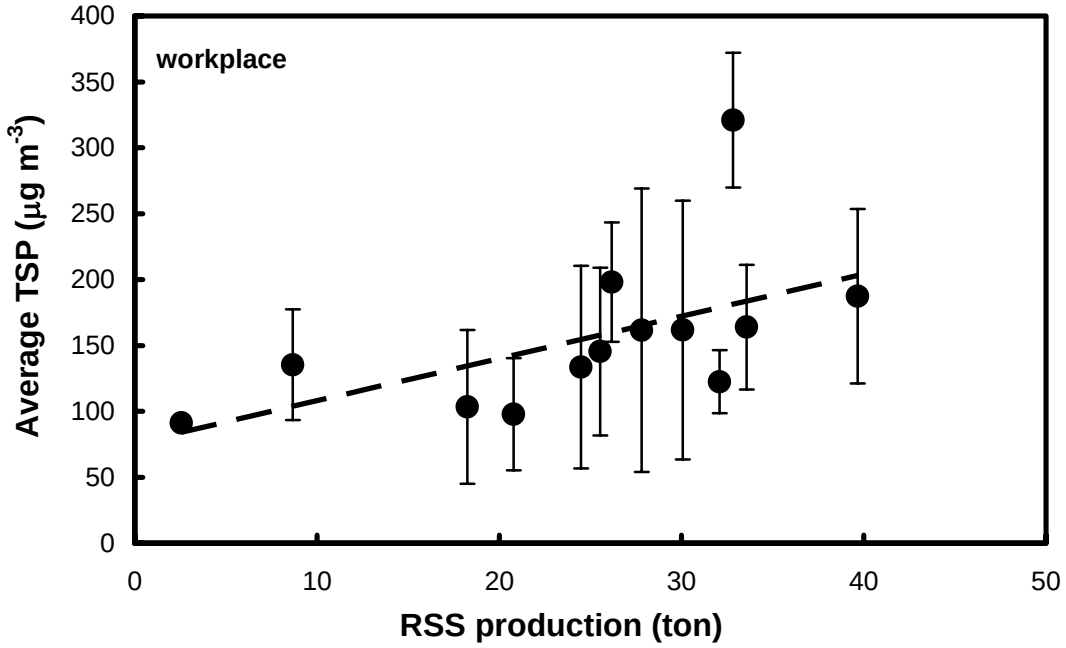

Figure 4.17 Relationship between the average monthly TSP at workplace area and the RSS production.

4.2.3 Concentrations of PAHs

In this study, 16 PAH compounds as described in section 4.1.3 were investigated.

TSP-bound PAH levels

Total PAH concentration refers to the sum of the concentration of 16 measured compounds. The total PAH at workplace area ranges from 2.89 to 655.41 ng m^{-3} depending strongly on the period. The increasing of TSP linearly enhances the concentration of PAH at the workplace sampling site as shown in Fig. 4.18.

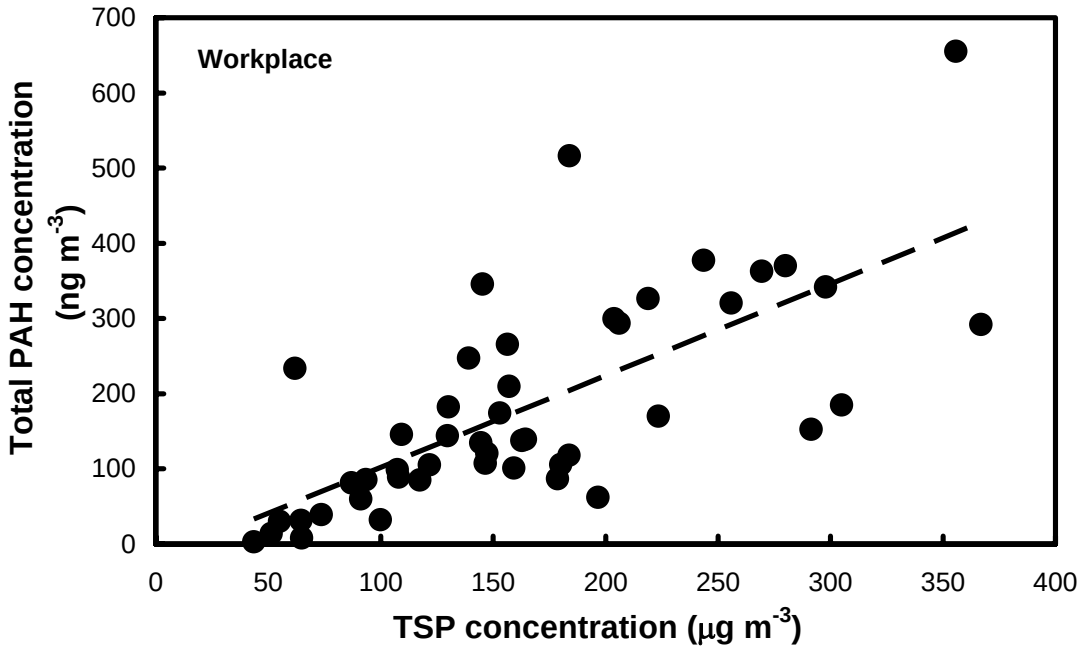

Figure 4.18 Relationship between the concentration of PAHs and the TSP at the workplace area.

Effect of RSS production

The change of PAH concentration under various RSS production level was studied. Monthly PAH concentrations and RSS production in the cooperative during January 2006 to January 2007 are shown in Fig. 4.19. Concentrations of total and 4-6 rings PAHs correspond well with the RSS production as shown in Fig. 4.20 and 4.21, where the total and 4-6 rings PAHs concentration and RSS productions are plotted. The PAH concentrations increase almost linearly with the RSS productions. A high RSS production implies higher use of rubber-wood for burning in the smoking rooms, and hence the smoke particles and the PAH concentrations are escalated.

Although concentration fluctuation are, in general, similar to the RSS production fluctuation, only a weak correlation were observed for total PAHs and 4-6 ring PAHs, respectively. This may be due to the influence of wood moisture content on the concentration of PAHs. Presence of water in the rubber-wood results in incomplete combustion and, hence, a cloud of smoke particles and PAHs. Therefore, when the moisture content is high, the resulted concentration of PAHs is also high.

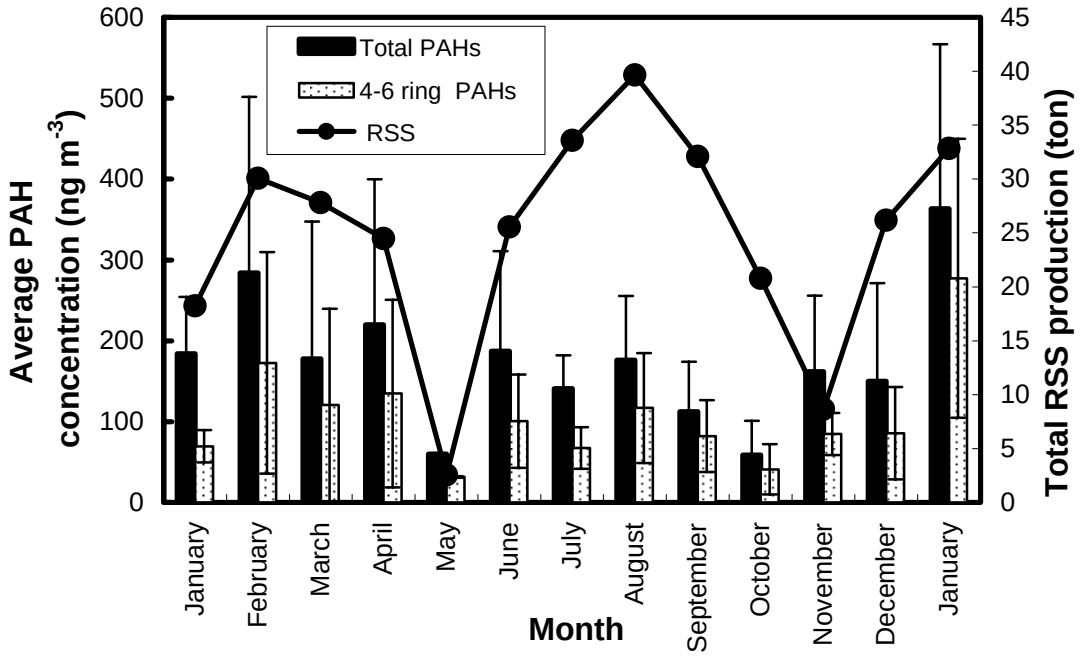

Figure 4.19 Average PAH concentration from workplace sampling and total RSS production during January 2006 to January 2007.

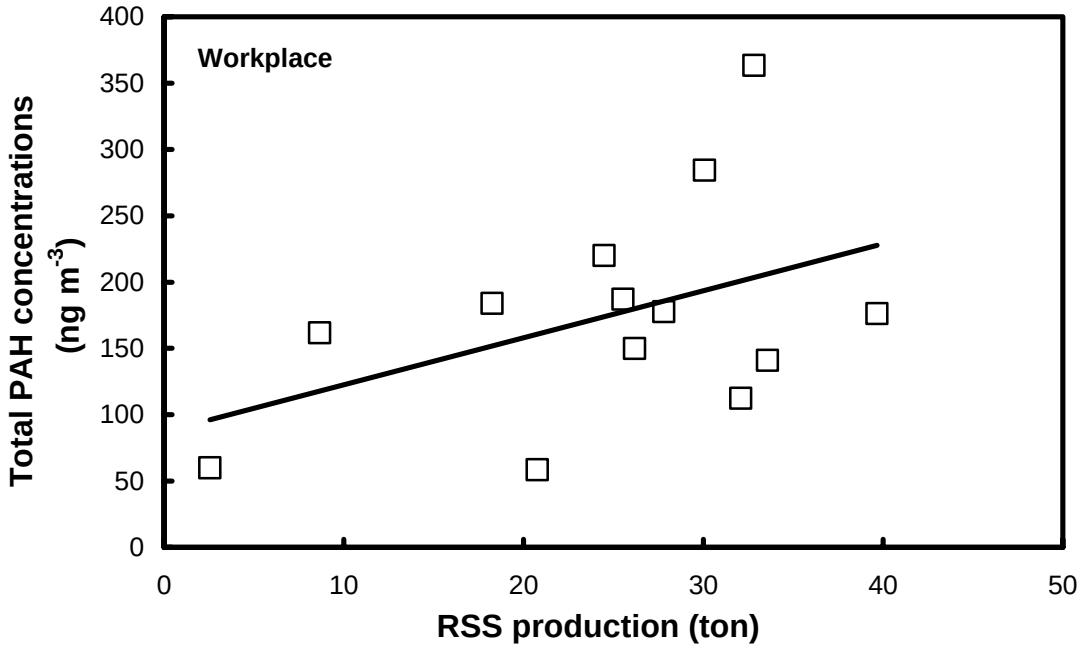

Figure 4.20 Relationship between total PAHs concentration at the workplace and RSS production.

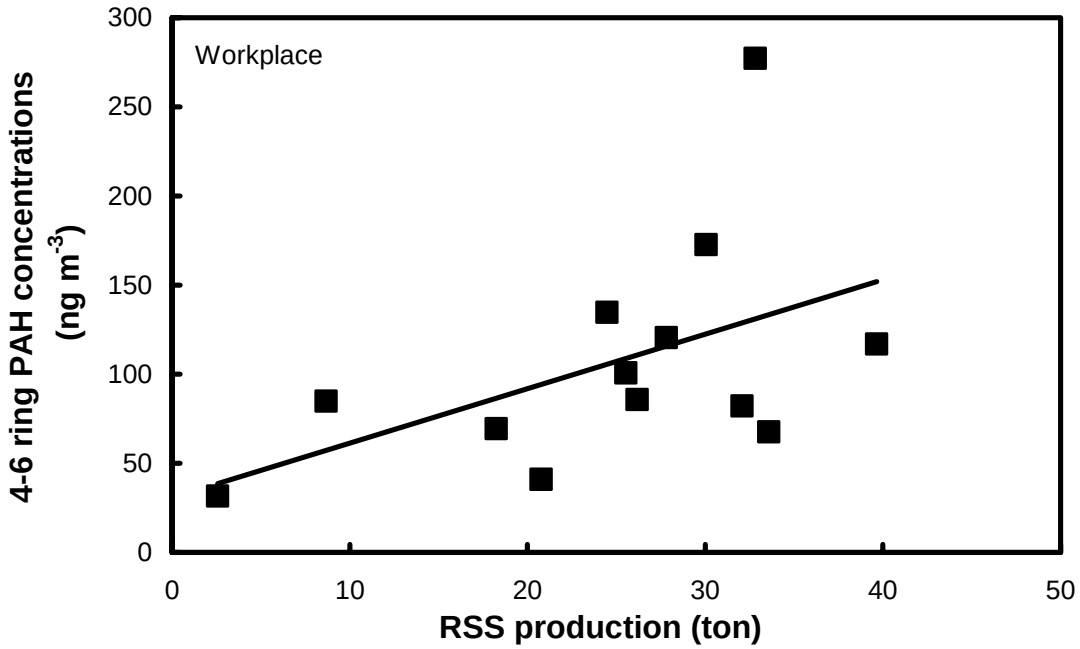

Figure 4.21 Relationship between concentration of 4-6 ring PAHs at the workplace and RSS production during January 2006 to January 2007.

Correlation with NO_2

The relationship between the concentration of PAHs and the concentration of NO_2 at various RSS production level was studied. Fig. 4.22 and 4.23 show the variation of total PAH concentration and NO_2 concentration at workplace sampling site 1 and site 2, respectively. The results show the concentrations of PAHs correlated with the concentrations of NO_2 as shown in Fig. 4.24 and 4.25. It was indicated that NO_2 and PAHs arise from combustion sources (Park at el., 2002). Fig. 4.24 shows the relationship between the concentrations of PAHs and NO_2 at workplace sampling site 1. The correlations have r-squared values of 0.37 and 0.48 for total PAH concentration and 4-6 ring PAH concentration, respectively. Fig 4.25 shows the relationship between the concentrations of PAHs and NO_2 at workplace sampling site 2. The correlations show r-squared values of 0.67 and 0.65 for total PAH concentrations and 4-6 ring PAH concentration, respectively. This indicates that NO_2 and PAHs in the workplace area arise from rubber-wood combustion.

Fig. 4.26 shows the NO_2 concentration at both workplace sites along with the RSS production. The concentration of NO_2 ranged from 3.64 to 25.39 ppb

and 5.42 to 25.92 ppb with an average concentration of 12.68 ppb and 13.69 ppb for workplace site 1 and site 2, respectively. An increase of the RSS production linearly enhances the concentration of NO_2 at both sampling sites in the workplace as shown in Fig. 4.27 with r-squared values of 0.49 and 0.92 for workplace sampling site 1 and workplace sampling site 2, respectively.

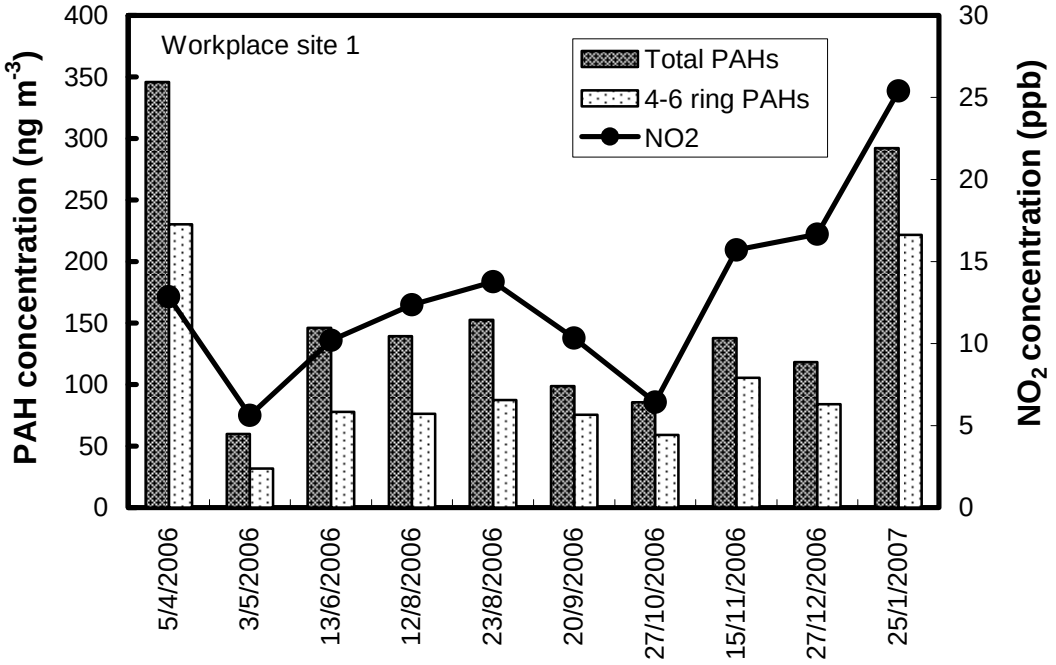

Figure 4.22 Concentration of PAHs and concentration of NO_2 at workplace sampling site 1 during January 2006 to January 2007.

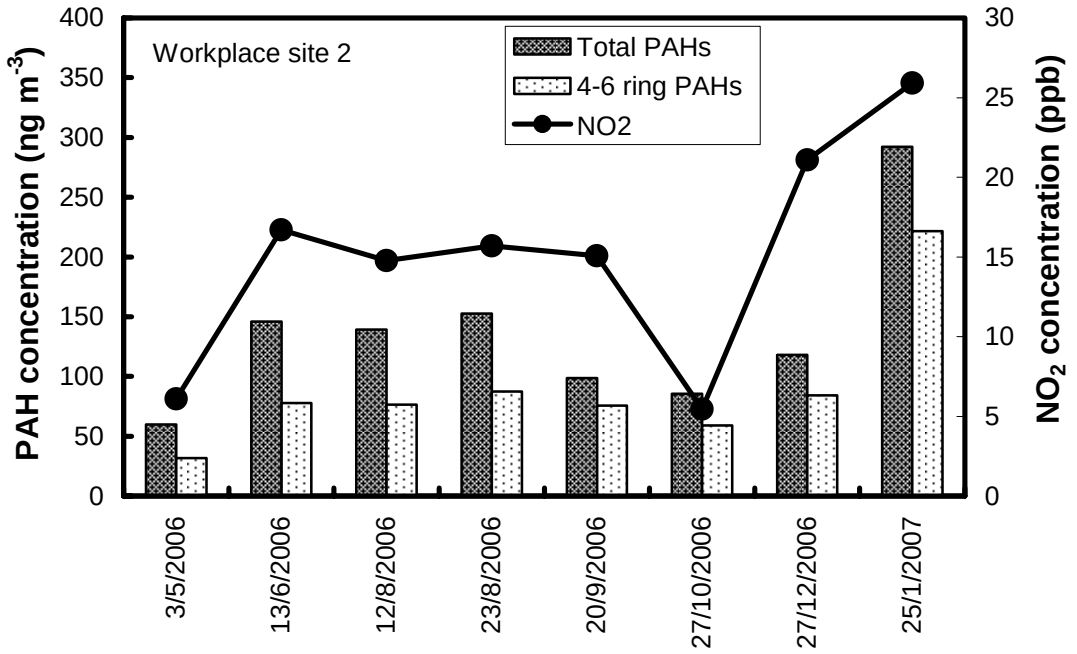

Figure 4.23 Concentration of total PAHs and concentration of NO_2 at workplace sampling site 2 during January 2006 to January 2007.

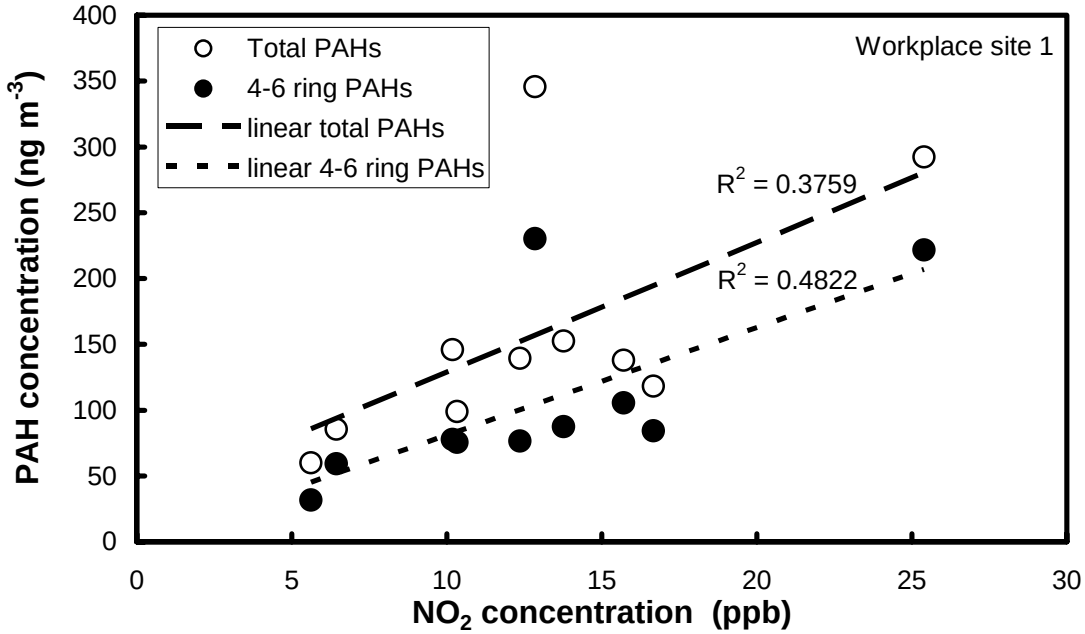

Figure 4.24 Relationship between concentrations of PAHs and concentration of NO_2 at workplace sampling site 1.

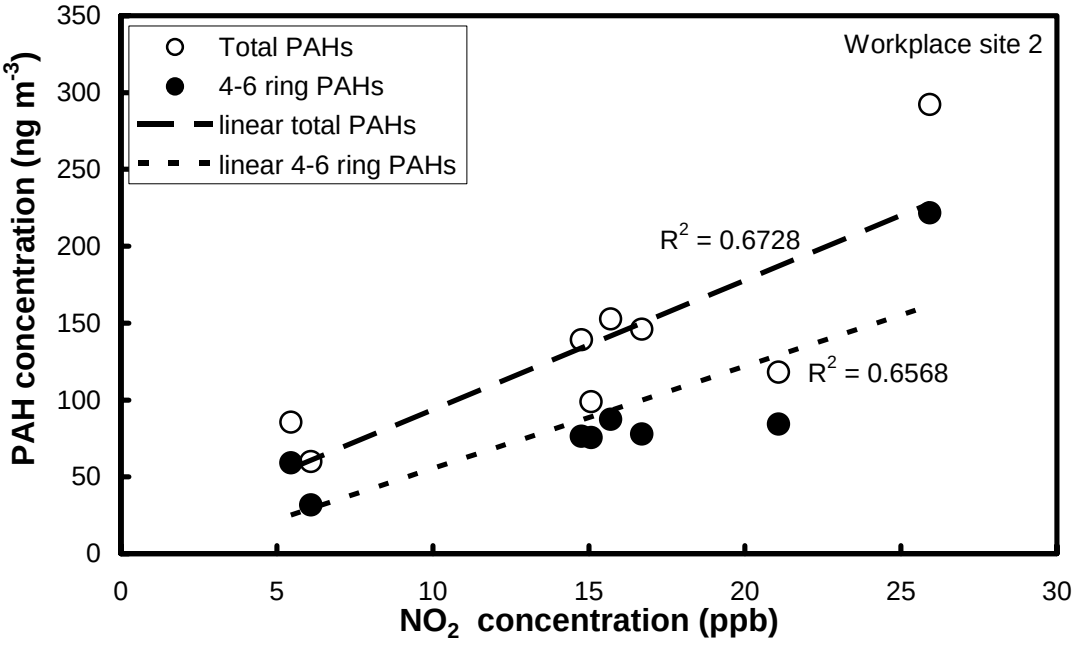

Figure 4.25 Relationship between concentrations of PAHs and concentration of NO_2 at workplace sampling site 2.

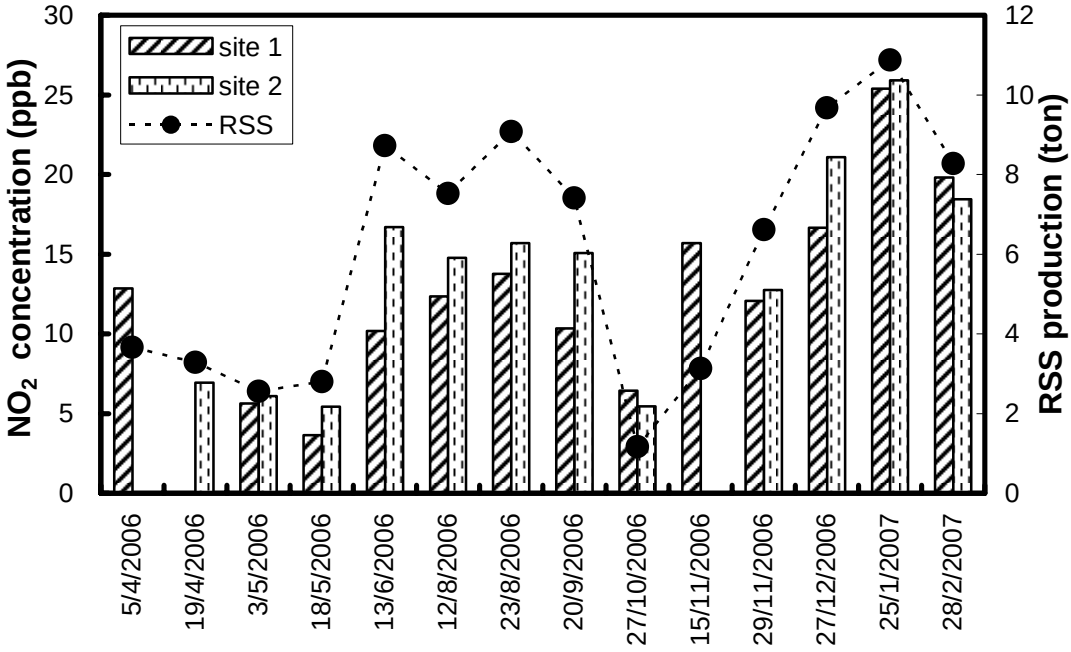

Figure 4.26 Concentration of NO_2 at workplace site 1 and site 2 and RSS production during January 2006 to January 2007.

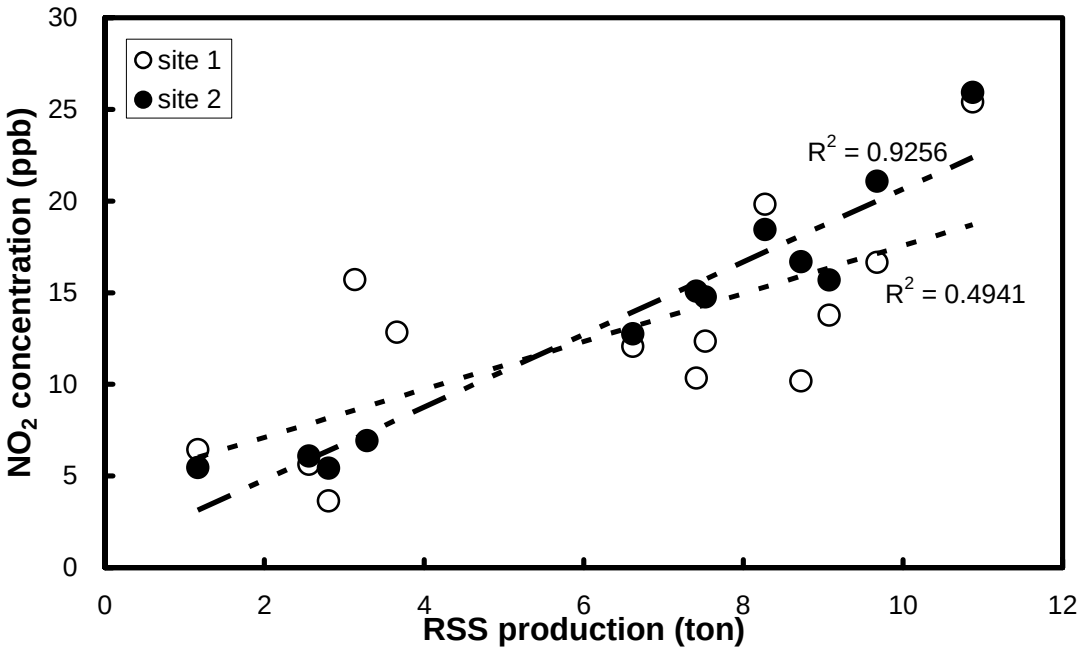

Figure 4.27 Relationship between NO_2 concentration and RSS productions.

4.2.4 Profile of PAHs

The composition profiles of PAHs by compounds in workplace particles generated from rubber-wood combustion in the smoking room are presented in Fig. 4.28. The mass fractions presented are average values from 47 samplings. It shows that the PAHs relative contribution was dominated by Nap, Act and Ace+Fle for 2-3 ring PAHs and BghiPe for 4-6 ring PAHs. The contribution of Act and BghiPe is 16.47% and 12.24% of total PAHs.

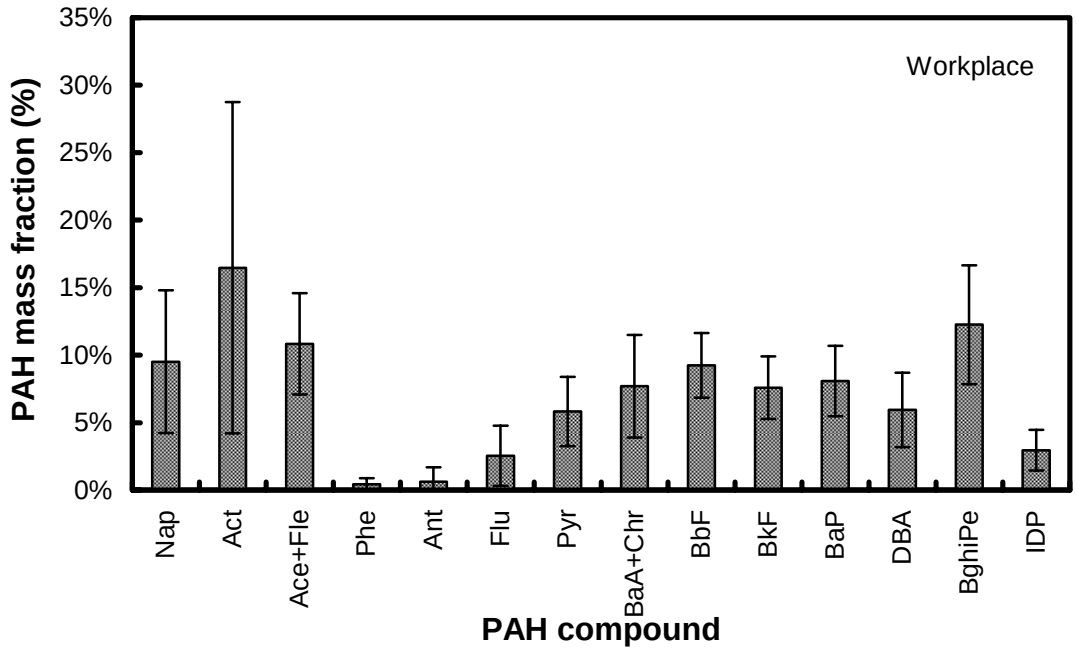

Figure 4.28 Average mass fraction of each PAH compound in TSP from workplace sampling (n = 47).

4.2.5 Size distribution of PAHs

Fig. 4.29 shows the mass ratio of PAH compositions in each particle size range at the workplace. The fractions of PAHs with larger molecular sizes (4-6 rings) are relatively high. This could be attributed very well to the particles generated from wood combustion in the source. Mass fraction of 4-6 ring PAHs were higher than 70% of total PAHs for particles smaller than 2-3 μm.

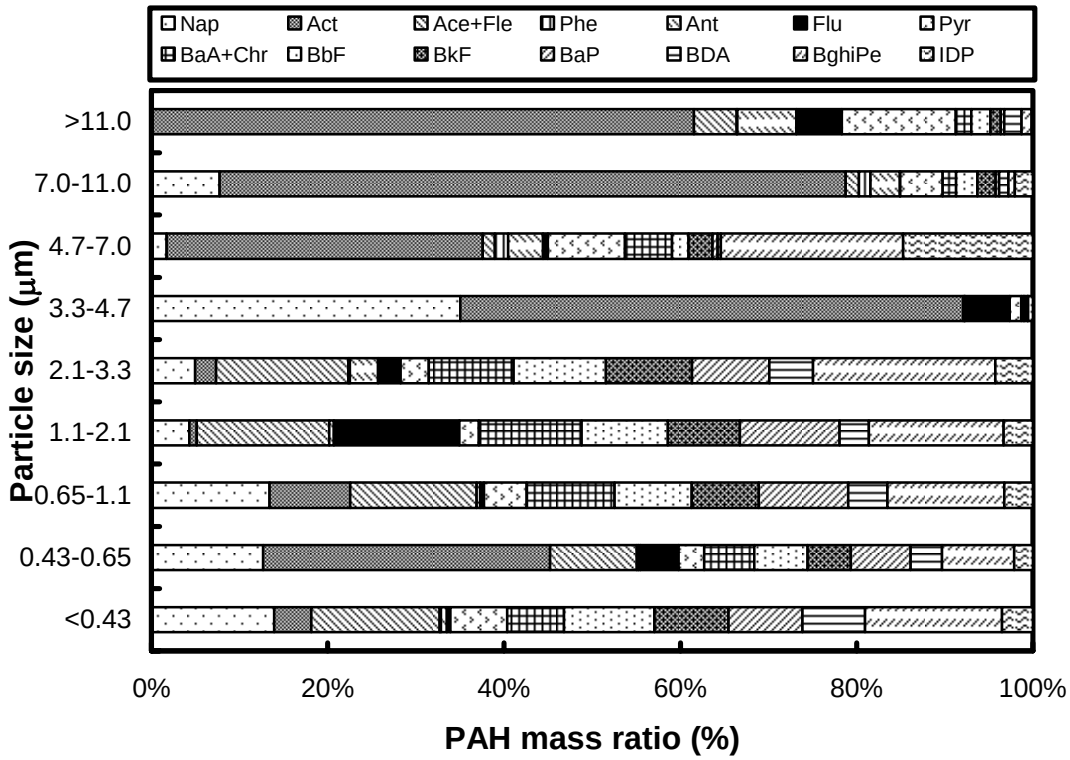

Figure 4.29 PAH mass ratio in each particle size range from workplace sampling sample #13.

4.3 Characteristics of ambient aerosol particles in Hat Yai City

In this section, the influence of smoke particles on atmospheric air of Hat Yai City, Songkhla Province, was evaluated. Physical and chemical characteristics of the ambient aerosol particles were investigated.

4.3.1 Size distribution of particles

The Size distribution of aerosol particles in Hat Yai City was measured using an identical eight-stage Andersen sampler (Dylec, AN 200). The samples were taken on the top floor of the four-story building of Computer Engineering Department, Faculty of Engineering, Prince of Songkla University (PSU) in Hat Yai City. The particle size distribution is shown in Fig. 4.30. The size distribution shows a bi-modal behavior, consisting of the accumulation mode aerosol (peak at 0.54 μm) from the

source emission and the coarse-mode (peak at 4.00 μm) probably from the soil dust from building and traffic.

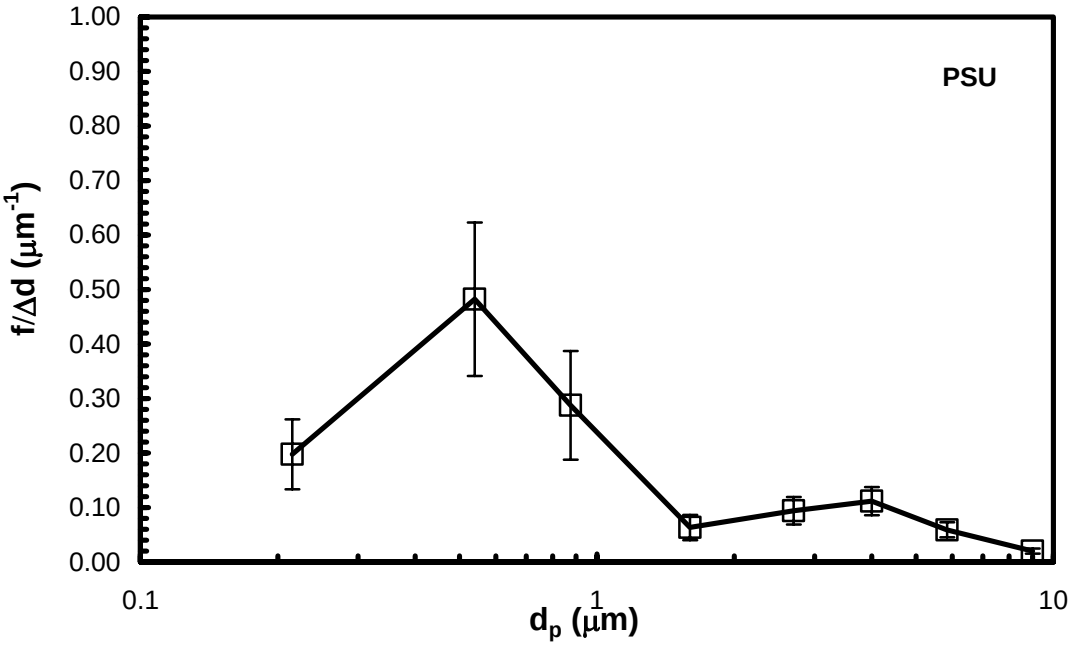

Figure 4.30 Size distribution of particulate matters from PSU sampling site.

4.3.2 Concentration of particles

The total suspended particulates (TSP) of ambient air from PSU sampling site were measured by using a portable high-volume air sampler (SIBATA, HV500F). TSP from PSU sampling site is about 31.86 μg m^{-3}. The variation of TSP ranged from 4.43 to 94.86 μg m^{-3}, with an average value of 31.86 ±16.63 μg m^{-3}.

Effect of RSS production

The effect of the amount of rubber-wood combustion on the particle concentrations was investigated. Fig. 4.31 shows monthly average TSP from the PSU sampling site during January 2006 to January 2007, along with RSS production from all rubber cooperatives in Songkhla Province. The relationship between the TSP and the RSS production is clear as shown in Fig. 4.32. An increase of RSS production linearly enhances the TSP. This probably indicates the contribution of RSS

production or, in turn, the amount of rubber-wood combusted in the RSS production, to the aerosol particles in the atmosphere of Hat Yai City.

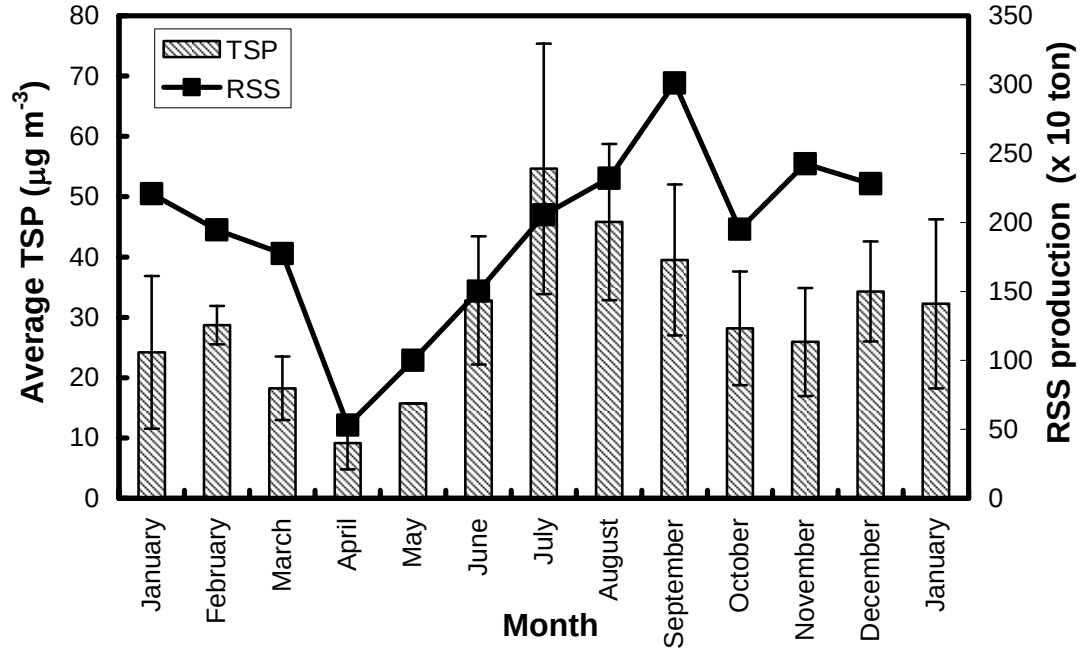

Figure 4.31 Effects of rubber production in Songkhla Province on the average monthly TSP of ambient air sampled from PSU during January 2006 to January 2007.

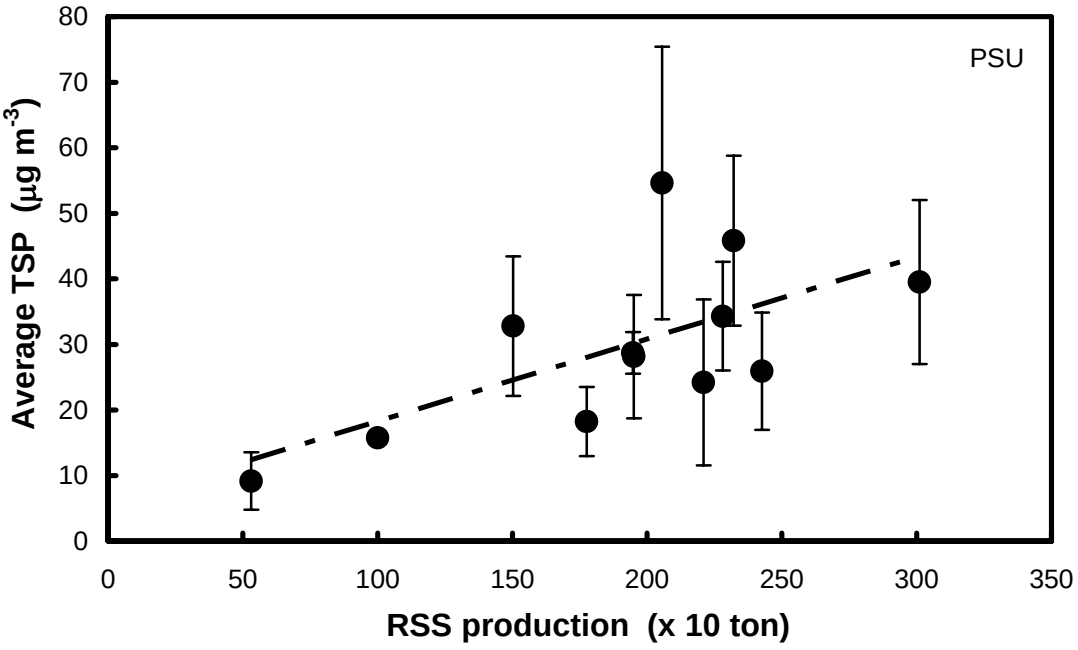

Figure 4.32 Relationship between the average monthly TSP at PSU and the RSS production.

Effect of precipitation

The effect of the precipitation on PM concentration was also observed. TSP is correlated to the meteorological conditions (Yang et al., 2005). Fig. 4.33 shows the monthly average of TSP, RSS production, and the precipitation during January 2006 to January 2007. The relationship between the amount of TSP and the precipitation during 3 periods for different wind directions is show in Fig. 4.34. The results indicate that TSP depends on the total precipitation, where the TSP decreases when the precipitation increases, during January-April and May-August. The results display a linear relation of TSP with precipitation. On the other hand, TSP increases slightly as the precipitation increases during September to December. This could be the effect of RSS production and wind direction. During this period the RSS production in Songkhla Province is higher than during other periods.

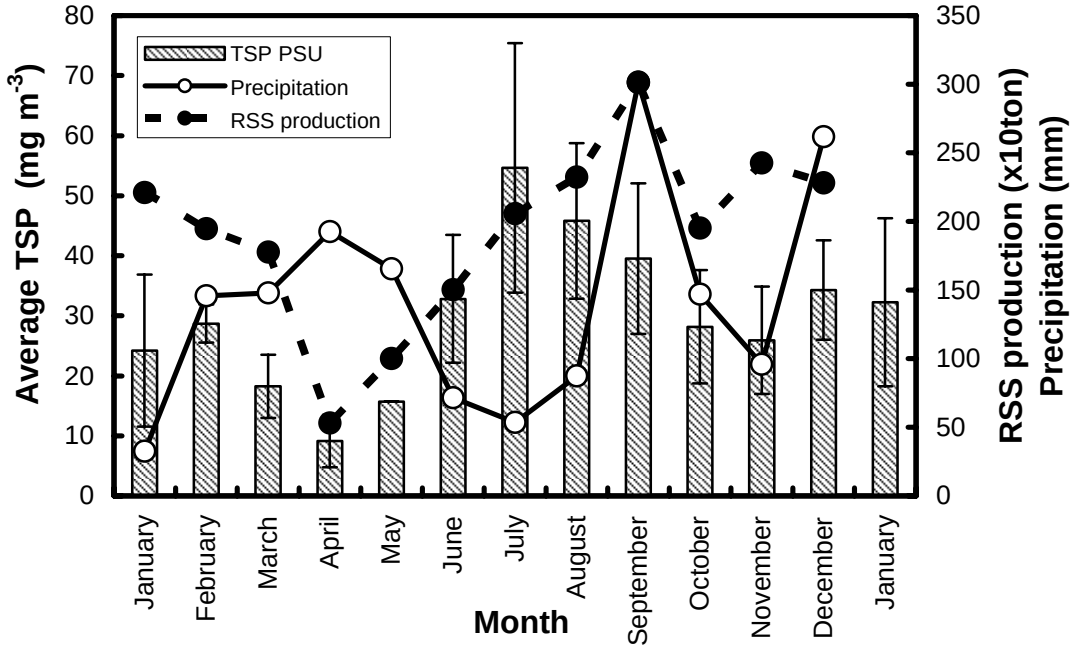

Figure 4.33 Average TSP of ambient air sampled from PSU, RSS production, and precipitation during January 2006 to January 2007.

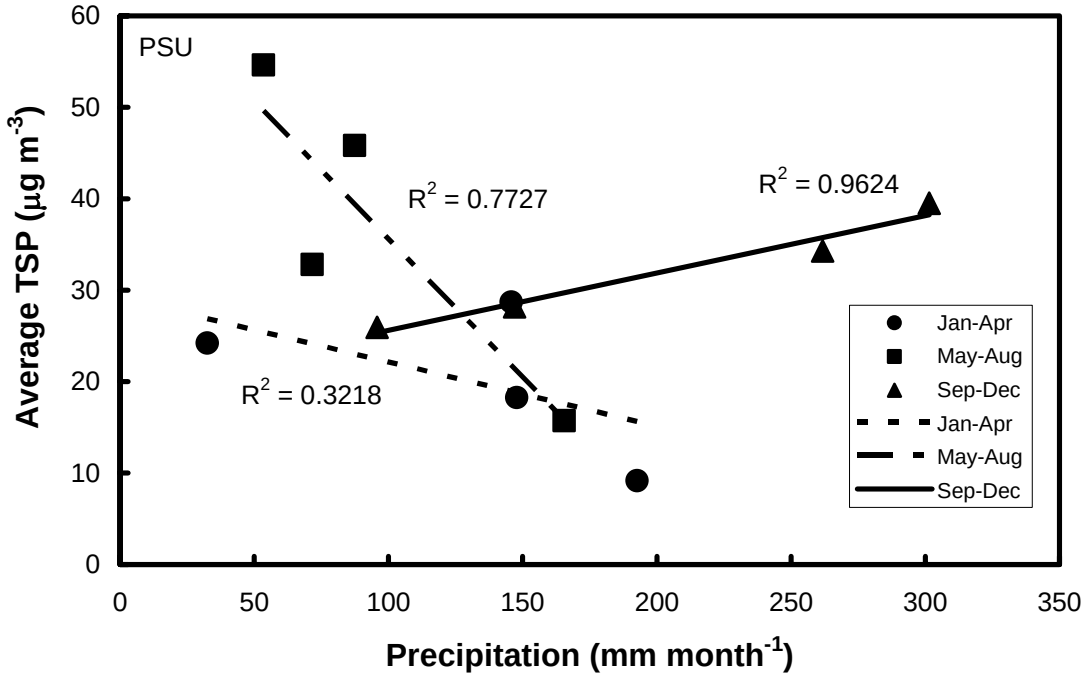

Figure 4.34 Relationship between the TSP and the precipitation at PSU for three periods in 2006.

4.3.3 Concentration of PAHs

TSP-bound PAH levels

Total PAH concentration refers to the sum of the concentration of 16 measured compounds. The total concentration of the 16 PAHs of samples from PSU sampling site varied from 1.17 to 18.29 ng m^{-3}. The average total PAH concentration at PSU is about ten times lower than that from the workplace. The maximum PAH concentration (18.29 ng m^{-3}) in ambient particles was observed on July 17, 2006, when the atmosphere in Hat Yai City was severely affected by smog from forest fires in Indonesia. In addition, the concentration of PAHs at PSU corresponds to the TSP. An increase of TSP linearly enhances the total PAH concentrations as shown in Fig. 4.35.

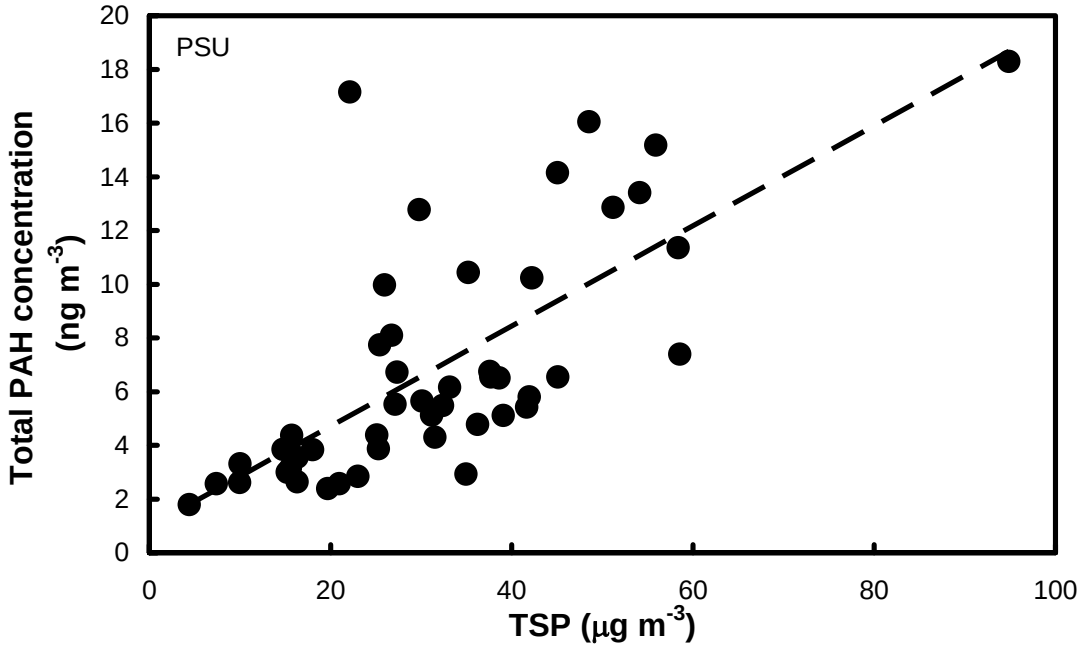

Figure 4.35. Relationship between the concentration of PAHs and TSP at PSU.

Effects of RSS production

The change of PAH concentration under various RSS production levels was also studied. Fig. 4.36 shows the monthly average PAH concentration and RSS production in 2006. A high RSS production level implies higher rubber-wood burning, and hence an increase in the smoke particles and higher total PAH concentrations are escalated.

The relationships between the concentrations of PAHs at PSU and RSS production in Songkhla Province are shown in Fig. 4.37 and 4.38 for total PAHs and 4-6 ring PAHs, respectively. The correlations exhibit trends, that the PAH concentration increases with respect to the RSS production. However, the correlations are not clear. This may result from the variation of air temperature, precipitation, and wind direction at the sampling site. For example, during September-December, the RSS production in Songkhla Province is high, while the precipitation at PSU is higher than 200 mm/month. The low correlation of PAHs concentration and RSS production in the year could partly result from the

precipitation in the rainy season. Moreover, PAHs at PSU sampling site were emitted from other sources, such as motor vehicle emissions.

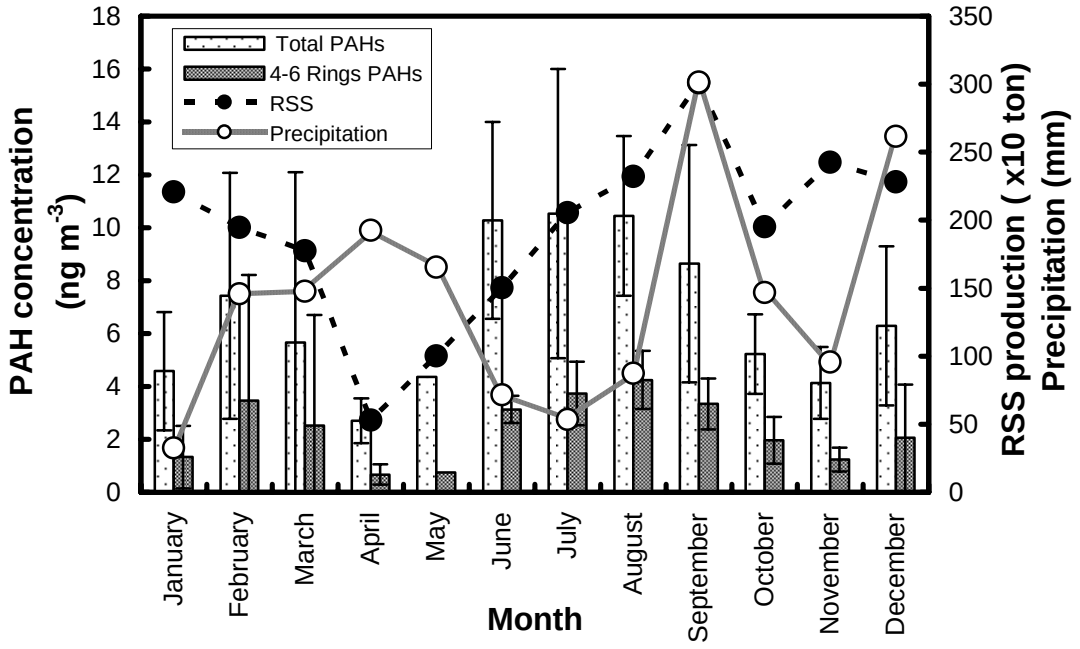

Figure 4.36 Average PAH concentration from PSU sampling, RSS production, and precipitation during January 2006 to January 2007.

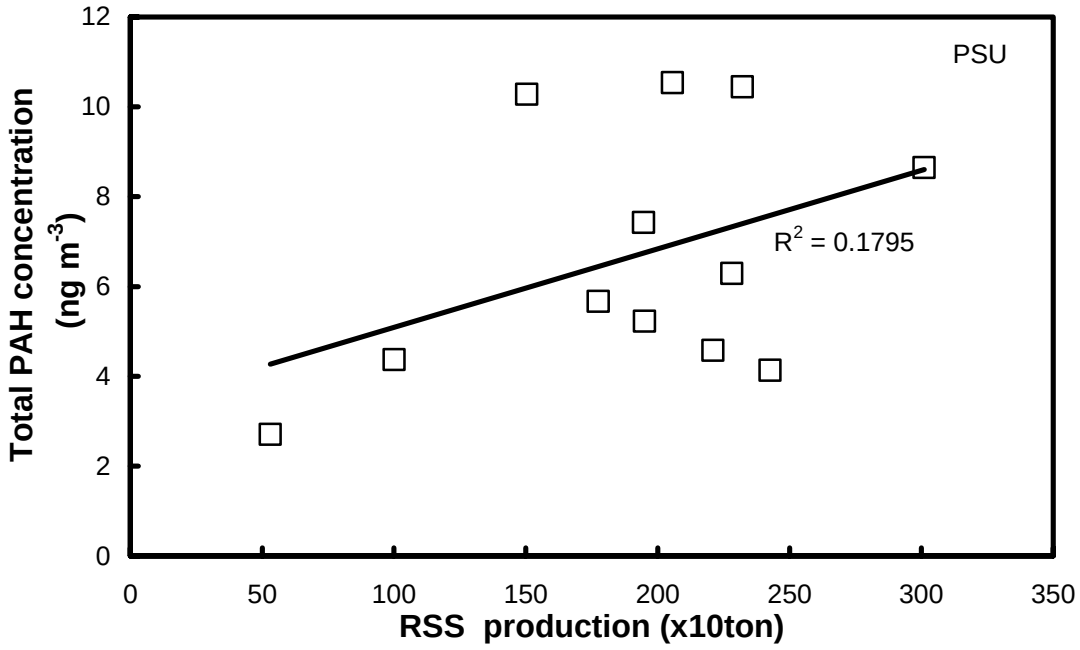

Figure 4.37 Relationship between total PAH concentration at PSU and RSS production.

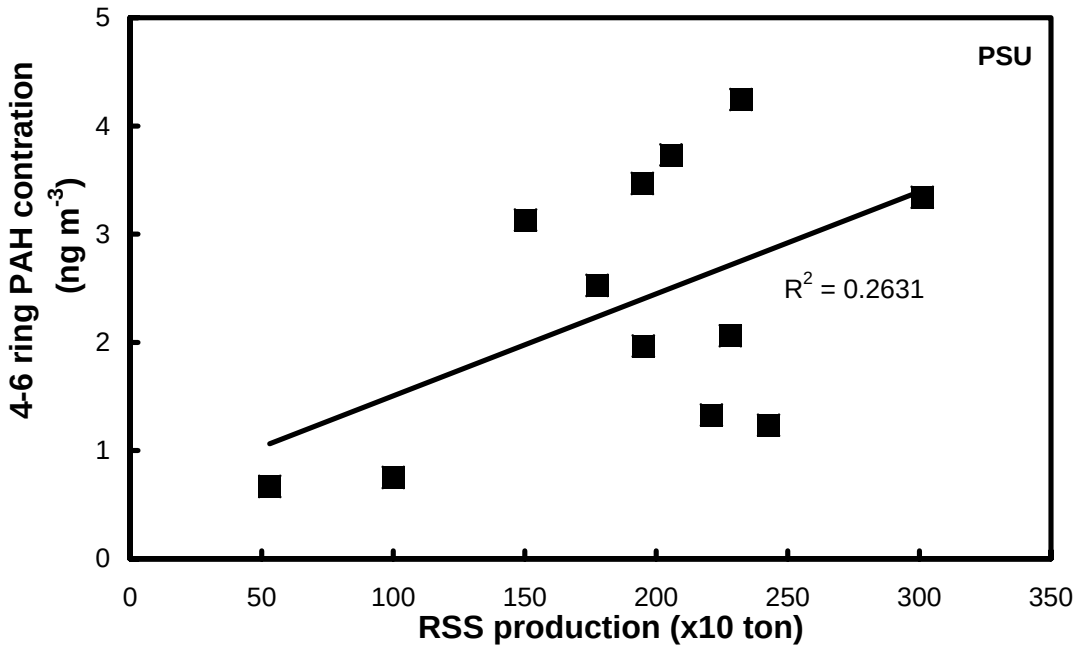

Figure 4.38 Relationship between concentrations of 4-6 ring PAHs at PSU and RSS production.

Effects of precipitation

The monthly precipitation in Songkhla Province in 2006 is shown in Fig. 4.36 along with the PAH concentration and RSS production. The result shows that the total PAHs and 4-6 ring PAH concentrations have a tendency to decrease when the precipitation increased as shown in Fig. 4.39 and 4.40, though they are not clear correlations. The concentration of total PAHs in ambient aerosol was lower than that from source and workplace sampling sites. The total PAH concentrations was highest in July with the maximum value of 10.53 ng m^{-3}, while the maximum value of 4-6 ring PAHs concentration occuredin August with a value of 4.24 ng m^{-3}. In April, the PAHs concentrations are lowest with values of 2.70 and 0.66 ng m^{-3} for total PAHs and 4-6 ring PAHs, respectively. The rubber sheet production level is also lowest in this month, while the precipitation is highest in this month.

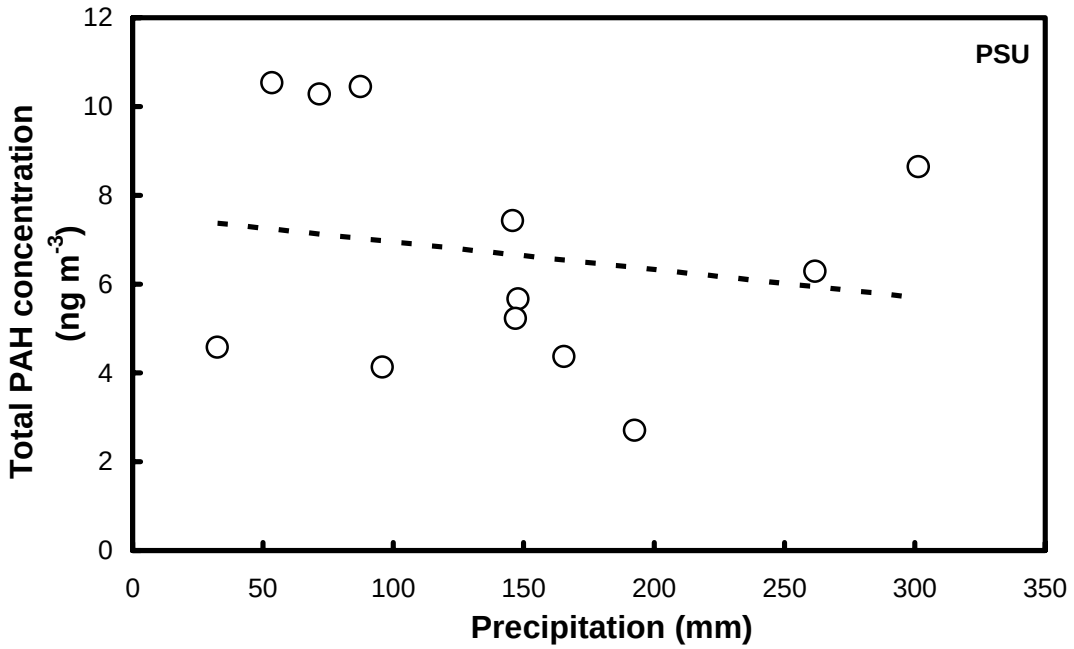

Figure 4.39 Relationship between total PAH concentration and the precipitation each month.

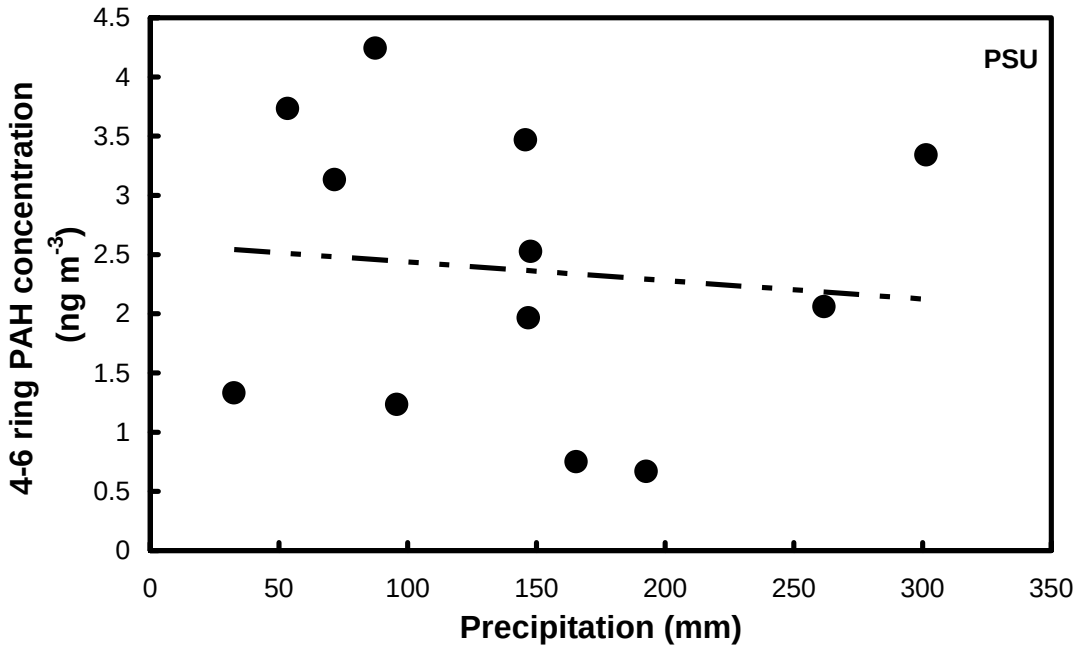

Figure 4.40 Relationship between 4-6 ring PAH concentration at PSU and precipitation.

Correlation with NO_2

The relationship between the concentrations of PAHs at PSU and NO_2 under various RSS production level was studied. NO_2 concentrations during sampling at PSU are shown in Fig. 4.41 along with the PAH concentrations. The result display that the concentrations of PAHs were correlated with the concentration of NO_2 with an r-squared values of 0.26 and 0.15 for total PAH and 4-6 ring PAH concentrations, respectively, as shown in Fig. 4.42. This weak correlation may be the effect of the precipitation in each sampling day, as the concentration of PAHs on particles were reduced with an increase of the precipitation. It was suggested that both NO_2 and PAHs arise from combustion sources (Park et al., 2002). More over NO_2 at PSU sampling site were emitted from other source, such as traffic emission and other combustion source.

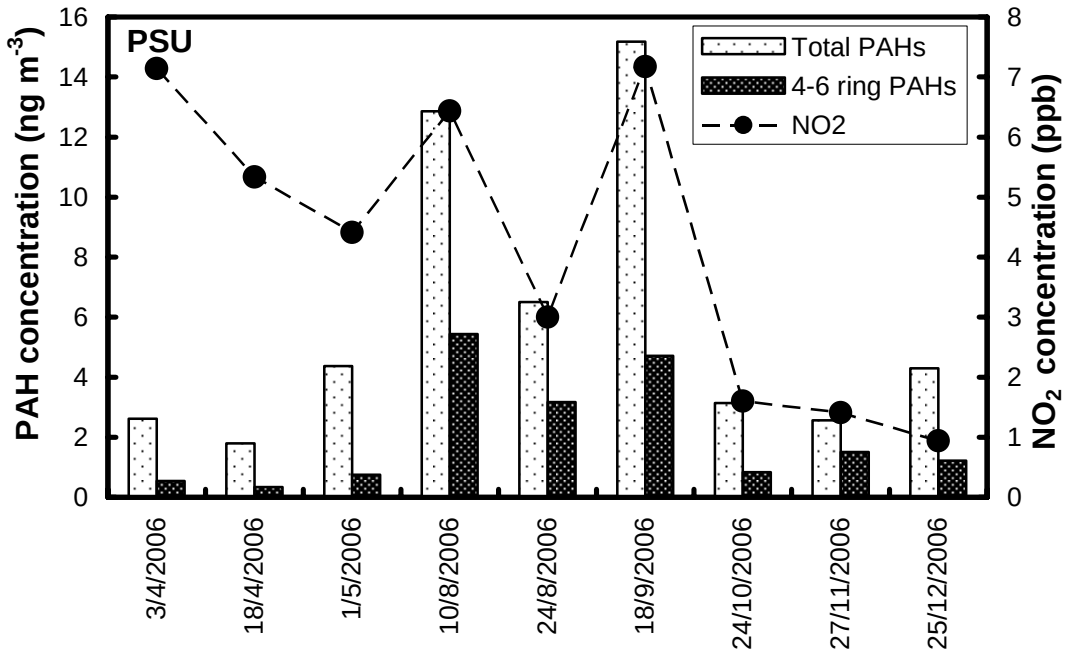

Figure 4.41 Concentrations of PAHs and concentrations of NO_2 at PSU during January 2006 to January 2007.

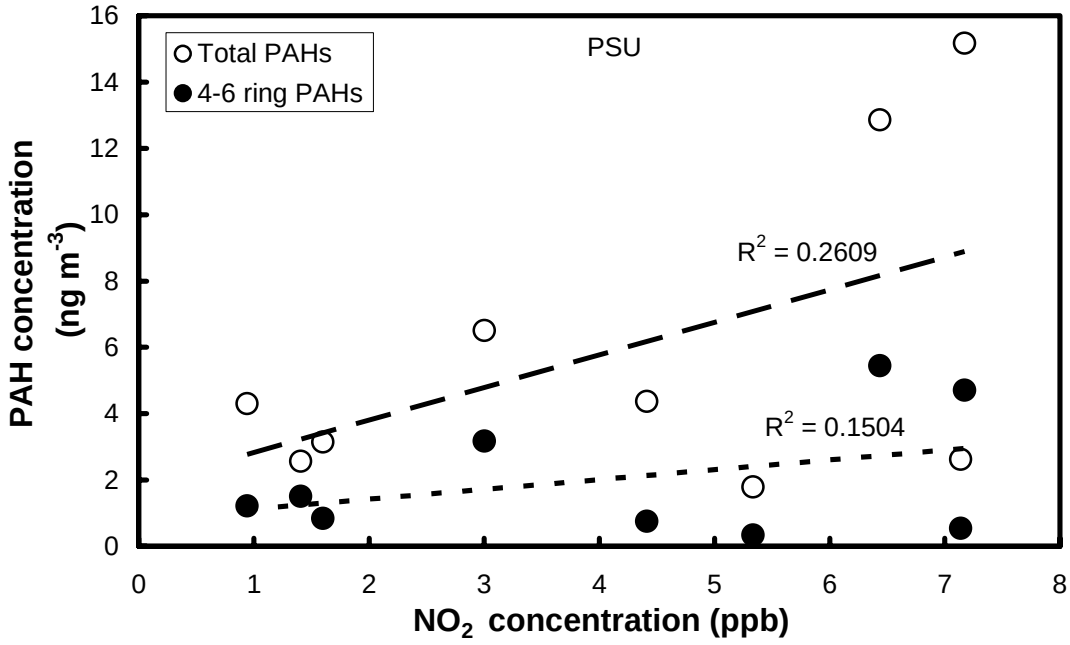

Figure 4.42 Relationship between concentrations of PAHs at PSU and concentration of NO_2.

4.3.4 Profile of PAHs

A profile of the average values of mass fraction for PAH compounds from the PSU samples is shown in Fig. 4.43. It is obvious that, Ace+Fle, Act, Nap, and BghiPe were predominant in this area. The 4-6 ring PAHs contributes to about 14.16-70.04% of the total PAHs. The variation may probably result from the temperature-dependence of PAHs gas-particle partitioning and other source emissions around the sampling site, especially at high ambient temperatures during the sampling period.

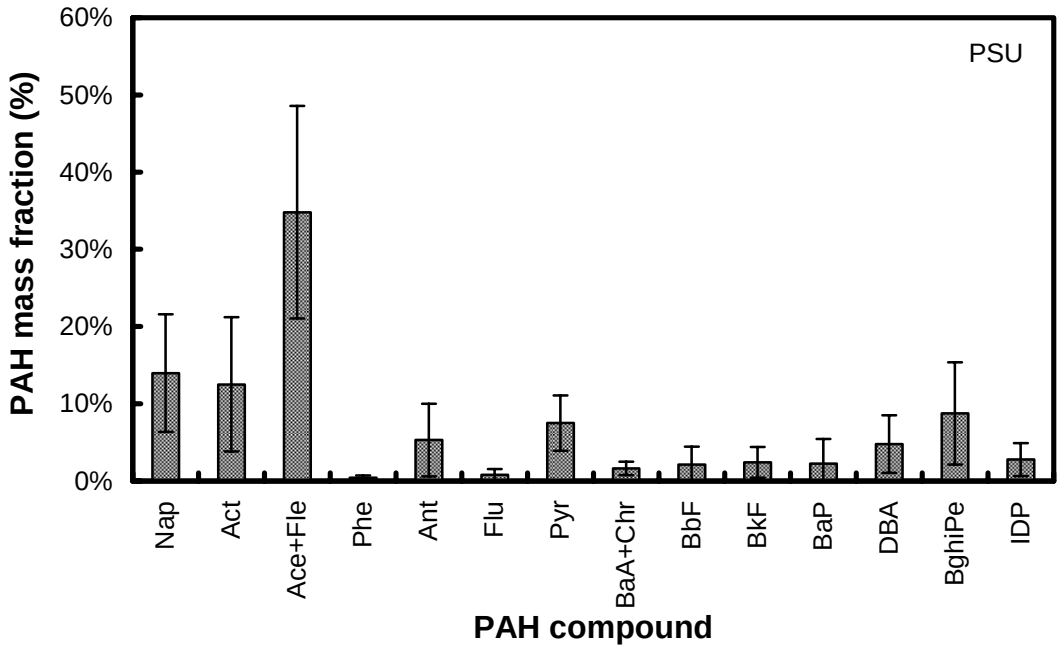

Figure 4.43 Average mass fraction of each PAH compound from PSU sampling (n = 47).

4.3.5 Size distribution of PAHs

Fig. 4.44 shows the mass ratios of PAH compositions at the PSU sampling site. Fractions of PAHs with larger molecular sizes with 4-6 rings show the highest values in the particle size range from 0.43 to 0.65 μm. The fraction of 2-3 rings PAHs compounds contribute more than 60% of the total PAHs for all particle size ranges.

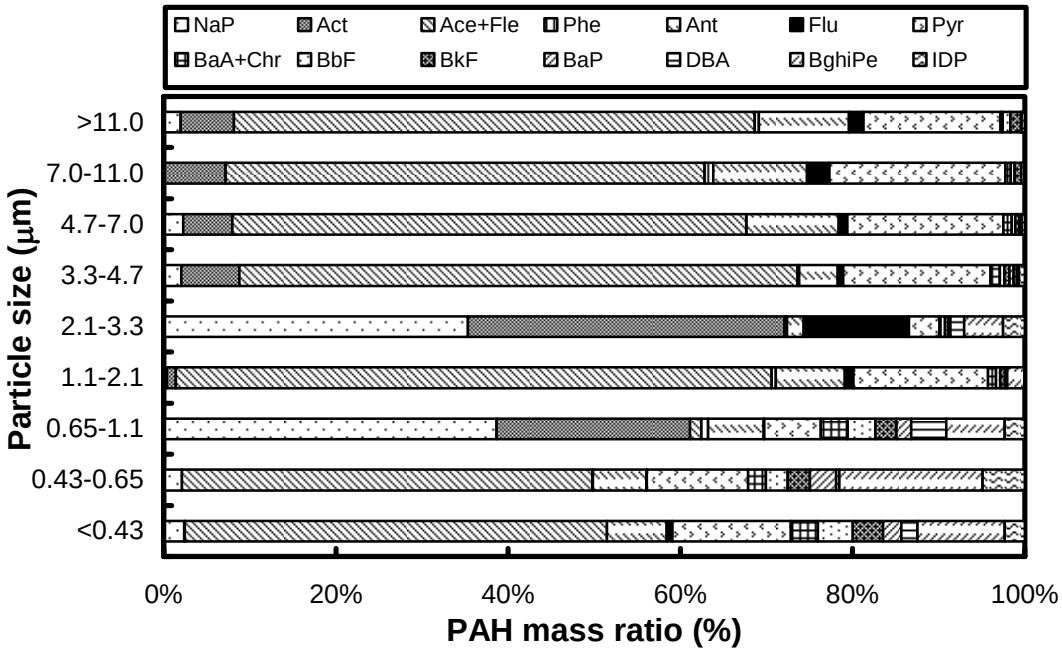

Figure 4.44 PAH mass ratio in each particle size range from PSU sampling (#13).

4.4 Comparison of particle characteristics in workplace and Hat Yai City

In this section, a comparative study between concentrations of particles and PAHs between workplace area and Hat Yai City are presented.

4.4.1 Concentrations of particles

The average TSP is about 15,806.11, 164.42 and 31.86 μg m^{-3} for particles sampled from source, workplace and Hat Yai City, respectively, as shows in Table 4.1. The TSP in workplace and ambient air at Hat Yai City are within the limit

regulated by the Thailand Pollution Control Department (330 μg m^{-3}) (http://www.pcd.go.th/info_serv/reg_std_airsnd01.html). TSP in the source is about two orders of magnitude higher than that in the workplace area.

Table 4.1 Average TSP at each sampling site.

Location	Sampling site	TSP (μg m^{-3})	SD
Source	1	15806.11	11739.67
WP	2	164.43	80.60
PSU	3	31.87	16.63

4.4.2 Concentrations of PAHs

The highest concentrations of total PAHs in TSP were observed in the source sampling site, followed by the workplace sampling. The concentration of PAHs in the source sampling was approximately hundred times higher than in the workplace area, while the concentrations of PAHs at PSU sampling site show a lower value. Average values and standard deviation of particulate PAH concentrations from source, workplace, and PSU sampling sites are listed in Table 4.2.

Table 4.2 Average concentration of PAHs at each sampling site.

Location	Total PAH concentration (ng m^{-3})		4-6 ring PAHs (ng m^{-3})	
	Average	SD	Average	SD
Source	21886.22	31952.62	15048.38	22668.71
WP	180.67	139.15	113.01	99.30
PSU	6.92	4.38	2.51	2.15

4.4.3 Size distribution of PAHs

Fig. 4.45 and 4.46, compare the total PAHs mass fraction and the concentration in particles for in each size range of particles sampled from workplace

and PSU. The PAH concentration in the workplace is about one order of magnitude higher than that in PSU, in almost all size ranges and especially for the fine particles smaller than 3-4 μm.

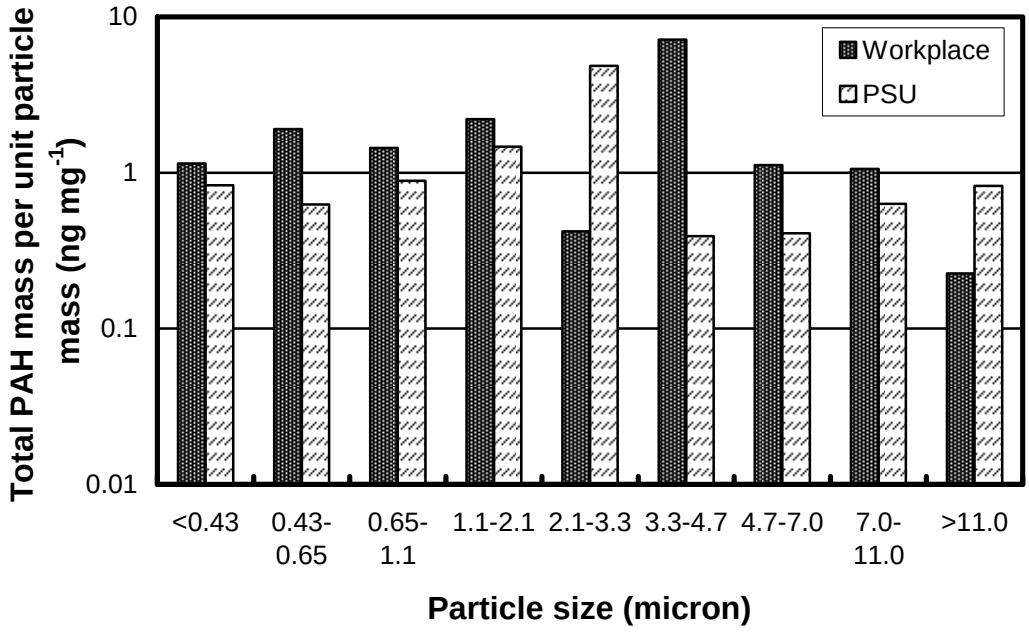

Figure 4.45 Total PAH mass per unit particle mass in each size of particles range of particles sampled at workplace and PSU.

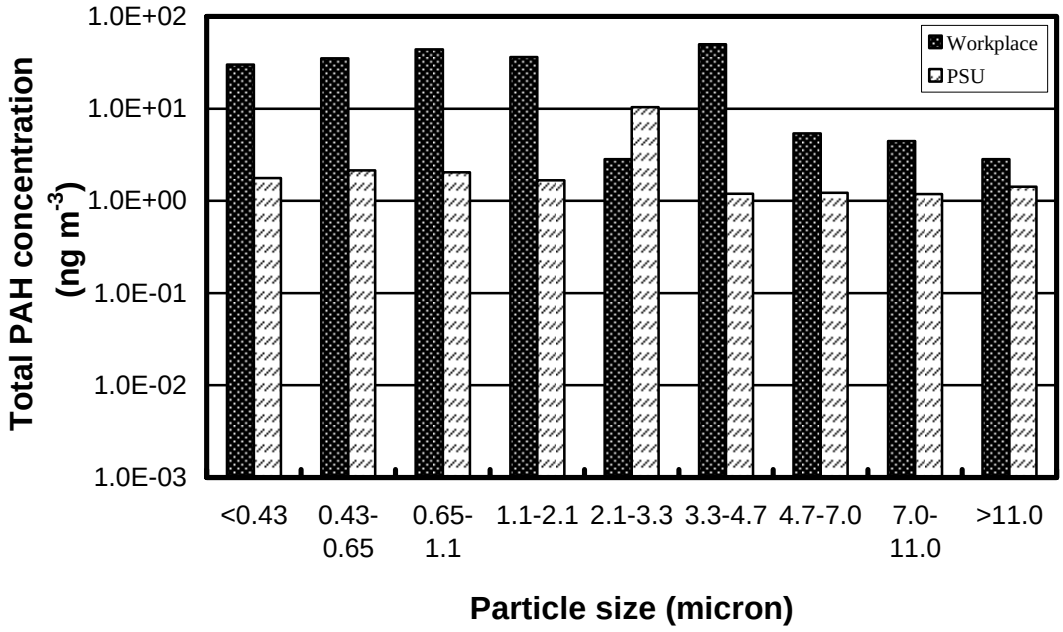

Figure 4.46 Total PAH concentration in each size range of particles sampled from workplace and PSU.

4.4.4 Profile of PAHs

Fig. 4.47 shows the contribution of each PAH to the total mass at each sampling site. The largest contributor to the total mass is different for the sampled air at each site. The largest contributor to the total mass for source and workplace were 4-6 rings PAHs, 64% and 62% to total mass for source and workplace sampling, respectively. This indicates the direct effect of smoke particles on the atmosphere in the working environment. The largest contributor to the total mass for PSU sampling was 2-3 ring PAHs, which accounted for 67%. Here, the effect of smoke particles to the city of Hat Yai seems to be less than to the workplace.

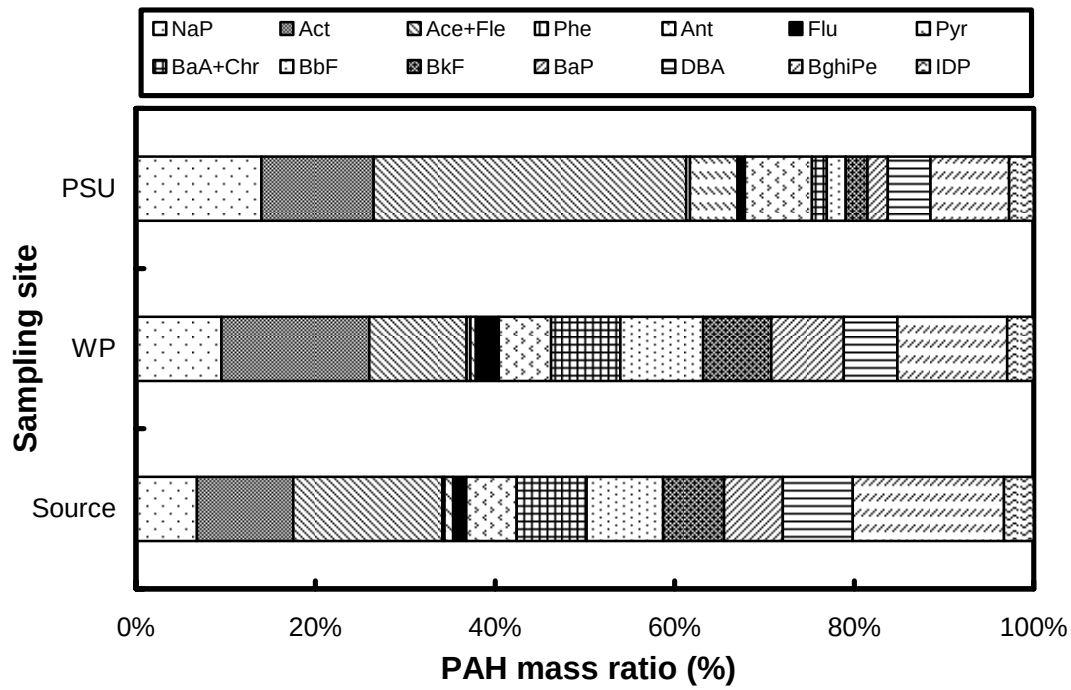

Figure 4.47 PAH mass ratio of samples from each sampling site.

4.4.5 Concentrations of NO_2

Fig. 4.48 shows a comparison of the concentration of NO_2 at the workplace sampling site 1, site 2, and PSU. Average concentrations of NO_2 at both sites of workplace and ambient air (PSU) were found to be less than the environmental standard value, which is 0.17 ppm.

(http://www.pcd.go.th/info_serv/reg_std_airsnd01.html).

The average concentration of NO_2 at PSU sampling site is about four times lower than that from workplace sampling. The maxima of NO_2 concentration at both sites of workplace were observed during the highest rubber production of cooperatives in the sampling period. The amount of rubber-wood used is proportional to the RSS production. It is clear that the concentration of NO_2, associated with the amount of rubber-wood used in combustion.

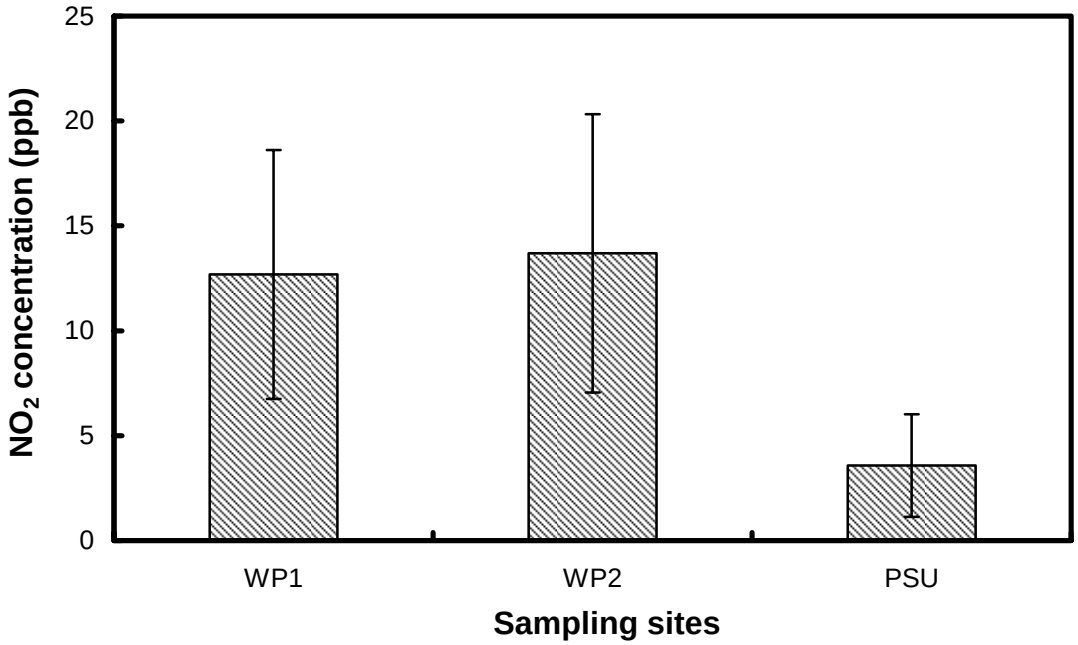

Figure 4.48 Average concentration of NO_2 at each sampling site and PCD standard (0.17 ppm for NO_2).

4.5 Source apportionment

In this section, the effects of wind direction on the relationship between the concentration of PAHs in ambient particles and the RSS production in Songkhla Province were investigated.

Frequency distributions of wind direction in 2006 are plotted in Fig. 4.49 (a), (b) and (c) for January-March, April-August, and September-December, respectively. The relationships between the PAH concentration and the RSS are show in Fig. 4.50 to 4.52. The correlations exhibit a linear increase of the 4-6 ring PAH concentration with respect to the RSS production for April-August and September-

December. The correlation is good with an r-squared value of 0.92 during April-August (Fig. 4.50), while during September-December the r-squared value is 0.4 (Fig.4.51). This weak correlation may be the effect of higher precipitation in this period. On the other hand the 4-6 rings PAH concentration during January-March shows an inverse correlation with the RSS as shown in Fig. 4.52. The concentration of PAHs decreased when the RSS production increased. During this period, the wind direction is east-northeast or from the Gulf of Thailand. This may be the reason why PAHs concentration is independent from the rubber sheet production in this period, while during April-August, the wind direction is west-southwest, where most of the wood-smoke generation sources are located upstream of the wind. This could be a reason for the strong correlation.

It is obvious that rubber-wood combustion in the rubber sheet smoking process was a source of air pollution in Hat Yai City. The high rubber sheet production implied higher rubber-wood burning in smoking cooperatives and, hence, the higher amounts of smoke particles and total PAH concentration.

The wind patterns affect the transport of aerosol particles in atmospheric air. The stability of the weather conditions and the ability to disperse are factors that profoundly influence the air quality of the urban areas of Hat Yai.

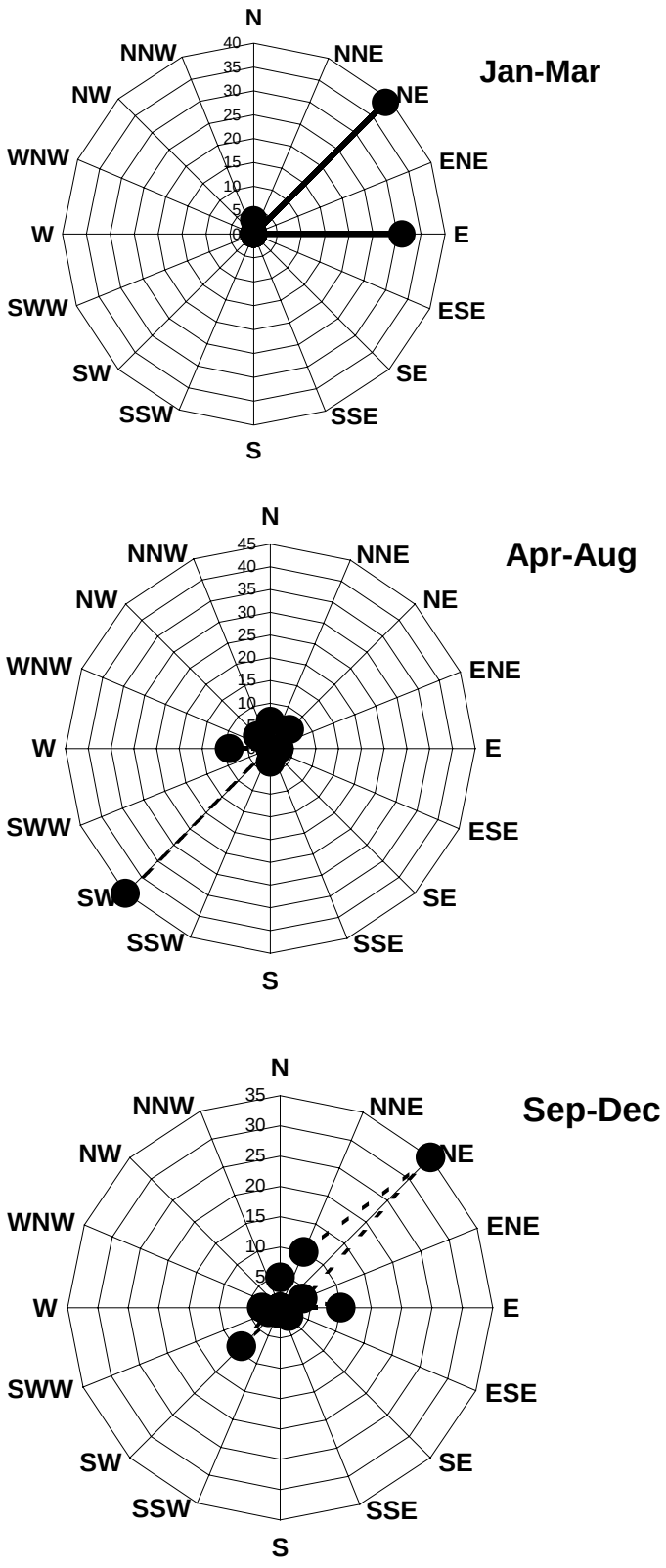

Figure 4.49 Frequency distribution of wind directions for three periods in Yai City in 2006.

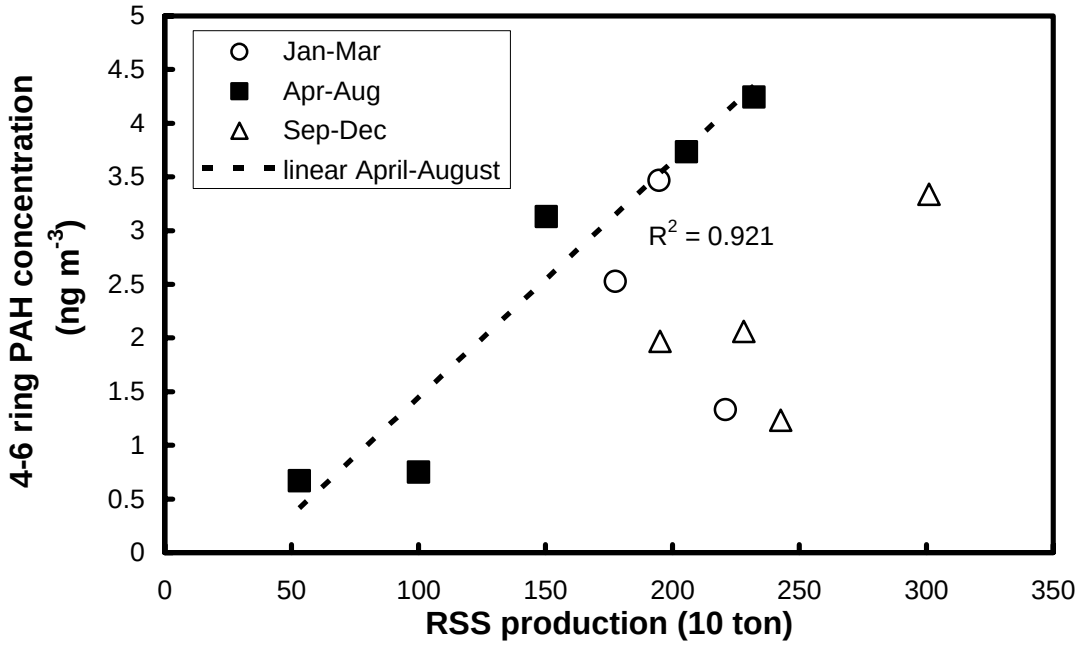

Figure 4.50 Relationship between concentrations of 4-6 ring PAHs at PSU and RSS production during April- August 2006.

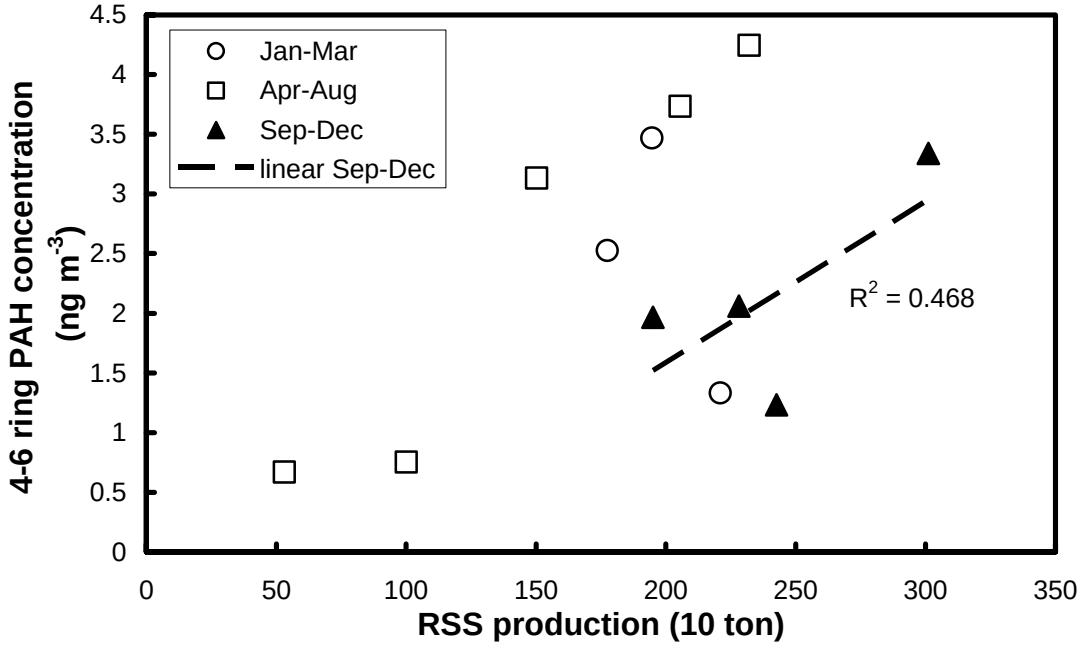

Figure 4.51 Relationship between concentrations of 4-6 ring PAHs at PSU and RSS production during September-December 2006.

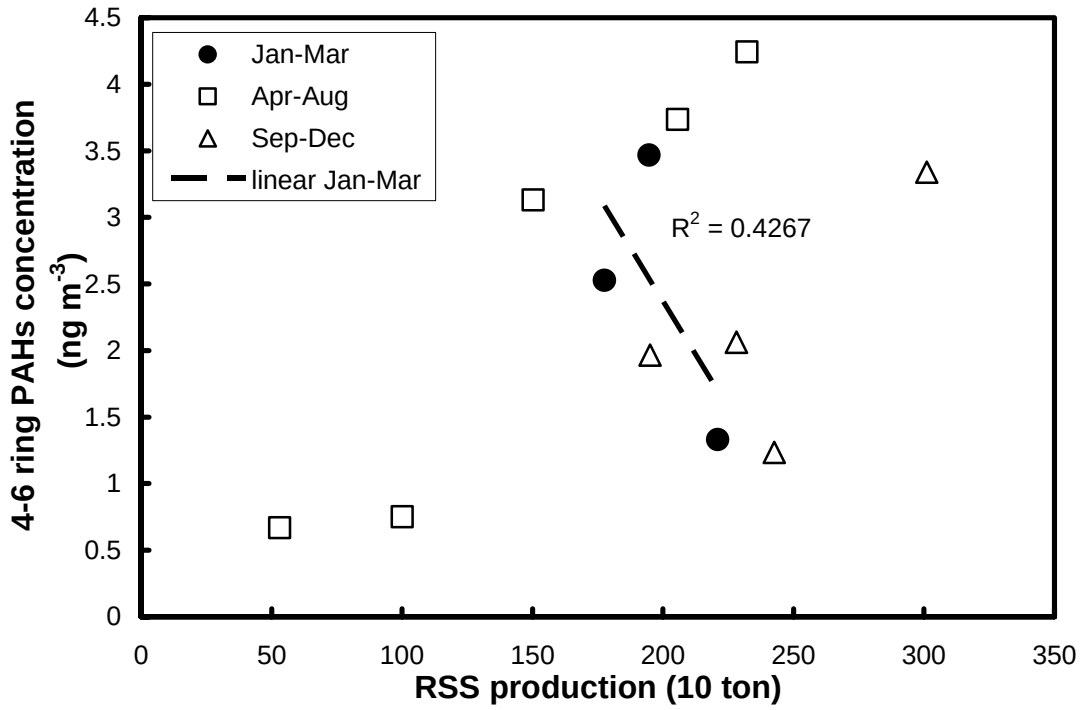

Figure 4.52 Relationship between concentrations of 4-6 ring PAHs at PSU and RSS production during January-March 2006.

CHAPTER 5
CONCLUSIONS

5.1 Conclusions

Physical and chemical characteristics of smoke particles from rubber-wood combustion in a rubber sheet smoking cooperative were studied. Ambient air in a workplace area and in Hat Yai City was evaluated to investigate the effect of the wood combustion. All samples were collected between January 2006 and January 2007. As a result of the present experimental study, the following conclusions can be reached:

(1) The smoke particle size distribution from source sampling measured using an 8-stage Andersen Sampler shows a single-mode behavior. the mass median aerodynamic diameter (MMAD) is 0.68 μm.

(2) The particle size distributions of workplace and ambient air show bi-modal behavior, with the accumulation-mode peak taking place at 0.54 μm particle size, and the coarse-mode peak taking place at 4.0 μm.

(3) The average total smoke concentration is about 15,806.11 μg m^{-3}. The total smoke concentration depends on the wood moisture content. An increase of the wood moisture content exponentially enhances the smoke concentration. The total smoke concentration also depends on the wood burning period. The smoke particles were reduced as the combustion time progresses.

(4) The average TSP in workplace sampling is about 164.42 μg m^{-3}. The TSP in workplace depends on RSS production. An increasing of the RSS production linearly enhances the TSP.

(5) The average TSP at PSU is about 31.86 μg m^{-3}. It depends on RSS production, precipitation, and wind direction. TSP decreased almost linearly when the precipitation increased.

(6) The average concentration of total PAHs from source is about 21,886.22 ng m^{-3}. PAH concentration in smoke particles depends on fuel wood moisture content. Increase of wood moisture content powerfully increases the PAH concentration. During the combustion, the PAH concentration is reduced as the time progresses. The correlation demonstrates a power function of PAH concentration with respect to the smoke particle concentration.

(7) The average concentration of total PAHs in workplace is about 180.67 ng m^{-3}. The PAH concentration is influenced by the RSS production.

(8) The average concentration of total PAHs at ambient air of PSU is about 6.92 ng m^{-3}. This behaviors of the PAH concentration is influenced by the precipitation, RSS production, and wind direction in a similar trend like those of TSP.

(9) The PAHs concentration inside the workplace was higher, particularly with larger numbers of aromatic rings in the fine fraction of particles, which may lead to serious health problems of the workers.

(10) The PAH distribution patterns varied with the sampling sites. Particle-bound PAHs from source and workplace are dominated by 4-6 ring PAH compounds, while PAHs from PSU are dominated by 2-3 ring PAH compounds.

(11) TSP and PAH concentrations in PSU are correlated with the amount of total rubber-wood combustion in Songkhla Province. However, the effect of smoke particles and PAHs to the city of Hat Yai seems to be less. This is because TSP and PAH concentration in PSU ambient air are low due to the decomposition of PAHs by sunlight. Moreover, PAH and TSP in PSU ambient may be affected by particulates emitted from diesel-engine vehicles.

5.2 Recommendation for future work

This study found that the particles and PAHs affected by the rubber-wood moisture contents and wood burning period. However, some experimental parameters could not be controlled, including excess air ratio and combustion temperature of rubber-wood combustion in the smoking room. Therefore, future work should be carried out under controlled conditions in the laboratory, to study the effects of fuel properties, furnace type, combustion temperature, excess air ratio, and the flue gas composition on particles and PAHs emitted. The information is important in the development of conditions of rubber-wood combustion in rubber smoking processes for control strategies leading to better air quality.

REFERENCES

Ecochem Analytic. PAHs. 2008.
http:// www.ecochem.biz/PAH/pah_primer.htm. (accessed 20/5/08), part of General Information about PAHs. Ecochem.biz/ (accessed 20/5/08).

PCD. Air Quality and Noise Standard. 2008.
http://www.pcd.go.th/info_serv/reg_std_airsnd01.html. (accessed 27/5/08), part of Air Quality Standards. http://www.pcd.go.th/ (accessed 27/5/08).

Bi,X., Sheng, G., Peng, P., Zhang, Z. and Fu, J. 2002. Extractable organic matter in PM10 from Liwan district of Guangzhou City, PR China, The science of The Total Environment. 300: 213-228.

Chao, C.Y.H., Kwong, P.C.W., Wang, J.H., Cheung, C.W. and Kendall, G. 2008. Co-firing coal with rice husk and bamboo and the impact on particulate matters and associated polycyclic aromatic hydrocarbon emissions, Bioresource Technology. 99: 83-93.

Choosong, T., Furuuchi, M., Tekasakul, P., Tekasakul, S., Chomanee, J., Jinno, T., Hata, M. and Otani, Y. 2007. Working environment in a rubber sheet smoking factory polluted by smoke from biomass fuel burning and health influences to workers, Ecotechnology. 13: 91-96.

Duan, J., Bi, X., Tan, J., Sheng, G. and Fu, J. 2005 The differences of the size distribution of polycyclic aromatic hydrocarbons (PAHs) between urban and rural sites of Guangzhou, China, Atmospheric Research. 78: 190-203.

Francisco, J., Juan, H., Ayala, M and Venerando, G. 2005. Emission of polycyclic aromatic hydrocarbons from combustion of agricultural and sylvicultural debris, Atmospheric Environment. 39: 6654-6663.

Furuuchi, M., Tekasakul, P., Murase, T., Otani, Y., Tekasakul, S. and Bai, Y. 2006. Characteristics of particulate emitted from rubber-wood burning, Journal of Ecotechnology Research. 12: 135-139.

Hays, M. D., Smith, N. D., Kinesy, J., Dong, Y. and Kariher, P. 2003. Polycyclic aromatic hydrocarbon size distribution in aerosol from appliances of residential wood combustion as determined by direct thermal desertion-GC/MS, Journal of Aerosol Science. 34: 1061-1084.

Hedberg, E., Kristensson, A., Ohlsson, C., Johnsson, P., Swietlicki, E., Vesely, V., Wideqvist, U. and Westerholm, R. 2002. Chemical and physical characterization of emission from brich wood combustion in a wood stove, Atmospheric Environment. 36: 4823-4837.

Leo, M.L. 2006. Polycyclic aromatic hydrocarbons. In: Chromatographic Analysis of the Environment, 3rd Ed. Boca Raton London: New York., Vol 93, pp 555-616.

Kalasee, W., Tekasakul, S., Otani, Y. and Tekasakul, P. 2003. Characteristic of soot Particles Produced from Rubberwood Combustion," Proceeding of the 2nd Asian Particle Technol. Penang, Malaysia, 2003. pp. 103-108.

Miguel, A. H., Eiguren-Fernandez, A., Jaques, P.A., Froines, J. R., Grant, B. L., Mayo, P. R. and Sioutas, C. 2004. Seasonal variation of the particle size distribution of polycyclic aromatic hydrocarbons and of major aerosol species in Claremont, California, Atmospheric Environment. 38: 3241-3251.

Martinis, D., Okamoto, A., Kado, N., Gundel, A. and Carvalho, R.F. 2002. Polycyclic aromatic hydrocarbons in a bioassay-fractionated extract of PM_{10} collected in Sao Paulo, Brazil, Atmospheric Environment. 36, 307-314.

Nielsen, T., Jsrgensen, E., Larsenb, J and Poulsenb, M. 1996. City air pollution of polycyclic aromatic hydrocarbons and other mutagens: occurrence, sources and health effects, The Science of the Total Environment. 189/190: 41-49.

Oanh, N.T.K., Albina, D.O., Ping, L. and Wang, X. 2005. Emission of particulate matter and polycyclic aromatic hydrocarbons from select cookstove-fuel systems in Asia, Biomass and Bioenergy. 28:579-590.

Oanh, N.T.K., Reuterga, L., Dung, N.,Yu, M and Yao, W. 2000. Polycyclic aromatic hydrocarbons in the airborne particulate matter at a location 40 km north of Bangkok, Thailand, Atmospheric Environment. 34: 4557-4563

Odabasi, M., Vardar, N., Sofuoglu, A., Tasdemir, Y. and Holsen, T. M. 1999. Polycyclic aromatic hydrocarbons (PAHs) in Chicago air, The Science of Total Environment. 227: 57-67.

Part, S.S., Kim, J.Y. and Kang, H.C. 2002. Atmospheric polycyclic aromatic hydrocarbons in Seaul, Korea, Atmospheric Environment. 36: 2917-2914.

Rehwagen, M., Muller, A., Massolo, L., Herbarth, O.and Ronco, A. 2005. Polycyclic aromatic hydrocarbons associated with particles in ambient air from urban and industrial areas, Science of the Total Environment. 348: 199-210.

Robinson, K.A. 1987. Chemical Analysis. Boston: Little Brow and Company. pp. 196-197.

Poppi, N. and Silva, M. 2005. Polycyclic aromatic hydrocarbons and other selected Organic compounds in ambient air of Campo Grande Coty, Brazil, Atmospheric Environment. 39: 2839-2850.

Promtong, M. and Tekasakul, P. 2007. CFD study of flow in natural rubber smoking-Room: I Validation with the present smoking-room, Applied Thermal Engineering. 27: 2113-2121.

Saez, F., Cabanas, A., Gonzalez, A., Murillo, J.M., Martinez, J.M., Rodriguez, J.J and Dorronsoro, J.L. 2003. Cascade impactor sampling to measure polycyclic aromatic hydrocarbons from biomass combustion processes, Biosystems Engineering. 86: 103-111.

Tang, N., Hattori, T., Taga, R., Igarashi, K., Yang, X., Tamura, K., Kakimoto, H., Mishukov, V.F., Toriba, A., Kizu, R. and Hayakawa, K. 2005. Polycyclic aromatic hydrocarbons and nitropolycyclic aromatic hydrocarbons in urban air particulates and their relationship to emission source in the Pan-Japan Sea countries, Atmospheric Environment. 39: 5817-5826.

Tekasakul, P., Furuuchi, M., Otani, Y., Tekasakul, S. and Sakano, T. 2005. Characteristics of particulate matters emitted from Rubberwood Burning and Effect on Atmospheric Air in Hat Yai, Thailand, Proceedings of AAC 2005, Mumbai, India, December 13-16.

Tekasakul, S., Tantichaowanan, M., Otani, Y., Kuruhongsa, P.and Tekasakul, P. 2006 Removal of soot particles in rubber smoking chamber by electrostatic precipitator to improve rubber sheet color, accepted for publication towards Aerosol and Air Quality Research Journal. 6: 1-14.

Tsapakis, M. and Stephanou, E.G. 2005. Occurrence of gaseous and particulate polycyclic aromatic hydrocarbons in the urban atmosphere: study of source and ambient temperature effect on the gas/particle concentration and distribution, Environmental Pollution. 133: 147-156.

Venkataraman, C., Thomas, S. and Kullkarni, P. 1999. Size distributions of polycyclic hydrocarbons-gas/particle partitioning to urban aerosols, Aerosol Science. 30: 759-770.

Venkataraman, C., Negi, G., Sardar, S.B. and Rastogi, R. 2002. Size distributions of polycyclic aromatic hydrocarbons in aerosol emission from biofuel combustion, Journal of Aerosol Science. 33: 503-518.

APPENDIX A

Table A-1 Concentration of 16 PAHs standard mix solutions at each level.

No.	Polycyclic aromatic hydrocarbon	Concentration (μg ml^{-1})				
		1st	2nd	3rd	4th	5th
1	Naphthalene	10.52	5.26	2.63	1.05	0.53
2	Acenaphthylene	21.03	10.52	5.26	2.10	1.05
3	Fluorene	12.65	6.3	3.16	1.26	0.63
4	Acenaphthene	1.03	0.52	0.26	0.10	0.05
5	Phenanthrene	1.04	0.52	0.26	0.10	0.05
6	Anthracene	2.14	1.07	0.53	0.21	0.10
7	Fluoranthene	0.97	0.48	0.24	0.10	0.05
8	Pyrene	2.09	1.04	0.52	0.21	0.10
9	Benz(a)anthracene	2.10	1.05	0.52	0.21	0.10
10	Chrysene	1.04	0.52	0.26	0.10	0.05
11	Benzo(b)fluoranthene	1.07	0.53	0.27	0.11	0.05
12	Benzo(k)fluoranthene	2.07	1.03	0.52	0.21	0.10
13	Benzo(a)pyrene	2.06	1.03	0.52	0.21	0.10
14	Dibenzo(a,h)anthracene	1.02	0.51	0.25	0.10	0.05
15	Benzo(g,h,i)perylene	10.52	5.26	2.63	1.05	0.53
16	Indeno(1,2,3-cd)pyrene	21.03	10.51	5.26	2.10	1.05

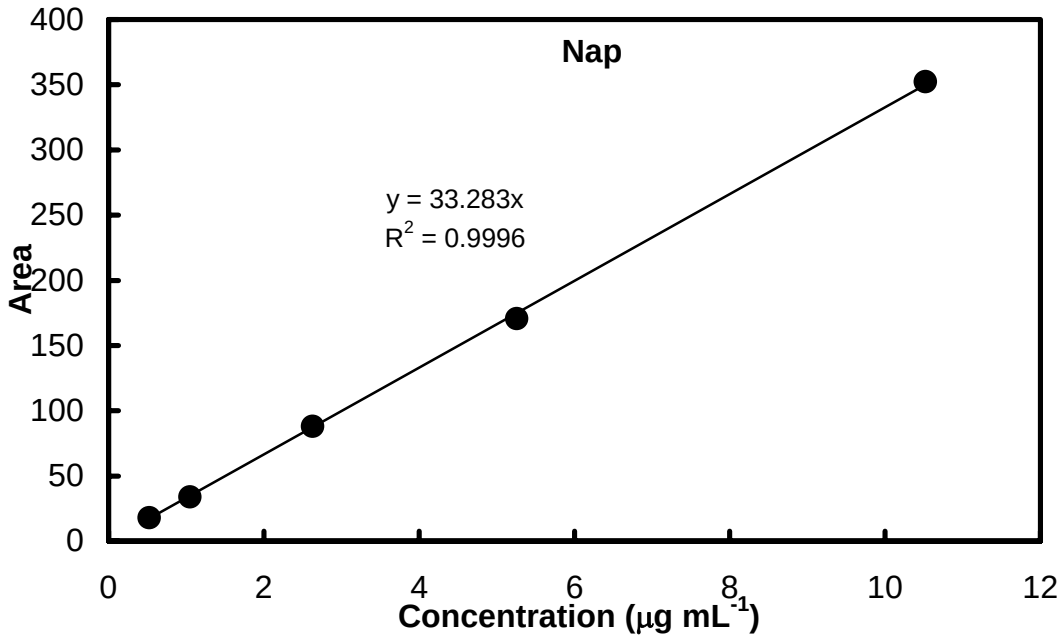

Figure A-1 Standard calibration curve of Naphthalene.

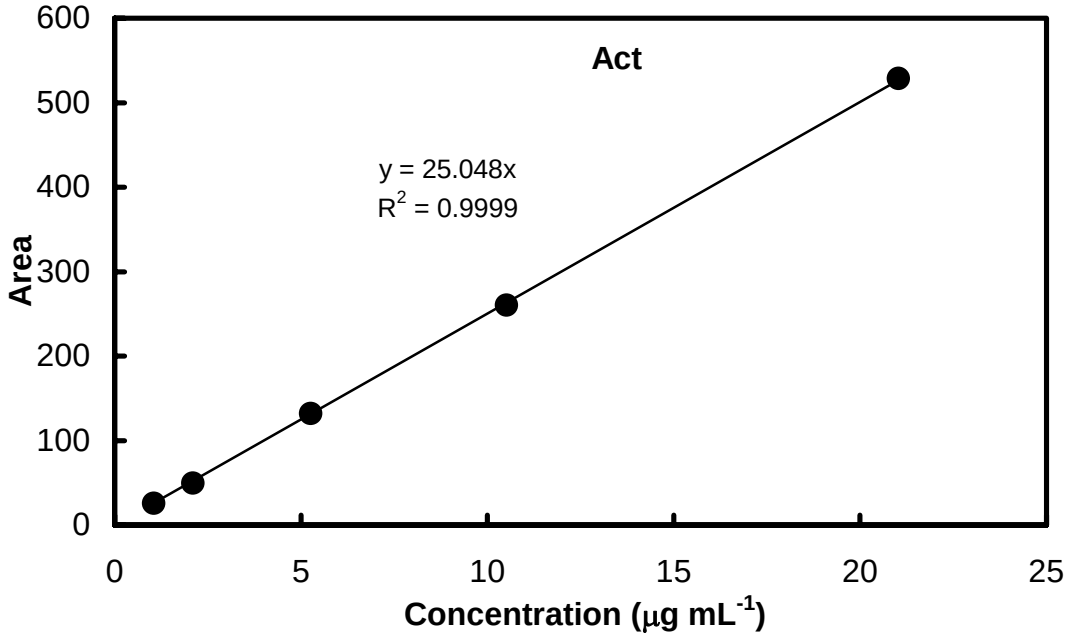

Figure A-2 Standard calibration curve of Acenaphthylene.

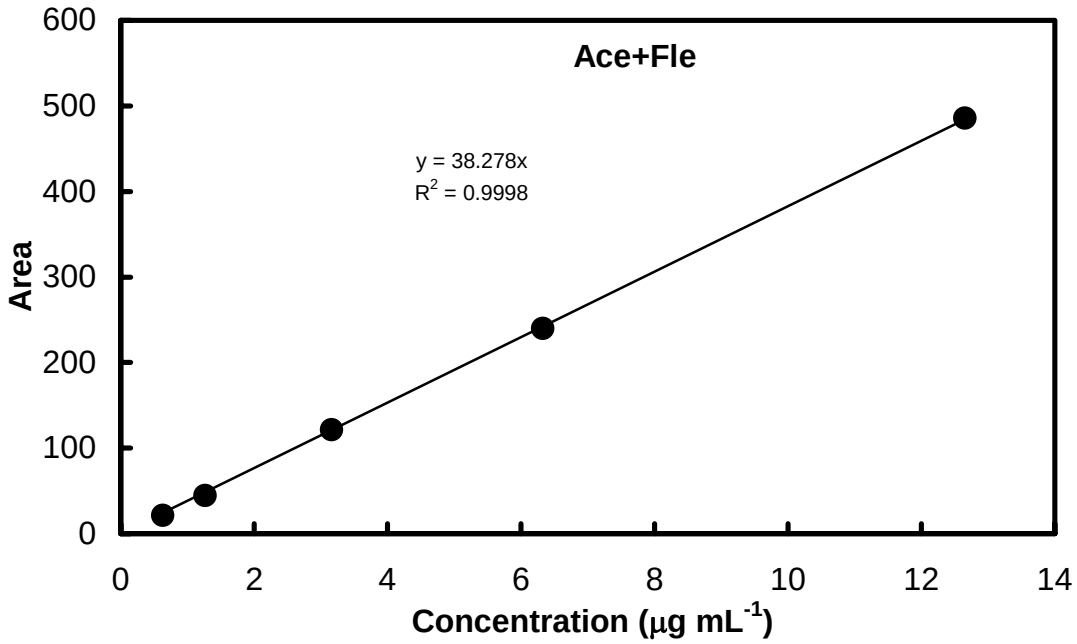

Figure A-3 Standard calibration curve of Fluorene + Acenaphthene.

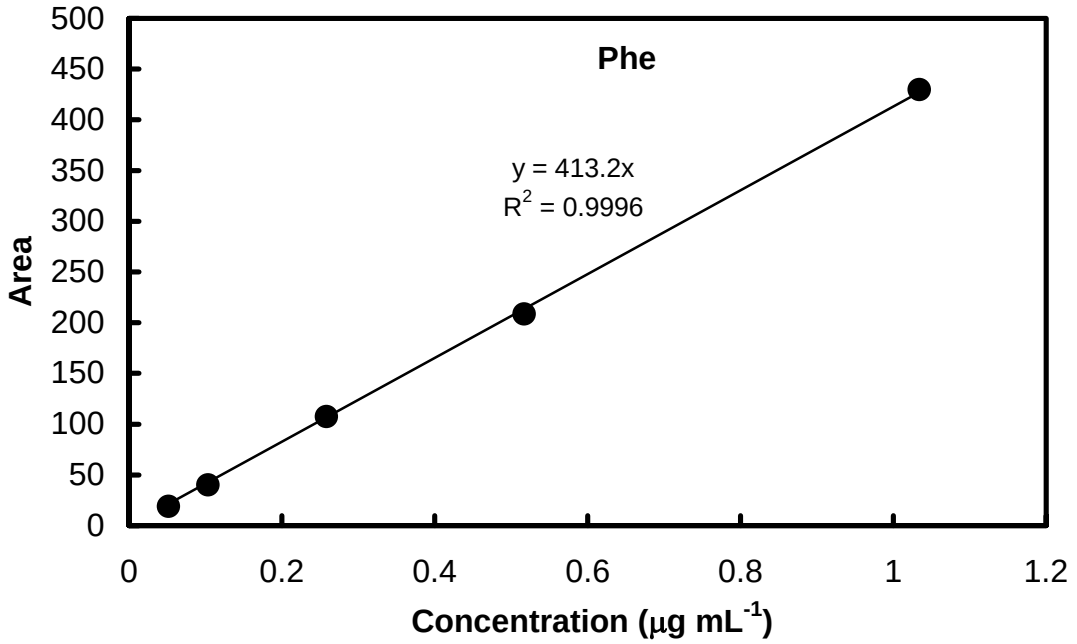

Figure A-4 Standard calibration curve of Phenanthrene.

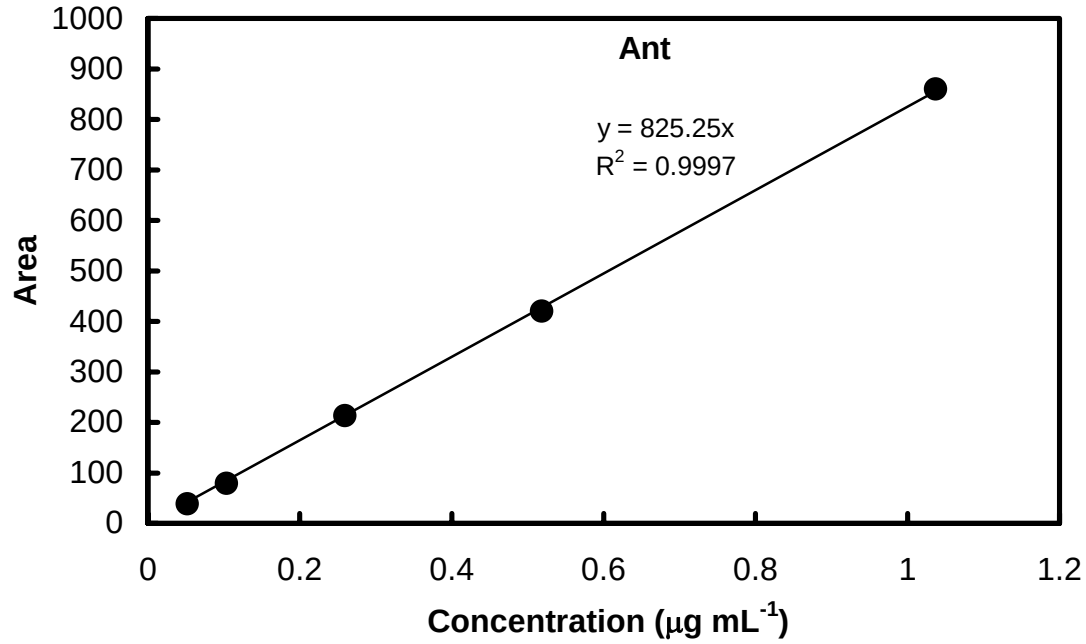

Figure A-5 Standard calibration curve of Anthracene.

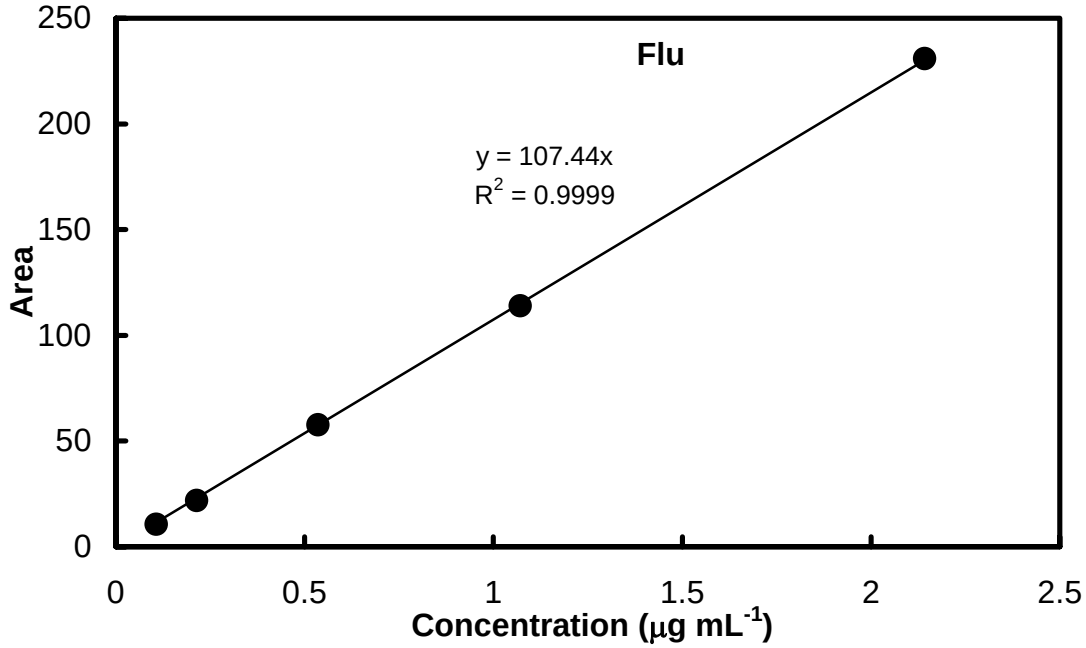

Figure A-6 Standard calibration curve of Fluoranthene.

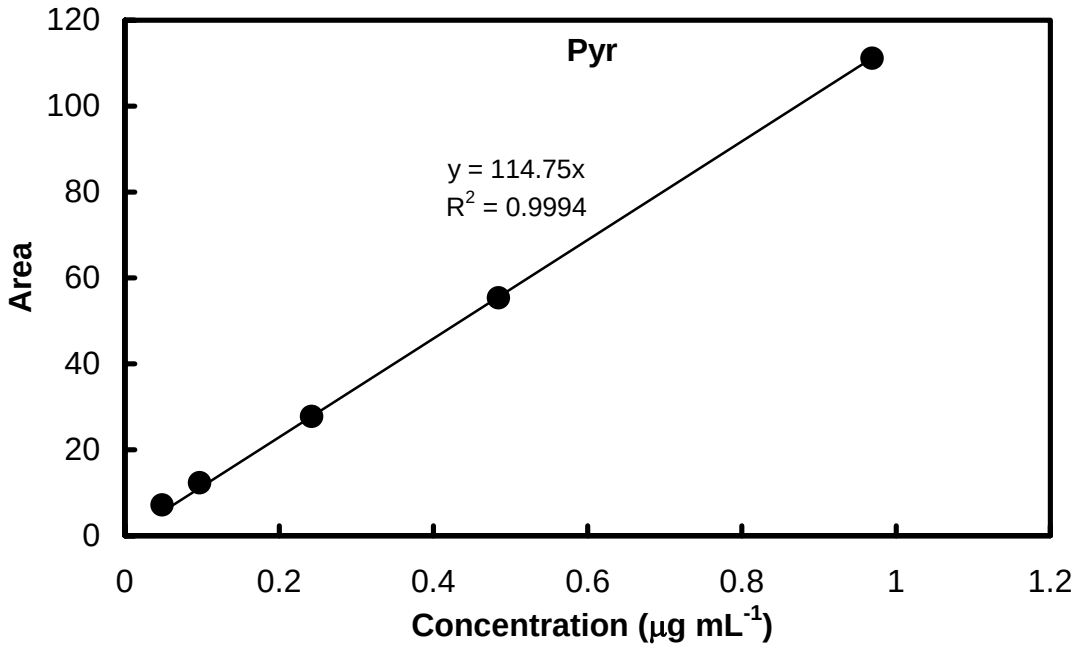

Figure A-7 Standard calibration curve of Pyrene.

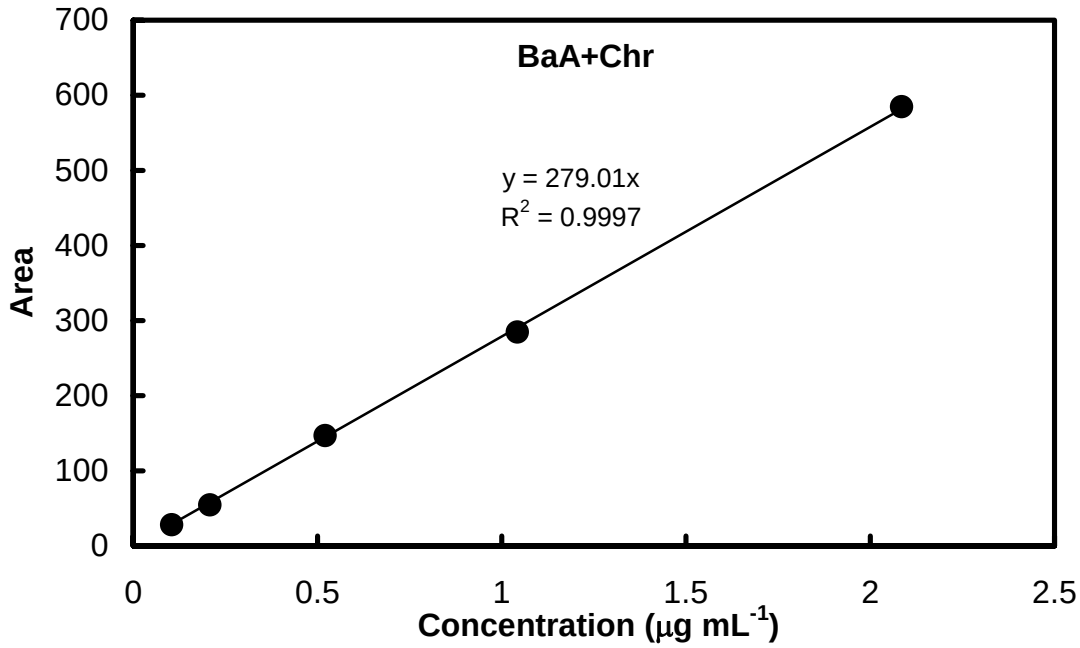

Figure A-8 Standard calibration curve of Benz(a)anthracene +Chrysene.

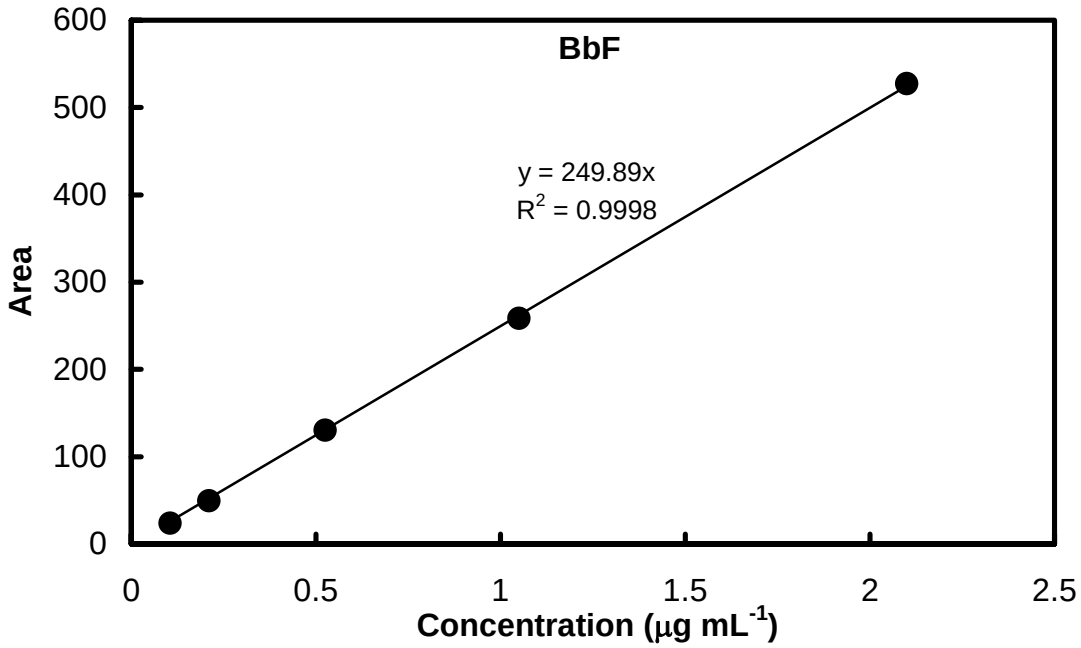

Figure A-9 Standard calibration curve of Benzo(b)fluoranthene.

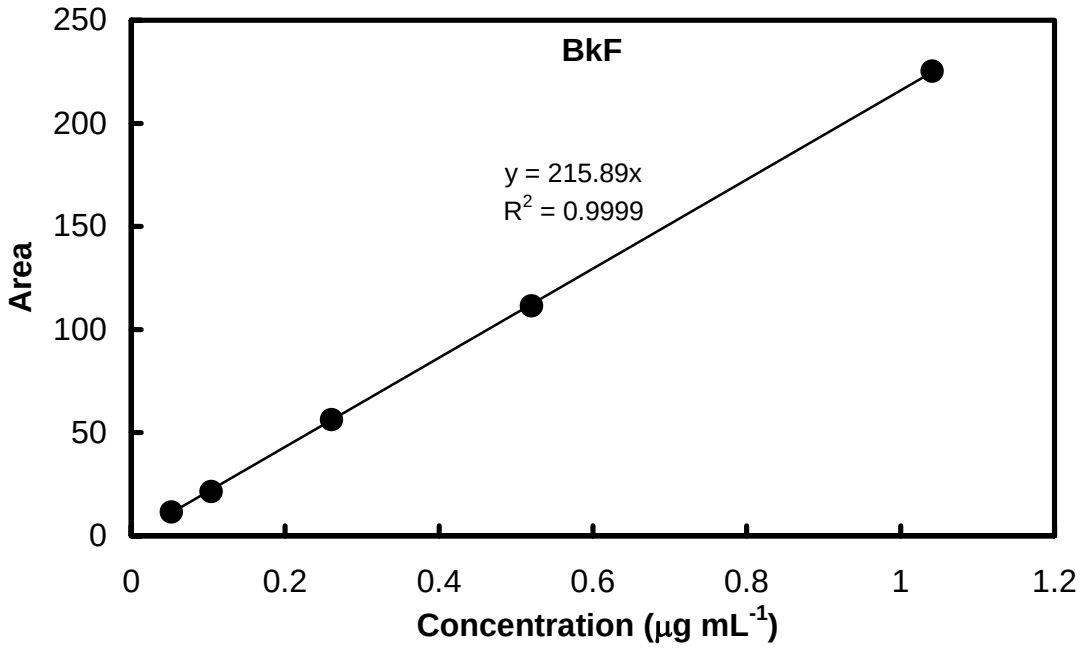

Figure A-10 Standard calibration curve of Benzo(k)fluoranthene.

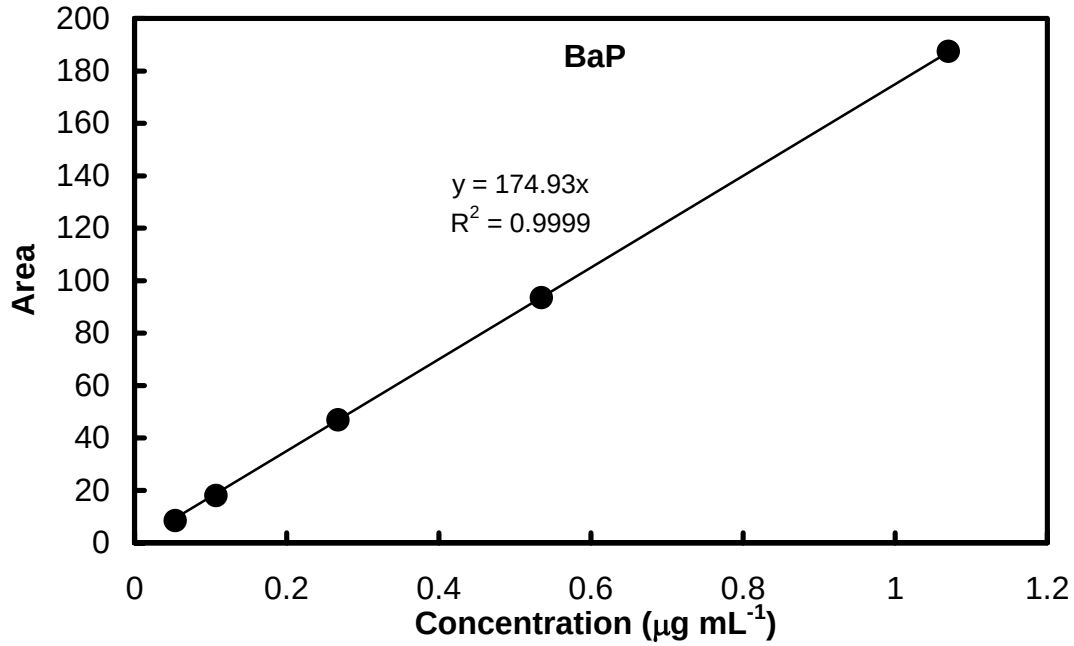

Figure A-11 Standard calibration curve of Benzo(a)pyrene.

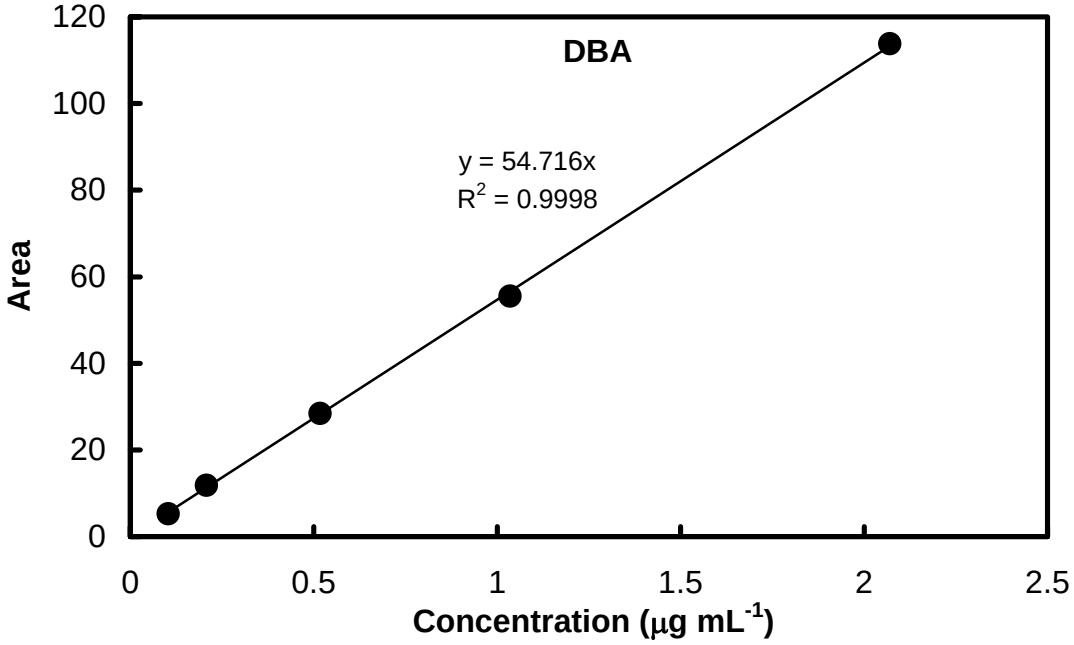

Figure A-12 Standard calibration curve of Dibenzo(a,h)anthracene.

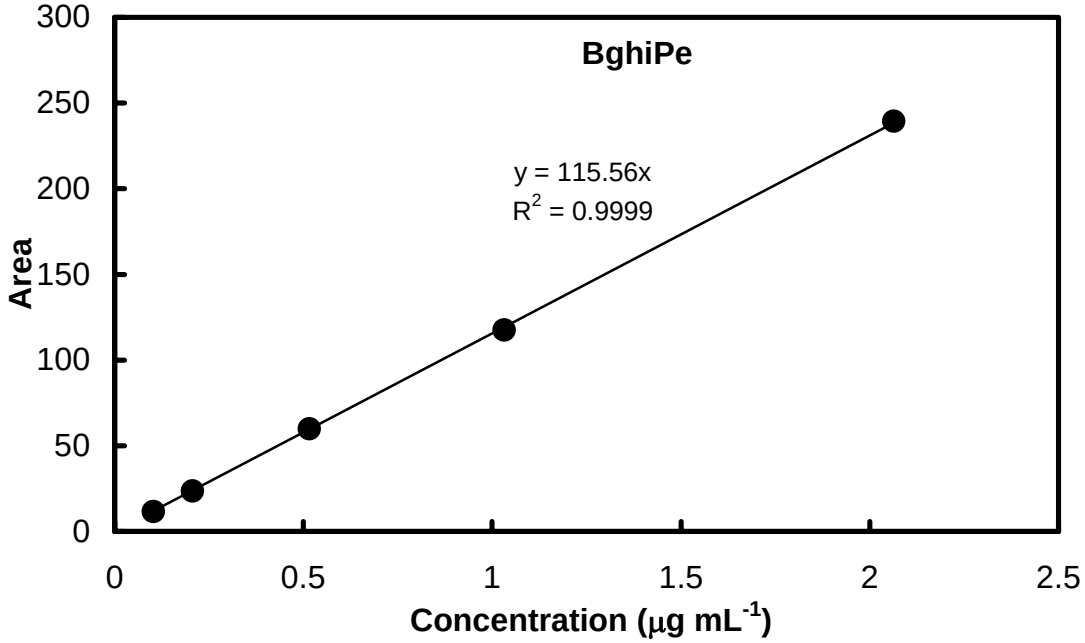

Figure A-13 Standard calibration curve of Benzo(g,h,i)perylene.

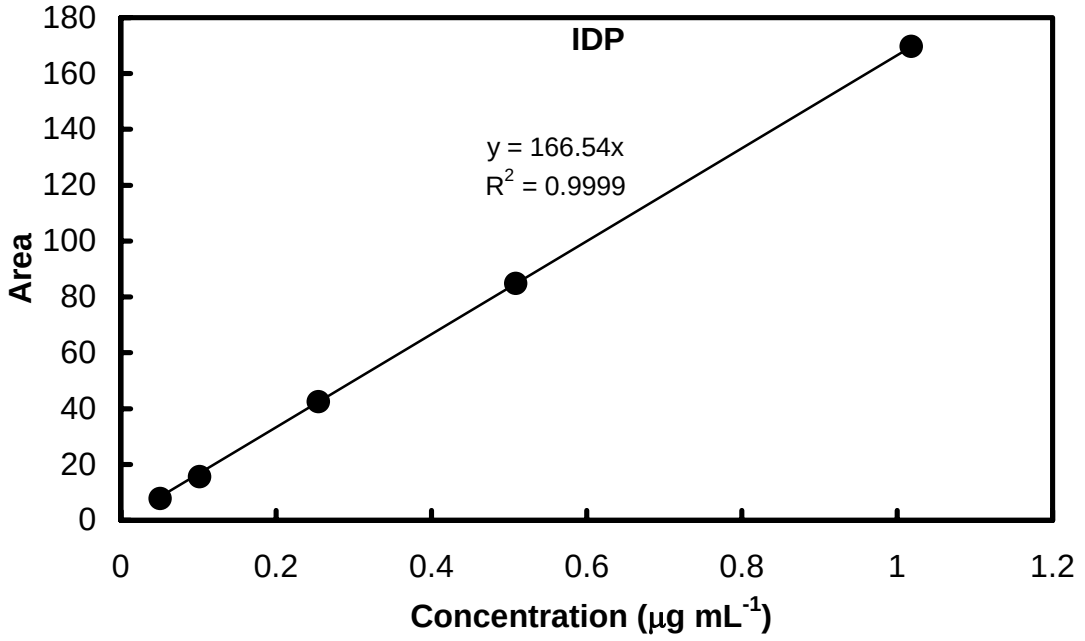

Figure A-13 Standard calibration curve of Indeno(1,2,3-cd)pyrene.

VITAE

Name Mrs. Jiraporn Chomanee

Student ID 4822132

Educational Attainment

Degree	Name of Institution	Year of Graduation
Bachelor of Science (Biotechnology)	Maejo University	2002

Scholarship Awards during Enrolment

The scholarship from Higher Education Development Project: Center of Excellence for Innovation in Chemistry (PERCH-CIC), funded by The Royal Thai Government.